Aus dem Institut für kardiovaskuläre Physiologie und Pathophysiologie
im Walter-Brendel-Zentrum für Experimentelle Medizin (WBex)
der Ludwig-Maximilians-Universität München

Direktor: Prof. Dr. med. Ulrich Pohl

Glutathion Peroxidase 4 (Gpx4)
Ein Modulator der Tumorangiogenese und Endothelintegrität

Kumulative Dissertation
zum Erwerb des Doktorgrades der Medizin
an der Medizinischen Fakultät der
Ludwig-Maximilians-Universität zu München

vorgelegt von

Markus Wortmann
aus
München

2015

Mit Genehmigung der Medizinischen Fakultät
der Universität München

Berichterstatter:	Prof. Dr. med. Ulrich Pohl
Mitberichterstatter:	Prof. Dr. Andreas Jung Priv. Doz. Dr. Axel Kleespies Priv. Doz. Dr. Gerald Schmid
Mitbetreuung durch die promovierte Mitarbeiterin:	Dr. med. vet. Heike Beck
Dekan:	Prof. Dr. med. dent. Reinhard Hickel
Tag der mündlichen Prüfung:	01.10.2015

Eidesstattliche Versicherung

-

Wortmann, Markus

Ich erkläre hiermit an Eides statt, dass ich die vorliegende Dissertation mit dem Thema

Glutathion Peroxidase 4 (Gpx4) – Ein Modulator der Tumorangiogenese und Endothelintegrität

selbstständig verfasst, mich außer der angegebenen keiner weiteren Hilfsmittel bedient und alle Erkenntnisse, die aus dem Schrifttum ganz oder annähernd übernommen sind, als solche kenntlich gemacht und nach ihrer Herkunft unter Bezeichnung der Fundstelle einzeln nachgewiesen habe.
Ich erkläre des Weiteren, dass die hier vorgelegte Dissertation nicht in gleicher oder in ähnlicher Form bei einer anderen Stelle zur Erlangung eines akademischen Grades eingereicht wurde.

Heidelberg, 04.10.2015

Markus Wortmann

Gewidmet

Meiner Familie

Inhaltsverzeichnis

Abkürzungsverzeichnis

12/15-Lox	12/15-Lipoxygenase
AIF	Apoptosis-Inducing Factor
bFGF	basic Fibroblast Growth Factor
eEPC	embryonale endotheliale Vorläuferzellen (embryonic Endothelial Progenitor Cells)
Gpx	Glutathion Peroxidase
Gpx4	Glutathion Peroxidase 4
$Gpx4^{iECKO}$	Endothelzellspezifischer Glutathion Peroxidase 4 Knockout
GSH	Glutathion
GSSG	Glutathion Disulfid
HETE	Hydroxyeicosatetraensäure
HPETE	Hydroperoxyeicosatetraensäure
NADPH	Oxidierte Form von Nicotinsäureamid-Adenin-Dinukleotid-Phosphat
PHGPx	Phospholipid Hydroperoxid Glutathion Peroxidase
PIGF	Placental Growth Factor
ROS	Reaktive Sauerstoffspezies (reactive oxygen species)
TAM	Tamoxifen ((Z)-1-(p-Dimethylaminoethoxyphenyl)-1,2-diphenyl-1-butene trans-2-[4-(1,2-Diphenyl-1-butenyl)phenoxy]-N,N-dimethylethylamine)
TROLOX	6-Hydroxy-2,5,7,8-tetramethylchroman-2-carbonsäure
VEGF-A	Vascular Endothelial Growth Factor A
αSMA	Alpha Smooth Muscle Actin

1 Einleitung

1.1 Die Familie der Glutathion Peroxidasen

Die Familie der Glutathion Peroxidasen (Gpx) umfasst bei Säugetieren insgesamt 8 verschiedene Enzyme. Die Glutathion Peroxidasen 1-4 und 6 sind durch ein konserviertes, aktives Zentrum mit der Aminosäurekombination Selenocystein, Glutamin, Tryptophan und Asparagin [4] charakterisiert. Bei Gpx5, 7 und 8 ist das Selenocystein durch Cystein, bei Gpx8 zusätzlich das Glutamin durch Serin ersetzt [5]. Genetische Mutanten, bei denen einzelne Aminosäuren des aktiven Zentrums ausgetauscht wurden, verdeutlichen, dass eine Veränderung des aktiven Zentrums zu einer deutlichen Verringerung der enzymatischen Aktivität der Glutathion Peroxidasen führt. Allein der Austausch von Selenocystein gegen Cystein verringert bei der Gpx4 die Reaktionsrate um drei Potenzstufen [6].

Die Hauptaufgabe der Glutathion Peroxidasen besteht in der Reduktion von H_2O_2 und Hydroperoxiden [1]. Hierbei reagiert das Selenocystein des aktiven Zentrums mit dem zu reduzierenden Molekül zu Selensäure und wird anschließend mittels zweier Moleküle Glutathion (GSH) wieder reduziert. Das Glutathion wird dabei zu Glutathion Disulfid (GSSG) umgesetzt (Abbildung 1) [1].

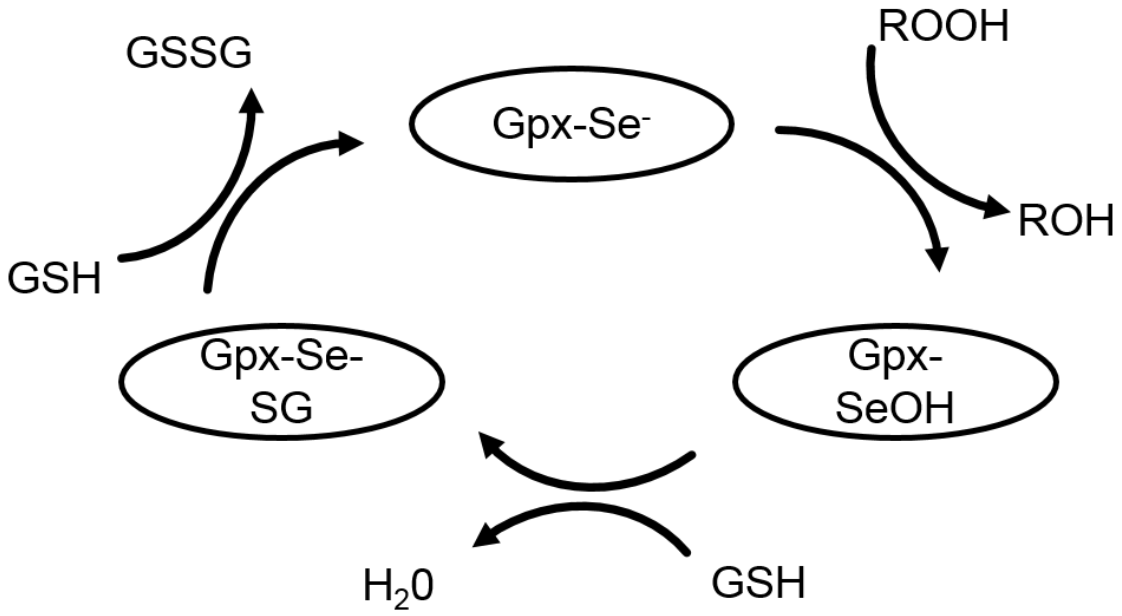

Abbildung 1: Funktionsweise der Glutathion Peroxidasen.

Das Selen (Se) im aktiven Zentrum der Glutathion Peroxidase reduziert das Hydroperoxid (ROOH) und wird dabei zur Selensäure (SeOH) umgesetzt. In zwei Reaktionsschritten unter Verbrauch jeweils eines Moleküls GSH wird die Selensäure wieder reduziert. Dabei entsteht im ersten Zwischenschritt ein Molekül H_20, im zweiten Zwischenschritt ein Molekül GSSG (Graphik adaptiert aus [1, 2]).

Neben dieser antioxidativen Funktion konnten den einzelnen Mitgliedern der Glutathion Peroxidase Familie in den letzten Jahren auch zell- und organspezifische Funktionen zugeordnet werden.

So führt zum Beispiel eine Überexpression von Gpx1 in einer Kreuzung aus 129/SVJ und C57BL/6 Mäusen zu einer erhöhten Insulinsekretion mit nachfolgendem Übergewicht und reduzierter Insulinsensitivität im Sinne eines Diabetes mellitus [7].

Gpx2 ist in mehreren humanen Tumorzelllinien, unter anderem bei Kolonkarzinomzellen [8] und Adenokarzinomzellen der Lunge [9], vermehrt exprimiert. Ein Gpx2-Knockdown in der humanen Kolon-Tumorzelllinie HT-29 führt zu einem verringerten Tumorwachstum, jedoch auch zu einer Erhöhung der Invasivität und Migrationsfähigkeit in entsprechenden *in vitro* Assays [10]. Somit ist letztendlich die Rolle der Gpx2 bei der Tumorinduktion, –progression und Metastasierung noch nicht vollständig geklärt.

Die Gpx3 ist die einzig bekannte Glutathion Peroxidase, die sezerniert wird [11]. Hauptsächlich wird die Gpx3 in Zellen der proximalen Nierentubuli gebildet und ins Blut abgegeben. Von dort aus bindet es extrazellulär vor allem an die Basalmembran der Nierentubuli in der Nierenrinde sowie an große Teile der Basalmembran der Epithelzellen des gesamten Gastrointestinaltraktes, beginnend im Magen und endend im Kolon [12, 13]. Gpx3 Knockout Mäuse haben keinen eindeutigen Phänotyp [13], jedoch wird der Gpx3 eine Rolle bei inflammatorischen Erkrankungen und Fettsucht zugeschrieben. Die genaue Funktion ist jedoch bislang unklar [1].

Die Gpx5 ist bei Mäusen nur im Nebenhoden exprimiert und schützt dort unter anderen die DNA vor einer Schädigung durch H_2O_2 [14].

Die physiologische Bedeutung der Gpx6 ist bislang unklar, jedoch wird eine Beteiligung an der Verarbeitung von Geruchsreizen vermutet [1]. Zudem wurde eine vermehrte Gpx6-Expression in der Kochlea in einem Tiermodell für Altersschwerhörigkeit [15] und in Toxoplasmose gondii-infizierten Zellen gefunden [16].

Ob auch die Gpx7 und 8 spezifische Zellfunktionen beeinflussen, ist bislang weitestgehend unklar. Sie scheinen aber bei der Faltung von Proteinen beteiligt zu sein. Die genaue Rolle dieser beiden Enzyme muss jedoch in Zukunft noch weiter spezifiziert werden [17].

1.2 Die Glutathion Peroxidase 4 (Gpx4)

Die Gpx4 wurde erstmalig 1982 durch Ursini et al. isoliert und als Enzym beschrieben, das biologische Membranen vor Peroxidation schützt. Daher rührt auch der alternative Name Phospholipid Hydroperoxid Glutathion Peroxidase (PHGPx) [18]. Gpx4 ist das einzige bekannte Enzym, das komplexe Biomoleküle wie oxidierte Phospholipide oder Cholesterine reduzieren kann [19, 20]. Dies gilt vor allem dann, wenn diese in Makromolekülen wie Lipoproteinen oder biologische Membranen integriert sind.
Gpx4 ist ein Monomer mit einer molekularen Masse von 20-22 kDa. Damit unterscheidet es sich von den meisten anderen Glutathion Peroxidasen, die entweder Dimere oder Tetramere bilden [21].

Ein weiterer Unterschied zu den anderen Mitgliedern der Gpx-Familie ist, dass die Gpx4 nicht nur auf Glutathion (GSH) als reduzierenden Kofaktor angewiesen ist. Auch Thiol-Gruppen von Proteinen, Dithiothreitol und Mercaptoethanol können als Kosubstrat fungieren (Abbildung 2) [1, 22].

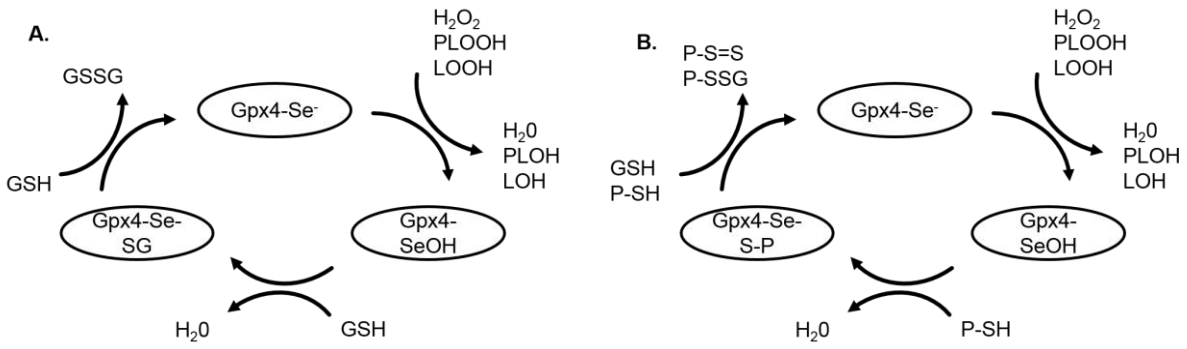

Abbildung 2: Funktionsweise der Gpx4.

Analog zu Abbildung 1 kann die Gpx4 auch oxidierte Phospholipide (PLOOH) und Lipide (LOOH) reduzieren. Als Kofaktor kommen neben GSH auch Proteine mit Thiol-Gruppen (P-SH) in Frage (Graphik adaptiert aus [1, 2]).

Insgesamt gibt es drei Isoformen der Gpx4, eine mitochondriale, eine nukleäre und eine zytosolische. Diese werden alle vom selben Gen kodiert [23]. Während die

zytosolische Form annähernd ubiquitär exprimiert wird, findet man die mitochondriale und nukleäre Form überwiegend im Hoden [24, 25]. Ein Knockout der mitochondrialen Gpx4-Isoform führt zur Unfruchtbarkeit durch eine veränderte Spermatozoen-Struktur [26]. Die nukleäre Form der Gpx4 ist mitverantwortlich für die Kondensation des Chromatins in den Spermatozoen [27, 28]. Allerdings führt ein Knockout der nukleären Gpx4 zu keiner Unfruchtbarkeit [29]. Der Grund hierfür ist noch nicht vollkommen klar, jedoch wird zumindest teilweise ein kompensierender Effekt der Gpx5 vermutet [1]. Geringe Konzentrationen an nukleärer Gpx4 sind auch in den Zellkernen von Nierenzellen nachweisbar, allerdings mit bislang unbekannter Funktion und Relevanz [30].

In diversen Studien mit Knockout-Mäusen, bei denen ein einzelnes antioxidatives Enzym ausgeknockt wurde, konnte gezeigt werden, dass das Fehlen einzelner Redox-Enzyme unter Basalbedingungen oft durch die Funktion anderer Enzyme kompensiert werden kann. Mäuse mit einem Gpx1-Knockout entwickeln sich zum Beispiel vollkommen normal und zeigen keine Anzeichen für Unfruchtbarkeit [31]. Selbes gilt für Mäuse mit einem ubiquitären Katalase-Knockout [32]. Auch ein Knockout von xCT, einer speziellen Untereinheit des Cystin/Glutathion-Antiporters, der für die intrazelluläre Bereitstellung von Glutathion verantwortlich ist und somit regulatorische Einflüsse bei der Redox-Regulation besitzt, hat keinen Effekt in einem *in vivo* Mausmodell, während Fibroblasten mit einem xCT-Knockout *in vitro* nicht überlebensfähig sind [33]. Die Gpx4 hingegen ist für die embryonale Entwicklung unentbehrlich. Ein Knockout des Enzyms resultiert in einer frühen embryonalen Letalität an Embryonaltag 7,5 [34].
Wird der Gpx4-Knockout erst in der adulten Maus induziert, führt dies innerhalb von 2 Wochen zum Tod der Tiere. Dabei konnte insbesondere eine Malfunktion der Mitochondrien der Leber sowie eine erhöhte Rate an apoptotischen Zellen der Leber und ein Verlust hippokampaler Neuronen nachgewiesen werden [35].
Mittels Zellkulturexperimenten gelang der Nachweis des entsprechenden Signalweges, der bei einem Verlust der Gpx4 zum Zelltod führt:
Ein Mangel an Gpx4 oder seines Hauptmetaboliten GSH führt zu einer gesteigerten Aktivität der 12/15-Lipoxygenase. Die daraus resultierende Lipidperoxidation führt über die Aktivierung des „Apoptosis-Inducing Factor“ (AIF) und dessen Translokation in den Zellkern zum Zelltod (Abbildung 3) [3]. Wichtig hierbei ist, dass dieser

Signalweg spezifisch über Lipidperoxidation wirkt. So kann der Zelltod durch lipophile Antioxidantien wie Vitamin E, seinem Isomer, α-Tocopherol oder dem wasserlöslichen Vitamin E Derivat 6-Hydroxy-2,5,7,8-tetramethylchroman-2-carbonsäure (TROLOX), effektiv verhindert werden [3]. Hydrophile Antioxidantien haben jedoch keinen Effekt.

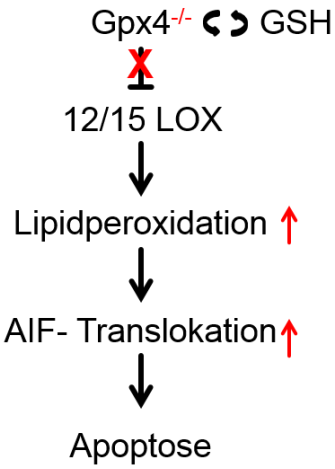

Abbildung 3: AIF vermittelte Apoptose durch erhöhte Lipidperoxidation.

Ein Gpx4 Knockout führt zu einem erhöhten Substratangebot für die 12/15 LOX. Konsekutiv steigt hierdurch die Lipidperoxidation in der Zelle. Dies löst eine vermehrte Translokation des AIF in den Zellkern aus. Hierdurch wird die Apoptose der Zelle induziert (Graphik adaptiert aus [3]).

Neben dem Schutz vor diesem Lipidperoxidation-abhängigen Weg der Apoptose hat die Gpx4 aber auch eine wichtige Regulatorfunktion in der Zellphysiologie. Unter anderem wird die Aktivität verschiedener Lipoxygenasen mit Funktionen im Arachidonsäurestoffwechsel direkt durch die Gpx4 kontrolliert. Zu nennen sind hier unter anderem die 5-, 12- und 15- Lipoxygenase [36, 37]. Die Gpx4 übt hierbei keine direkte hemmende Wirkung auf die untergeordneten Lipoxygenasen aus. Vielmehr führt eine regelrechte Funktion der Gpx4 zu einer reduzierten Konzentration an Hydroperoxyeicosatetraen- und Hydroxyeicosatetraensäuren, die wiederum als Substrat für die Lipoxygenasen dienen. Im Falle einer durch Selenmangel reduzierten Gpx4 Aktivität kann es in Leukozyten (RBL-1 Zellen) zu einer 8-fach erhöhten Freisetzung von LOX Metaboliten, wie Leukotrien B4 oder HETEs, kommen [36]. Eine Überexpression von Gpx4 führt konsekutiv zu einer erniedrigten Leukotrien Produktion [38].

Auch die Aktivität von Rezeptor Tyrosinkinasen, die wichtige transmembranöse Signalwege wie den des Platelet Derived Growth Factor β (PDGF-β) – Rezeptors vermitteln, wird durch Lipidperoxide und somit durch die Gpx4-Aktivität moduliert [39].

So führt die erhöhte Konzentration an Lipidperoxiden in Folge einer reduzierten Gpx4-Aktivität zu einer Oxidation von Tyrosin-Phosphatasen, die wiederum die Aktivität der Rezeptor-Tyrosinkinasen verringern.
In der humanen Endothelzelllinie ECV 304 konnte zudem gezeigt werden, dass eine Überexpression von Gpx4 die NFκB Induktion durch Interleukin-1, und somit einen der wichtigsten Signalwege in der Antwort auf inflammatorische Stimuli, komplett unterbindet [40].

Somit hat die Gpx4 neben ihrer einzigartigen Rolle als protektives Enzym gegen Membran-Lipidperoxidation eine Vielzahl von physiologischen Aufgaben. Diese umfassen eine regulatorische Funktion im Arachidonsäurestoffwechsel und bei zentralen inflammatorischen Signalwegen, sowie eine Interaktion mit Rezeptor-Tyrosinkinasen. Letzteres wiederum bedeutet auch einen direkten Einfluss der Gpx4 auf die Migrations- und Wachstumsfähigkeit von Zellen.

1.3 Die Bedeutung von reaktiven Sauerstoffspezies (ROS) und Gpx4 im Gefäßsystem

Nur ein intaktes Endothel ermöglicht auch eine regelrechte Gefäßfunktion. Durch multiple Interaktionen mit intraluminalen Zellen sowie Zellen der Gefäßwand reguliert das Endothel u.a. den Gefäßtonus, Thrombogenität, inflammatorische Prozesse, verschiedene Signalwege und die Gefäßpermeabilität [41].

Eine Dysfunktion des Endothels kann beispielsweise zur Entstehung von atherosklerotischen Läsionen, Vasospasmus, erhöhter Thrombogenität, Proliferation, „Remodelling“ der Gefäßwand sowie zu einer erhöhten Expression inflammatorischer Marker beitragen [41].
Eine vermehrte Konzentration von Sauerstoffradikalen (ROS) gilt als eine der Hauptursachen für endotheliale Dysfunktion [42, 43].

Unter bestimmten Formen der mechanischen Aktivierung, z.B. niedrigem oszillatorischem Shear Stress, können Endothelzellen dauerhaft NADPH Oxidase abhängig vermehrt Superoxidanionen produzieren [44]. Auch andere Enzyme wie die Xanthin Oxidase, verschiedene mitochondriale Enzyme der Atmungskette, die

endotheliale NO-Synthase und verschiedene Lipoxygenasen [45, 46] können zur ROS Produktion in Endothelzellen beitragen. Hierzu zählt auch die 12/15-LOX, die durch Gpx4 kontrolliert wird und eine hohe Expression im Endothel aufweist.

Außerdem trägt die Aktivierung des Renin-Angiotensin-Aldosteron-Systems, das eines der wichtigsten klinischen Ziele der antihypertensiven Therapie darstellt, zu einer Erhöhung des oxidativen Stresses bei. Eine Angiotensin-II Applikation über mehrere Tage führt bei Ratten nicht nur zu einer deutlichen Erhöhung des Blutdruckes, sondern auch zu einer vermehrten Bildung von Sauerstoffradikalen in der Gefäßwand sowie zu mangelnder Gefäßdilatation nach Acetylcholin Stimulation [47]. Dieser Effekt wird maßgeblich durch die Stimulation und erhöhte Expression der NADH/NADPH Oxidase vermittelt. Zellkulturexperimente haben ergeben, dass diese Induktion in sämtlichen Zellen der Gefäßwand, unter anderem auch in den Endothelzellen, erfolgt [48]. Eine Therapie mit Angiotensin-II führt jedoch nur zu einem geringen Blutdruckanstieg, wenn gleichzeitig die NADH/NADPH Oxidase gehemmt wird [49]. Dies verdeutlicht die Bedeutung der ROS Induktion durch das Renin-Angiotensin-Aldosteron System.

Klinisch gesehen kann bei Patienten mit arterieller Hypertonie ein erhöhtes Maß an oxidativem Stress anhand zirkulierender Biomarker nachgewiesen werden [50].

Trotz dieser experimentellen Ergebnisse, die eine pathophysiologische Rolle von ROS bei Gefäßerkrankungen wahrscheinlich machen, haben klinische Studien mit Antioxidantien bislang nur zu enttäuschenden Ergebnissen in der Primär- und Sekundärprävention kardiovaskulärer Ereignisse geführt [46, 51]. Dies mag unter anderem daran liegen, dass entweder die falschen Patienten, die falschen Antioxidantien oder die falsche Dosierung gewählt wurden [52].

Während ROS früher nur eine toxische Wirkung zugeschrieben wurde, haben sie in den letzten Jahren vermehrt Bedeutung als Signalmoleküle und somit auch für die physiologische Funktion der Zellen der Gefäßwand gewonnen [53, 54]. Heute werden ROS als wichtige Signalmoleküle in der Feinabstimmung der zellulären Reaktion auf unterschiedliche Stimuli betrachtet. Toxisch wirken sie nur, wenn ihre Konzentration zu hoch ist [54]. Wie bereits beschrieben werden zum Beispiel Rezeptor Tyrosinkinasen direkt durch die Lipidperoxidkonzentration reguliert [39]. Auch die Oxidation von

Cystein zu Cystin dient bei vielen Transkriptionsfaktoren, wie NF-κB und Egr-1, der Redox-abhängigen Regulation [17]. Selbiges gilt auch für die Oxidation von Fe^{2+} zu Fe^{3+} bei HIF-Prolyl-Hydroxylasen, die zu einer Aktivierung von HIF-1α führt [55]. Diese Signalwege sind für eine regelrechte Zellphysiologie unerlässlich. Somit kann ein ungezielter Einsatz von Antioxidantien bei manchen Patienten sogar schädlich sein [46].

Aus diesem Grund ist es von großer Bedeutung, die genaue Funktion der einzelnen Enzyme, die an der Regulation des oxidativen Stresses beteiligt sind, genauer zu verstehen. Dies soll in Zukunft neue, möglichst gezielte antioxidative Therapieansätze ermöglichen.

Die Untersuchung der funktionellen Bedeutung von Redoxenzymen gestaltet sich jedoch oftmals schwierig, da ein Knockout eines einzelnen Enzyms durch die verstärkte Expression und/ oder gesteigerte Aktivität eines anderen Enzyms kompensiert werden kann. Die beteiligten Radikale sind zudem oft kurzlebig und instabil, so dass deren Nachweis technisch aufwendig ist.

Wie bereits beschrieben schützt die Gpx4, sowohl *in vivo* als auch *in vitro*, vor einem durch erhöhte Lipidperoxidation induzierten Zelltod und hat multiple Interaktionen mit verschiedenen zellulären Signalkaskaden.

Ob die Gpx4 jedoch auch direkt in Zellen des Gefäßsystems, vor allem im Gefäßendothel mit seiner zentralen Bedeutung für die Gefäßfunktion, eine Rolle spielt, ist bislang unklar. Weiterhin bleibt unklar, ob eine Störung der Gpx4-Funktion in Zellen, die durch die Freisetzung von Wachstumsfaktoren die Angiogenese stimulieren, einen Einfluss auf diese Angiogeneseprozesse hat.

Aus diesem Grunde wurden im ersten Teil dieser Arbeit transformierte Fibroblasten mit einem Gpx4-Knockout generiert und diese in Mäuse implantiert. Ziel war es zu untersuchen, ob eine veränderte Sekretion an angiogenen Faktoren der Fibroblasten, verursacht durch den Gpx4-Knockout und nachgeschaltete Signalwege, zu einer Veränderung der Tumorvaskularisation führt.

Im zweiten Teil dieser Arbeit wurden Mäuse mit einem induzierbaren, endothelspezifischen Gpx4-Knockout generiert, anhand derer der Einfluss des Gpx4-Knockouts mit nachfolgender erhöhter Lipidperoxidation im Endothel selbst *in vivo* untersucht werden sollte. Hierbei wurde, analog zu dem in Vorarbeiten beschriebenen Phänotyp *in vitro*, ein Untergang der Endothelzellen sowie eine Veränderung der Antithrombogenität der Endothelzellen durch den Einfluss der erhöhten Lipidperoxidation erwartet.

2 Eigene Arbeiten

2.1 Absence of Glutathione Peroxidase 4 Affects Tumor Angiogenesis through Increased 12/15-Lipoxygenase Activity

Manuela Schneider, **Markus Wortmann**, Pankaj Kumar Mandal, Warangkana Arpornchayanon, Katharina Jannasch, Frauke Alves, Sebastian Strieth, Marcus Conrad and Heike Beck

Neoplasia. 2010 Mar;12(3):254-63.

Da in kultivierten Zellen ein Gpx4-Knockout ohne Substitution von lipophilen Antioxidantien zum Zelltod führt, sind Gpx4-Knockout Zellen nur begrenzt zur Analyse des Einflusses der Gpx4 auf ROS-abhängige Zellfunktionen geeignet. Dies gilt vor allem für länger andauernde Prozesse wie Tumorentwicklung und -wachstum.

Um dieses Problem zu lösen und eine Differenzierung der Gpx4-Funktion in zeitlich verschiedenen Stadien untersuchen zu können, wurden Zellen mit einem induzierbaren Gpx4-Knockout mittels eines sogenannten „Cre/loxP-Rekombinationssystems“ generiert. Die letzten 3 Exons des Gpx4 Gens wurden mit zwei loxP-Sequenzen flankiert, die später als Schnittstellen für das Restriktionsenzym Cre-Rekombinase dienten. Diese Zellen werden auch als „gefloxte“ Zellen bezeichnet. Wenn diese Zellen mit Cre-Rekombinase transfiziert werden, schneidet diese an den entsprechenden loxP-Sequenzen. Die dazwischen liegende DNA-Sequenz wird entfernt und kann nicht mehr abgelesen werden. Das Enzym wird nicht mehr in einer funktionellen Form exprimiert.

Um eine gezielte Induktion des Knockouts zu bestimmten Zeitpunkten zu ermöglichen, wird die Cre-Rekombinase in Form eines MerCreMer Proteinkomplexes in Fibroblasten transfiziert, die das gefloxte Gpx4 Gen enthalten. Dabei wir ein Vektor verwendet, auf dem die Sequenz der Cre-Rekombinase durch die Sequenz zweier MER-Proteine (mutated murine estrogen receptor ligand-binding domain) flankiert wird. Durch dieses genetische Konstrukt wird ein Fusionsprotein aus der Cre-Rekombinase und zwei MER-Proteinen synthetisiert. Ein Übertritt in den Zellkern und eine Induktion des Knockouts ist somit nicht möglich. Erst nach Zugabe von Tamoxifen dissoziiert dieser Proteinkomplex aufgrund der Rezeptoreigenschaften der MER-Proteine. Die Cre-Rekombinase kann nun in den Zellkern übertreten und der Knockout

wird induziert (Abbildung 4) [56].

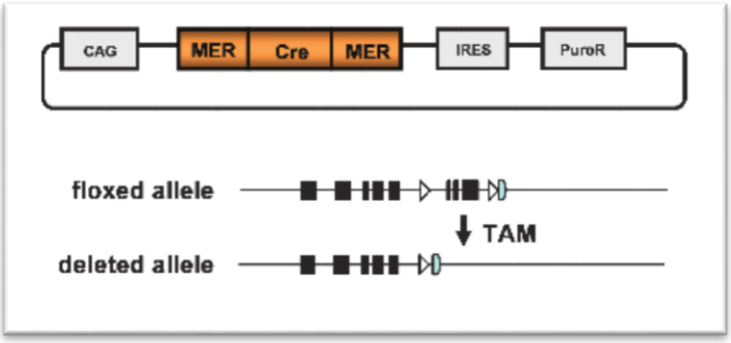

Abbildung 4: Knockout Strategie.

Die gefloxten Fibroblasten wurden mit dem MERCreMER tragenden Plasmid transfiziert. Durch die Zugabe von Tamoxifen wird der Gpx4-Knockout durch die Deletion der mit loxP-Sequenzen flankierten Exons induziert.

Auf diese Weise stand ein induzierbares Knockout-Modell zur Verfügung, das eine Kultivierung der Zellen unter Standard Zellkultur Bedingungen ermöglicht, bei denen ein Gpx4 Knockout jederzeit durch die Zugabe von Tamoxifen induziert werden kann. Die entsprechenden Fibroblasten wurden in einem weiteren Schritt mit dem Protoonkogen *c-Myc* und dem Onkogen *Ha-ras*^{V12} transfiziert, um ihnen Tumorzelleigenschaften zu verleihen. Trotz dieser erneuten Transfektion verhielten sich die Zellen genauso wie die nicht transfizierten Zellen. Genetische Schäden, die zu einem funktionellen Phänotyp führen, wurden durch die Transfektion also nicht induziert.

Vergleichbar mit ähnlichen Befunden an anderen Zelllinien [3], starben diese transfomierten Fibroblasten unter normalen Zellkulturbedingungen ohne Zugabe von lipophilen Antioxidantien innerhalb von 48 Stunden nach Induktion des Gpx4-Knockouts ab. Wie erwartet konnte dieser Zelltod durch die Zugabe von lipophilen Antioxidantien oder durch eine Hemmung der 12/15-LOX verhindert werden. Hydrophile Antioxidantien zeigten jedoch keinen rettenden Effekt. Die Transfektion der Onkogene hatte keinen Effekt auf die Knockout Induktion. Die transformierten Zellen verhielten sich diesbezüglich also genauso wie die nicht transformierten.

Um die Auswirkung des Gpx4-Knockouts auf die Interaktion der transformierten Fibroblasten mit Proteinen der extrazellulären Matrix zu überprüfen, wurden sie anschließend in Matrigel eingebettet. Matrigel ist eine Mixtur aus verschiedenen Komponenten der extrazellulären Matrix, die aus Engelbreth-Holm-Swarm Sarkomen

isoliert wird. Verwendung findet Matrigel vor allem in *in vitro* Experimenten, bei denen eine Interaktion von Zellen mit einer extrazellulären Matrix untersucht werden soll [57].

Obwohl die Gpx4$^{-/-}$-Fibroblasten unter Zellkulturbedingungen nur mit Zugabe entsprechender protektiver Antioxidantien überleben, bilden sie in Matrigel auch ohne Zugabe lipophiler Antioxidantien Tumorzellspheroide. Weder in Bezug auf die Größe noch auf die Anzahl der Tumorspheroide war ein signifikanter Effekt des Gpx4-Knockouts nachweisbar.
Der genaue Grund hierfür ist bislang unbekannt. Jedoch zeigte sich auch unter Zellkulturbedingungen, dass Zellen die Induktion des Knockouts überlebten, wenn sie konfluent waren und somit einen engen Zell-Zell Kontakt zueinander hatten.

Auch *in vivo*, nach subkutaner Implantation in C57Bl/6 Mäuse, überlebten die transformierten Gpx4$^{-/-}$-Fibroblasten und formten Tumore.
Diese waren 16 Tage nach Implantation sowohl in Größe und Volumen vergleichbar mit den entsprechenden Wildtyptumoren (Abbildung 5).

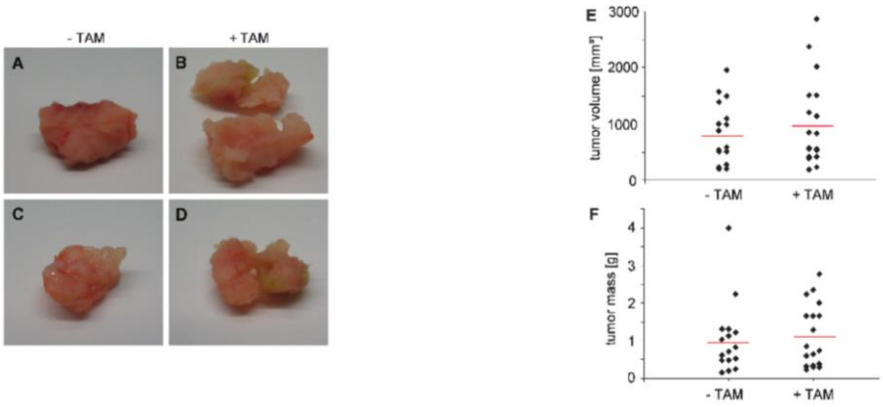

Abbildung 5: Tumorexperimente mit transformierten Gpx4$^{-/-}$-Fibroblasten.

Die transformierten Fibroblasten bilden Tumore, wenn sie subkutan in C57/Bl6 Mäuse implantiert werden, unabhängig davon ob sie mit Tamoxifen behandelt werden (B und D) oder nicht (A und C). Ebenso verursacht die Induktion eines Gpx4-Knockouts keinen Unterschied in Bezug auf das Tumorvolumen (E) oder die Tumormasse (F).

Ein wichtiger Unterschied war jedoch ein erhöhter Anteil an mitotisch aktiven Zellen. Dieser wurde durch einen höheren Anteil an apoptotischen, TUNEL positiven-Zellen kompensiert, so dass es insgesamt nicht zu einem vermehrten Tumorwachstum kam. Der genaue Grund hierfür bleibt jedoch bislang unklar.

Histologische Analysen des Tumorgefäßsystems mittels eines gegen Endothelzellen gerichteten Antikörpers (anti-CD31), zeigten jedoch einen deutlichen vaskulären Phänotyp. In den Gpx4$^{-/-}$-Tumoren fehlten weitestgehend Gefäße mit größerem Lumen. Dafür war das Netzwerk aus Kapillaren und kleinen Gefäßen signifikant dichter. Zusätzliche Analysen mit einem gegen alpha Smooth Muscle Actin (αSMA) gerichteten Antikörper erbrachten einen signifikant geringeren Anteil an vollständig ausgebildeten, mit αSMA-positiven Zellen (glatte Gefäßmuskelzellen oder Perizyten) umgebenen Gefäßen (Abbildung 6).

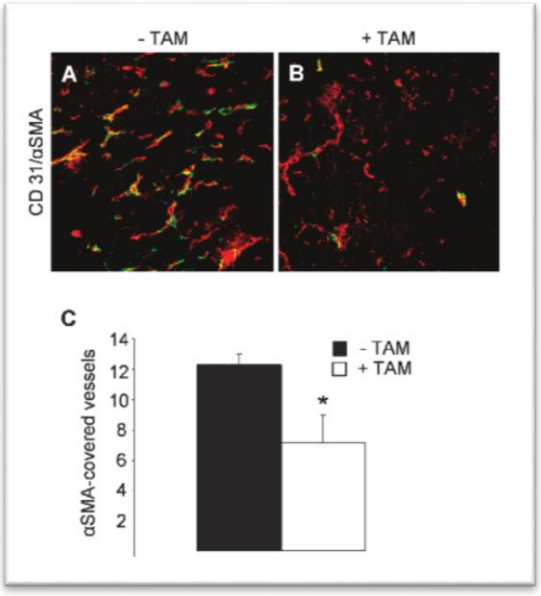

Abbildung 6: Reduzierte Dichte an αSMA-positiven Zellen bei den Gpx4$^{-/-}$-Tumoren.

Die Gpx4$^{-/-}$-Tumore (B) zeigen in der Doppelfärbung gegen CD31 (rot) als Endothelzellmarker sowie gegen αSMA (grün) als Marker für glatte Muskelzellen und Perizyten eine deutlich verminderte Dichte an αSMA-positiven Zellen. Als Vergleich dienten Tumore derselben transformierten Fibroblasten, bei denen jedoch der Gpx4-Knockout nicht induziert worden war (B).

Um den Grund der veränderten Morphologie der Tumorgefäße in den Gpx4$^{-/-}$-Tumoren zu untersuchen, wurde die Konzentration mehrerer endothelialer Wachstumsfaktoren (Vascular Endothelial Growth Factor A (VEGF-A), Placental Growth Factor (PIGF) und basic Fibroblast Growth Factor (bFGF)) in Tumorgewebs-Lysaten bestimmt. Die Proben zeigten jedoch keine signifikanten Konzentrationsunterschiede. Dieses Negativergebnis war vermutlich durch die Heterogenität des Tumorgewebes zu erklären.

Im Überstand der transformierten Gpx4$^{-/-}$- Fibroblasten unter *in vitro* Bedingungen war die Konzentration von bFGF jedoch signifikant erhöht, die von VEGF-A signifikant erniedrigt.

Dieser Konzentrationsanstieg von bFGF kann beispielsweise durch eine vermehrte Aktivität der 12/15-LOX erklärt werden [58].
In der Literatur ist beschrieben, dass eine verringerte bFGF-Produktion mit einem Rückgang der Dichte der Blutgefäße einhergeht, wobei in diesem Fall auch eine Abnahme des Gefäßdurchmessers beschrieben ist [59, 60]. Eine direkte Inhibition von bFGF führt zu einer reduzierten Neovaskularisation und wird aktuell als antiangiogene Therapie bei verschiedenen Tumorerkrankungen evaluiert [61].
Dies ist insofern kongruent zu den oben genannten Daten, da bei Gpx4$^{-/-}$-Tumoren genau das Gegenteil, also eine erhöhte bFGF Konzentration mit höherer Dichte an Tumorgefäßen, auftritt.

Erfolgte während des subkutanen Wachstums der Gpx4$^{-/-}$-Tumore eine systemische Therapie der Mäuse mit Baicalein, einem spezifischen Inhibitor der 12/15-Lipoxygenase, waren diese Veränderungen am Tumorgefäßsystem deutlich geringer ausgeprägt. So konnte eine deutliche Abnahme der Kapillardichte, eine signifikante Zunahme der Tumorgefäßdurchmesser sowie eine Zunahme der αSMA- positiven Zellen beobachtet werden (Abbildung 7).

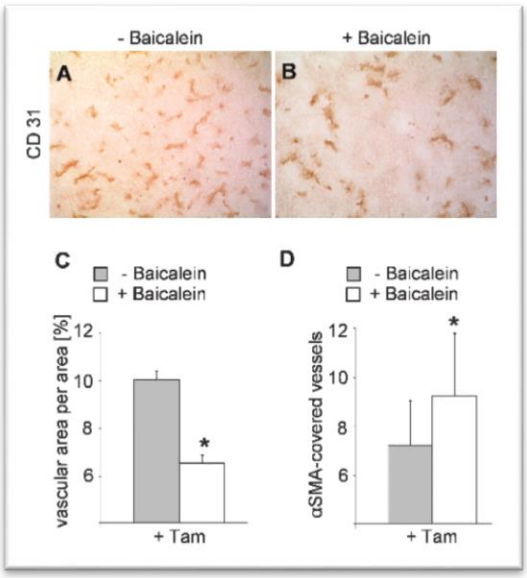

Abbildung 7: Baicalein Therapie.

Während Gp4$^{-/-}$-Tumore ohne Baicalein Behandlung eine deutlichen vaskulären Phänotyp zeigen (A), führt eine Therapie mit Baicalein zu einer Normalisierung des Tumor Gefäßsystems sowohl in Bezug auf die Gefäßdichte als auch in Bezug auf die mit αSMA-positiven Zellen umgebenen Gefäße (B-D).

Zusammenfassend führt ein Gpx4-Knockout in transformierten Fibroblasten unter Zellkulturbedingungen zum Zelltod. Wenn diese Zellen jedoch in Matrigel als extrazelluläre Matrix implantiert werden, überleben sie trotz des induzierten Gpx4

Knockouts, wobei der Grund hierfür bislang unklar bleibt.

Werden transformierte Gpx4$^{-/-}$-Fibroblasten subkutan in Mäuse implantiert, bilden sie im Vergleich zu Wildtyptumoren Tumoren gleicher Größe. Diese unterscheiden sich jedoch in der Morphologie des Tumorgefäßsystems deutlich. Der Gpx4-Knockout führt über einen 12/15-Lipoxygenase vermittelten Signalweg zu einem Anstieg der bFGF Freisetzung. Dies wiederum führt zu einer reduzierten Bildung von großen Tumorgefäßen und einer höheren Dichte an kleinen Mikrogefäßen, die wiederum weniger αSMA-positiven Zellen aufweisen. Durch eine Behandlung mit einem Inhibitor der 12/15-Lipoxygenase kann dieser Phänotyp rückgängig gemacht werden. Es bilden sich, vergleichbar mit den Kontrolltumoren, wieder größere Gefäße mit geringerer Dichte, die zudem eine erhöhte Anzahl an αSMA-positiven Zellen besitzen.

2.2 Combined Deficiency in Glutathione Peroxidase 4 (Gpx4) and Vitamin E Causes Multi-Organ Thrombus Formation and Early Death in Mice

Markus Wortmann*, Manuela Schneider*, Joachim Pircher, Juliane Hellfritsch, Michaela Aichler, Naidu Vegi, Pirkko Koelle, Peter Kuhlencordt, Axel Walch, Ulrich Pohl, Georg W. Bornkamm, Marcus Conrad and Heike Beck

Circ Res. 2013 Aug 2;113(4):408-17. Epub 2013 Jun 14. (* equal contribution)

Zur Analyse der bisher weitgehend unbekannten Funktion der Gpx4 im Endothel wurden transgene Mäusen mit einem endothelspezifischen, induzierbaren Gpx4-Knockout ($Gpx4^{iECKO}$) generiert. Dieses Mausmodell basiert auf dem bereits beschriebenen „cre-loxP"-Modell. Die letzten drei Exons des Gpx4-Gens werden hierbei durch zwei „loxP"-Sequenzen flankiert, die durch die Cre-Rekombinase ausgeschnitten werden. Somit wird der Knockout induziert. In diesem speziellen Modell wurde die Cre-Rekombinase unter die Kontrolle des Cdh5-Promoters gestellt, der in der adulten Maus nur im Endothel aktiv ist [62]. Dadurch wird auch die Cre-Rekombinase nur im Endothel transkribiert. Für einen induzierbaren Knockout wird die Cre-Rekombinase wiederum durch MER-Proteine (mutated murine estrogen receptor ligand-binding domain) blockiert. Durch die Gabe von Tamoxifen dissoziieren diese MER-Proteine, der Knockout wird induziert (Abbildung 8) [62].

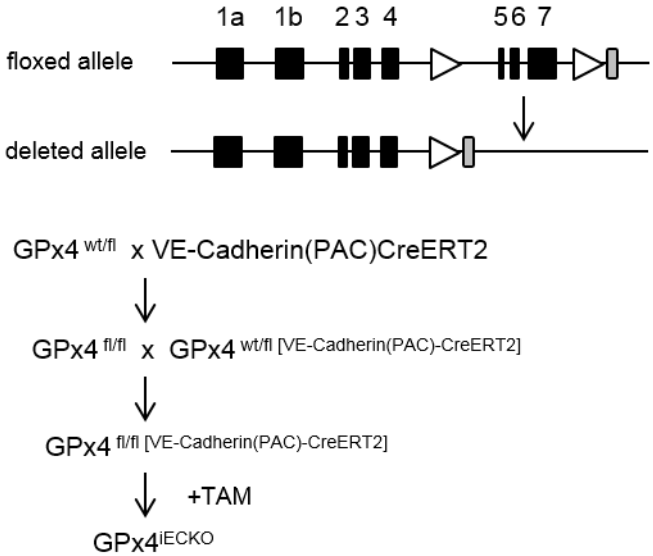

Abbildung 8: Knockout Strategie der induzierbaren, endothelspezifischen Gpx4-Knockout Mäuse.

Die Exons 5-7 des Gpx4 Gens sind mit sogenannten „loxP"-Sequenzen flankiert. Durch Zugabe von Tamoxifen kann die Cre-Rekombinase, die vorher durch die MER-Proteine blockiert und somit im Zytosol gehalten wird, in den Zellkern übertreten und den Knockout induzieren. Durch den Cdh-5 Promoter wird erreicht, dass die Cre-Rekombinase nur in Endothelzellen expremiert wird.

Um die Effektivität des Knockout Modells zu quantifizieren wurden Endothelzellen aus Herz und Lunge isoliert und mittels Western Blot die Gpx4-Proteinmenge bestimmt. Der endothelspezifische Knockout führt zu einer circa 75%igen Reduktion der Gpx4-Expression. Dass keine komplette Reduktion der Proteinmenge erreicht werden konnte, liegt daran, dass die Knockout-Induktion durch das „cre-loxP"-System nicht zu einem vollkommenen Knockout führt [62, 63]. Zudem gelingt die Isolierung der Endothelzellen mit dem auf magnetischer Wirkung basierenden „MACS Cell Separation" System nicht in absoluter Reinheit.

Da für verschiedene Zelllinien *in vitro* bereits gezeigt werden konnte, dass ein Gpx4-Knockout zum Zelltod führt [3, 64], wurde primär ein starker Effekt des endothelialen Gpx4-Knockouts im Gefäßsystem der Tiere *in vivo* erwartet. Andererseits könnte man auch in Analogie zu den Gpx4-defizienten Tumorzellen mit ihrer erhöhten bFGF-Sezernierung vermuten, dass es auch in Endothelzellen zu einer verstärkten bFGF-Sekretion kommt und dadurch angiogene Prozesse stimuliert werden [65].

Überraschenderweise zeigten die Gpx4^{iECKO}-Mäuse nach Tamoxifen-induzierter Gpx4-Deletion über einen Beobachtungszeitraum von insgesamt 6 Monaten keinen offensichtlichen Phänotyp, weder in Hinsicht auf das Überleben noch in Bezug auf die Morphologie der Blutgefäße. Letzteres wurde mittels verschiedener histologischer und immunhistochemischer Färbungen analysiert. Explantierte und in Matrigel eingebettete Ringe der thorakalen Aorta aus den Gpx4^{iECKO}-Mäusen bildeten jedoch weniger und kürzere Gefäßaussprossungen im sogenannten *ex vivo* „Aortic Ring" Modell (Abbildung 9). Dies wurde als Hinweis auf einen endothelialen Funktionsdefekt gedeutet.

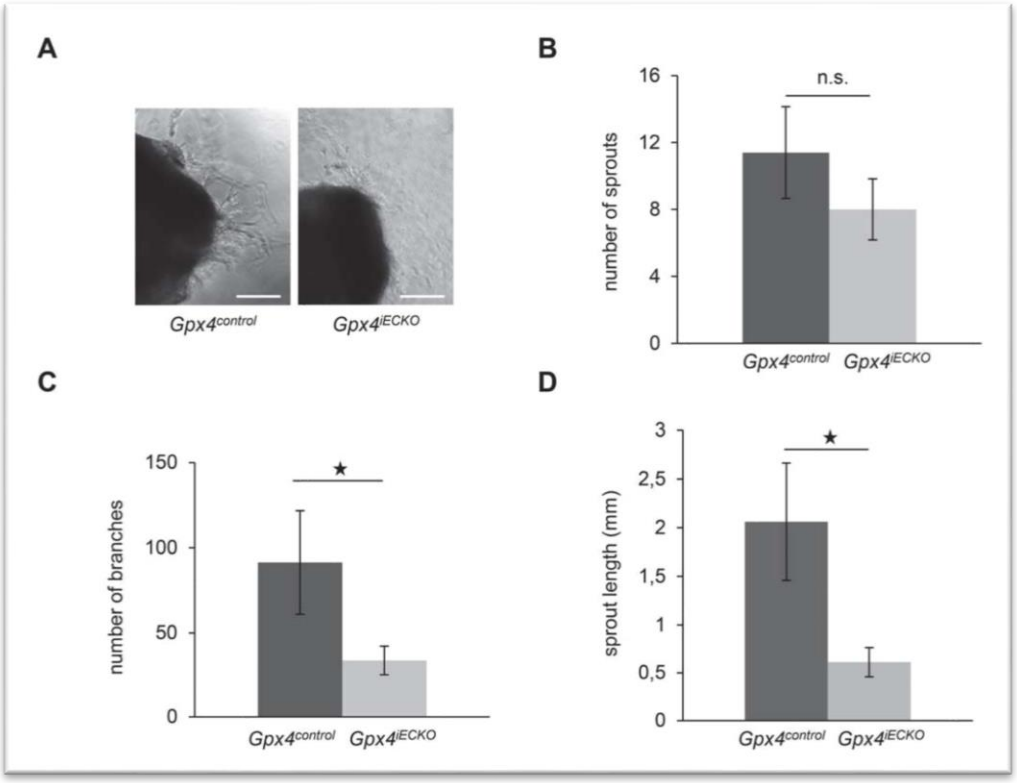

Abbildung 9: Aortic Rings als ex vivo Modell für Angiogenese.

Ringe aus der thorakalen Aorta werden explantiert und in Matrigel eingebettet (A). Die Ringe aus Gpx4^{iECKO}-Mäusen bilden zwar dieselbe Anzahl an Aussprossungen, diese sind aber signifikant kürzer (D) und bilden weniger Verzweigungen (C).

Um diese divergente Situation mit dem fehlenden Phänotyp *in vivo* und endothelialer Funktionseinschränkung *ex vivo* näher zu analysieren, wurden aus Mausembryonen „embryonale endotheliale Vorläuferzellen (embryonic Endothelial Progenitor Cells, eEPCs)“ isoliert und als Ersatz für die nur in begrenztem Ausmaß gewinn- und kultivierbaren Gefäß-Endothelzellen in Zellkultur weiter untersucht. Wie auch in verschiedenen anderen Zelllinien starben die eEPCs, sobald der Gpx4-Knockout in Kultur induziert wurde. Dieser Zelltod konnte durch eine Substitution des Zellkulturmediums mit TROLOX, einem wasserlöslichen Derivat von Vitamin E, effektiv verhindert werden. Somit verhielten sich die endothelialen Progenitorzellen unter *in vitro* Bedingungen idem zu anderen Zelllinien mit Gpx4-Knockout [3, 64].

In diesem Kontext ist es von Bedeutung, dass die Mausdiät, die zur Aufzucht und Fütterung der Versuchstiere verwendet wurde, hochgradig mit verschiedenen Vitaminen, unter anderem auch Vitamin E, angereichert war.

Mit der Hypothese, dass der hohe Vitamin E Gehalt in der Standarddiät die Mäuse vor

dem Effekt des endothelialen Gpx4-Knockout schützt, wurden Gpx4^{iECKO}-Mäuse für mehrere Monate auf eine Vitamin E-Mangeldiät gesetzt, bevor der Knockout induziert wurde.

Unter diesen Bedingungen konnten nun, analog zur Vitamin E-Mangel Situation in den *in vitro* Experimenten, deutliche Effekte beobachtet werden. Im Gegensatz zu den Kontroll-Knockout-Tieren starben circa 80% der Gpx4^{iECKO}-Mäuse unter Vitamin E-Mangeldiät innerhalb der ersten beiden Wochen nach Knockout-Induktion (Abbildung 10).

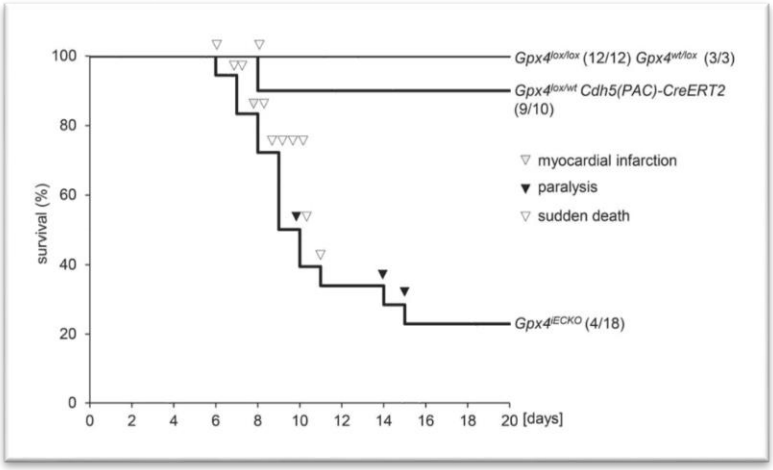

Abbildung 10: Die Induktion des endothelspezifischen Gpx4-Knockouts unter Vitamin E-Mangel führt zum Tod.

Im Vergleich zu den Kontrollgruppen (Gpx4$^{lox/lox}$, Gpx4$^{wt/lox}$ und Gpx4$^{lox/wt}$) führt die Induktion des endothelspezifischen Knockouts (Gpx4^{iECKO}) innerhalb von 2 Wochen bei circa 80% der Knockout-Mäuse zum Tod.

Die histologischen Analysen zeigten Thromben in multiplen Organen, die dann wiederum zu makroskopisch sichtbaren Infarkten führten. Mittels einer sogenannten TUNEL-Färbung konnten lokal auftretende, einzelne apoptotische Endothelzellen als mögliche Ursache der Thromben ausgemacht werden. Anhand elektronenmikroskopischer Aufnahmen der Aorta sowie der Nierenglomeruli konnte gezeigt werden, dass der endothelzellspezifische Gpx4-Knockout zu einem partiellen Ablösen einzelner Endothelzellen von der Basalmembran führt (Abbildung 11). Apoptotische Endothelzellen wiederum sind pro-thrombogen, nicht nur weil durch ihre Ablösung die Basalmembran freiliegt und dort lokal Thromben entstehen können, sondern auch, weil *in situ* befindliche, apoptotosische Endothelzellen weniger

antithrombogene Moleküle exprimieren [66].

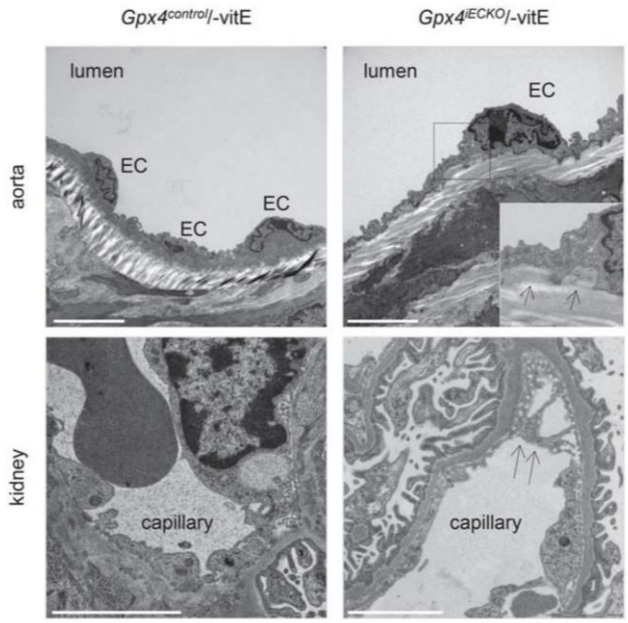

Abbildung 11: Elektronenmikroskopische Aufnahmen der Aorta und der Nieren.
In den Aorten und Nierenglomeruli der Gpx4^{iECKO}-Mäuse zeigte sich ein partielles Ablösen der Endothelzellen.

Durch die Verwendung von Knockout-Systemen, die auf der Verwendung der Cre-Rekombinase basieren, können jedoch auch unspezifische, teilweise letale Schäden verursacht werden [67].
Um auszuschließen, dass der letale Phänotyp des endothelzellspezifischen Gpx4-Knockouts unter Vitamin E-Mangel nicht auf einem Nebeneffekt der Cre-Rekombinase beruht, wurde ein zusätzliches Langzeit-Experiment durchgeführt. Hierbei wurde zuerst unter normaler, Vitamin E reicher Diät der Knockout induziert. Nach 6 Wochen Wartezeit, in denen sich die Mäuse von möglichen unspezifischen Effekten der Cre-Rekombinase-Induktion erholen konnten, erfolgte das Umsetzen auf eine Vitamin E-Mangeldiät. Hierbei starben während der Beobachtungszeit von 12 Wochen insgesamt 40% der Tiere (Abbildung 12).

Für diesen abgeschwächten Phänotyp gibt es zwei mögliche Erklärungen. Einerseits könnten sich die Mäuse während der Zeit unter der protektiven Vitamin E reichen Diät potentiell an den endothelspezifischen Gpx4-Knockout partiell adaptiert haben, da der akute oxidative Stress in der Phase der Induktion des Gpx4-Knockouts möglicherweise durch Vitamin E abgefangen wurde. Andererseits wäre es möglich, dass die hohe Letalität bei einer Induktion des Knockouts unter einer bereits bestehenden Vitamin E-Mangeldiät eine Kombination des Schadens durch den Gpx4-Knockout und die

unspezifischen Nebenwirkungen der Cre-Rekombinase ist. Diese Frage lässt sich jedoch im Rahmen dieser Experimente nicht eindeutig beantworten.

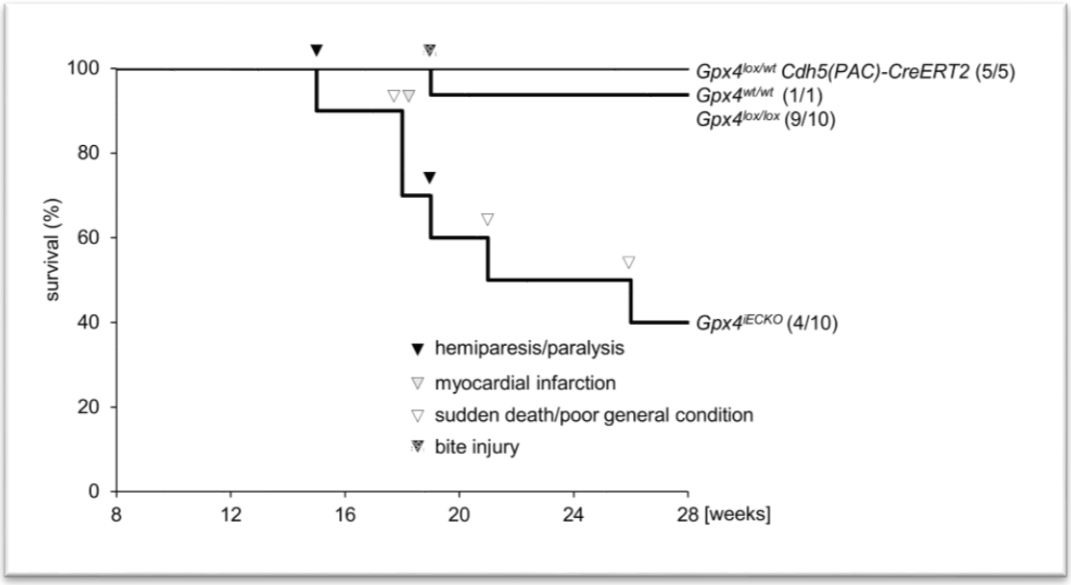

Abbildung 12: Die Adaptation an den Knockout führt zu einem abgeschwächten Phänotyp.

Wird der endothelspezifische Gpx4-Knockout unter einer Vitamin E reichen Diät induziert und die Mäuse sekundär auf eine Vitamin E-Mangeldiät umgesetzt, sterben deutlich weniger $Gpx4^{iECKO}$-Mäuse als bei Knockout-Induktion unter Vitamin E-Mangeldiät.

Auf eine genaue Quantifizierung des Vitamin E-Spiegels unter der verwendeten Vitamin E-Mangeldiät musste in diesem Projekt verzichtet werden, da dies technisch sehr aufwendig ist und zudem eine ungleiche Verteilung von Vitamin-E in verschiedenen Organen vorliegt. Aus Studien ist jedoch bekannt, dass eine Vitamin E-Mangeldiät für 14 Wochen zu einer circa 70%igen Reduktion des Vitamin-E Spiegels im Blut [68] beziehungsweise zu einer circa 80%igen Reduktion in Lysaten der Haut führt [69]. Limitierend muss hier jedoch angemerkt werden, dass es keine standardisierte Vitamin E-Mangeldiät gibt und der Vitamin E-Gehalt der verwendeten Spezialdiäten oftmals nur unzureichend bekannt ist und sich somit von Studie zu Studie auch unterscheiden kann.

Zusammenfassend führte der endothelzellspezifische Gpx4-Knockout bei Mäusen unter Vitamin E-Mangeldiät zu einer vermehrten Apoptose von Endothelzellen und somit zumindest fokal zu einem direkten Kontakt des Blutes mit der stark thrombogenen Basalmembran. Durch die sich entwickelnden Thromben entstanden multiple Infarkte in verschiedenen Organen, die zu unterschiedlichen Krankheitsbildern (wie Lähmungserscheinungen und Niereninfarkten) oder zum Tod der Mäuse führten.

Unter einer Diät mit hohem Vitamin E-Gehalt zeigen dieselben Mäuse dagegen keinen nachweisbaren Phänotyp. Ein hoher Vitamin E-Spiegel kann also den endothelzellschädigenden Effekt des endothelialen Gpx4-Knockouts verhindern.
Somit konnte erstmals gezeigt werden, dass bei einem endothelialem Gpx4-Mangel ein ausreichender Vitamin E-Spiegel vonnöten ist, um die Endothelfunktion aufrecht zu erhalten und lebensbedrohliche thromboembolische Krankheitsbilder zu verhindern.

3 Zusammenfassung

Während Sauerstoffradikalen früher lediglich eine toxische Funktion zugeschrieben wurde, ist inzwischen bekannt, dass sie auch eine wichtige physiologische Bedeutung haben. In eng regulierten Konzentrationsbereichen kontrollieren sie nicht nur die Differenzierung von Zellen, sondern auch deren Proliferation, Seneszenz und Apoptose [17, 53].

Vermehrtem oxidativen Stress, im Sinne einer erhöhten Konzentration an Sauerstoffradikalen, sei es durch eine vermehrte Bildung oder eine verringerte Reduktion durch antioxidative Enzyme, wird jedoch pathophysiologisch eine kausale Rolle bei vielen verschiedenen, meist chronisch inflammatorischen Erkrankungen beigemessen. Als Beispiele sind hier Krebserkrankungen [70], Diabetes mellitus [71] und neurodegenerative Erkrankungen [72] aufzuführen. Auch die Zellalterung wird zu großen Teilen einer chronischen Schädigung durch Sauerstoffradikale zugeschrieben [73].

Des Weiteren werden auch eine Reihe kardiovaskulärer Erkrankungen, wie zum Beispiel arterieller Hypertonus und Atherosklerose, mit einem erhöhten oxidativen Stress in Zusammenhang gebracht.

Dennoch haben klinische Studien mit Antioxidantien zur Therapie von kardiovaskulären Erkrankungen bislang keinen Vorteil erbracht [51], in einigen Studien haben sich sogar nachteilige Effekte gezeigt. Eine mögliche Erklärung wäre, dass durch eine ungezielte Therapie die Konzentration unterschiedlicher ROS so verändert wird, dass auch deren physiologische Funktion als kurzlebige Signalmoleküle gestört wird.

Aus diesem Grund ist eine differenzierte Erforschung der spezifischen Funktionen einzelner Redox-Enzyme notwendig. Dies dient sowohl dem Verständnis ihrer physiologischen Bedeutung als auch der Rolle, die sie in der Pathophysiologie verschiedener Erkrankungen spielen. Eine gezieltere antioxidative Therapie könnte dann in Zukunft auch bessere Ergebnisse bei der Primär- und Sekundärprophylaxe verschiedener Krankheitsbilder ermöglichen.

Die Gpx4 unterscheidet sich von anderen antioxidativen Enzymen insbesondere dadurch, dass sie das einzige bekannte Enzym ist, welches oxidierte Phospholipide oder Cholesterine reduzieren kann, selbst wenn diese in komplexen Makromolekülen integriert sind. Zudem hat die Gpx4 einen regulierenden Einfluss auf den Arachidonsäurestoffwechsel und verschiedene physiologische Signalwege, wie zum Beispiel Rezeptor-Tyrosinkinasen oder die AIF-vermittelte Apoptose.
Über die Rolle der Gpx4 im Gefäßsystem liegen jedoch nur wenige Informationen vor.

Im ersten Teilprojekt wurde der Effekt eines Gpx4-Knockouts in transformierten Fibroblasten auf die Tumorangiogenese untersucht. Hierbei kommt es über einen 12/15-Lipoxygenase vermittelten Signalweg zu einer verringerte Sekretion von VEGF-A in Kombination mit einer erhöhten Sekretion von bFGF. Dies führt zwar zu keiner Änderung der Tumorgröße im Vergleich zu Kontrolltumoren; jedoch hat der Gpx4-Knockout einen Einfluss auf die Tumorgefäße. Diese weisen eine veränderte Morphologie mit kleineren Gefäßlumina sowie einer reduzierten Anzahl an αSMA-positiven Zellen auf.

Im Allgemeinen zeigt das durch solide Tumore zur Blutversorgung akquirierte Tumorgefäßnetzwerk im Vergleich zu normalen Gefäßen eine Vielzahl von Unterschieden. Unter anderem sind die Tumorgefäße oft dilatiert und korkenzieherartig gewunden, zeigen eine höhere Permeabilität und auch die Endothelzellen und glatten Muskelzellen weisen deutliche morphologische Unterschiede auf [74]. Der Normalisierung des Tumorgefäßnetzwerkes wird in der modernen Tumortherapie eine steigende Bedeutung zugerechnet, weil durch eine Reduktion der unphysiologisch hohen Permeabilität eine Reduktion der Metastasierung erreicht werden kann. Ebenso verbessert sich die Anflutung und Verteilung von systemisch verabreichten Chemotherapeutika und somit deren Wirksamkeit [75].

In diesem Kontext konnte gezeigt werden, dass die Gpx4 zu einer partiellen Normalisierung der Tumorgefäße beiträgt.

Eine Erklärung für dieselbe Tumorgröße trotz des durch den Gpx4-Knockout veränderten Gefäßsystems könnte sein, dass Gpx4 auch in den Tumorzellen selbst wichtige Signalwege steuert und somit das Tumorwachstum beeinflusst [76]. Die

genaue Rolle der Gpx4 in der Tumorprogression ist bislang unbekannt, wobei vorwiegend ein inhibitorischer Effekt auf das Tumorwachstum postuliert wird [77]. Erschwerend kommt hinzu, dass die Gpx4 in verschiedenen Tumorzelllinien unterschiedlichen Einfluss auf das Tumorwachstum hat [76] und dieser zusätzlich von der Phase des Tumorwachstums abhängig ist [77].

Im zweiten Teilprojekt konnte gezeigt werden, dass eine Kombination aus einem endothelzellspezifischen Knockout von Gpx4 und Vitamin E-Mangel zu lebensbedrohlichen Thrombosen im Mausmodell führt. Durch eine ausreichende Vitamin E-Gabe kann dieser Phänotyp komplett verhindert werden.

Obwohl mehrere Studien keine eindeutigen Effekte einer Vitamin E-Therapie auf die Inzidenz von kardiovaskulären Erkrankungen gezeigt haben [51, 78], konnte in der „Women's Health Study" ein protektiver Effekt einer Vitamin E-Supplementierung bezüglich venöser Thrombosen nachgewiesen werden. Dies war vor allem bei Frauen relevant, die in der Vorgeschichte bereits eine Thrombose erlitten hatten [79].
In diesem Zusammenhang wären weitere umfangreiche klinische Studien notwendig, um Patienten mit Funktionseinschränkungen der Gpx4 zu selektieren und zu verifizieren, ob diese wirklich von einer Vitamin E-Gabe profitieren.

Da Mäuse mit einem endothelzellspezifischen Gpx4-Knockout eine endotheliale Dysfunktion aufweisen und dies einer der Hauptursachen für die Entstehung von Plaques ist, liegt eine Beteiligung der Gpx4 an der Entstehung von Atherosklerose nahe. Eine Überexpression von Gpx4 im Mausmodell reduziert wie erwartet die Bildung von atherosklerotischen Läsionen [80]. Auch in der Pathophysiologie der Atherosklerose spielt die Angiogenese eine wichtige Rolle [81]; die letztendliche Bedeutung der Gefäßneubildung bei dieser Erkrankung bleibt jedoch unklar. So kann ein positiver Effekt denkbar sein, wenn zum Beispiel hochgradige Stenosen durch die Ausbildung von Kollateralkreisläufen kompensiert werden. Andererseits führt das vermehrte Einwachsen von Gefäßen in atherosklerotische Plaques zu einer erhöhten Rupturgefahr [81].
Obwohl der Effekt des Gpx4-Knockouts in den transformierten Fibroblasten auf die Tumorangiogenese nicht direkt auf die Angiogenese im Zuge atherosklerotische Prozesse übertragen werden kann, ist eine Rolle der Gpx4 in diesem Kontext absolut

denkbar.
So geht zum Beispiel die Sekretion von bFGF durch Mastzellen mit einer erhöhten Angiogenese in atherosklerotischen Plaques einher [82]. Auch hier könnte die Gpx4 einen regulatorischen Einfluss haben.
Sollten sich die Erkenntnisse der bFGF-Regulation durch Gpx4 auch bei kardiovaskulären Erkrankungen bestätigen, würde dies unter Umständen eine doppelte Bedeutung der Gpx4 bei diesen Erkrankungen nahelegen: Einerseits spielt die Gpx4 eine Rolle bei der endothelialen Dysfunktion, andererseits wäre eine Regulation der Angiogenese durch Gpx4 denkbar. Um die genaue Funktion der Gpx4 in diesem Rahmen weiter zu spezifizieren sind jedoch weitere Studien notwendig.

Zusammenfassend wurden im Rahmen dieser Dissertationsarbeit sowohl der direkte Effekt eines Gpx4-Knockouts im adulten Endothel selbst, als auch der Effekt eines Gpx4-Knockouts in transformierten Fibroblasten auf das proliferierende Tumorgefäßsystem untersucht.
Dies trägt zum weiteren Verständnis der komplexen pathophysiologischen Einflüsse einer mangelnden Gpx4-Aktivität und der damit einhergehenden erhöhten Lipidperoxidation auf das Gefäßsystem bei.
Da die Gpx4 neben der antioxidative Funktion auch eine Vielzahl spezifischer Funktionen hat, ist ein genaues Verständnis der Funktion der Gpx4 in einzelnen Zelltypen notwendig, um neue, antioxidative Therapieformen für Gefäßerkrankungen zu entwickeln.

4 Literaturverzeichnis

1. Brigelius-Flohe, R. and M. Maiorino, *Glutathione peroxidases.* Biochim Biophys Acta, 2013. **1830**(5): p. 3289-303.
2. Hawkes, W.C. and Z. Alkan, *Regulation of redox signaling by selenoproteins.* Biol Trace Elem Res, 2010. **134**(3): p. 235-51.
3. Seiler, A., et al., *Glutathione peroxidase 4 senses and translates oxidative stress into 12/15-lipoxygenase dependent- and AIF-mediated cell death.* Cell Metab, 2008. **8**(3): p. 237-48.
4. Tosatto, S.C., et al., *The catalytic site of glutathione peroxidases.* Antioxid Redox Signal, 2008. **10**(9): p. 1515-26.
5. Toppo, S., et al., *Evolutionary and structural insights into the multifaceted glutathione peroxidase (Gpx) superfamily.* Antioxid Redox Signal, 2008. **10**(9): p. 1501-14.
6. Maiorino, M., et al., *Probing the presumed catalytic triad of a selenium-containing peroxidase by mutational analysis.* Z Ernahrungswiss, 1998. **37 Suppl 1**: p. 118-21.
7. McClung, J.P., et al., *Development of insulin resistance and obesity in mice overexpressing cellular glutathione peroxidase.* Proc Natl Acad Sci U S A, 2004. **101**(24): p. 8852-7.
8. Al-Taie, O.H., et al., *Expression profiling and genetic alterations of the selenoproteins GI-GPx and SePP in colorectal carcinogenesis.* Nutr Cancer, 2004. **48**(1): p. 6-14.
9. Woenckhaus, M., et al., *Smoking and cancer-related gene expression in bronchial epithelium and non-small-cell lung cancers.* J Pathol, 2006. **210**(2): p. 192-204.
10. Banning, A., et al., *Glutathione Peroxidase 2 Inhibits Cyclooxygenase-2-Mediated Migration and Invasion of HT-29 Adenocarcinoma Cells but Supports Their Growth as Tumors in Nude Mice.* Cancer Res, 2008. **68**(23): p. 9746-53.
11. Whitin, J.C., et al., *Extracellular glutathione peroxidase is secreted basolaterally by human renal proximal tubule cells.* Am J Physiol Renal Physiol, 2002. **283**(1): p. F20-8.
12. Burk, R.F., et al., *Glutathione peroxidase-3 produced by the kidney binds to a population of basement membranes in the gastrointestinal tract and in other tissues.* Am J Physiol Gastrointest Liver Physiol, 2011. **301**(1): p. G32-8.
13. Olson, G.E., et al., *Extracellular glutathione peroxidase (Gpx3) binds specifically to basement membranes of mouse renal cortex tubule cells.* Am J Physiol Renal Physiol, 2010. **298**(5): p. F1244-53.
14. Chabory, E., et al., *Epididymis seleno-independent glutathione peroxidase 5 maintains sperm DNA integrity in mice.* J Clin Invest, 2009. **119**(7): p. 2074-85.
15. Tanaka, C., et al., *Expression pattern of oxidative stress and antioxidant defense-related genes in the aging Fischer 344/NHsd rat cochlea.* Neurobiol Aging, 2012. **33**(8): p. 1842 e1-14.
16. Xu, X., et al., *Reactive oxygen species-triggered trophoblast apoptosis is initiated by endoplasmic reticulum stress via activation of caspase-12, CHOP, and the JNK pathway in Toxoplasma gondii infection in mice.* Infect Immun, 2012. **80**(6): p. 2121-32.
17. Brigelius-Flohe, R. and L. Flohe, *Basic principles and emerging concepts in the redox control of transcription factors.* Antioxid Redox Signal, 2011. **15**(8): p. 2335-81.
18. Ursini, F., et al., *Purification from pig liver of a protein which protects liposomes and biomembranes from peroxidative degradation and exhibits glutathione peroxidase activity on phosphatidylcholine hydroperoxides.* Biochim Biophys Acta, 1982. **710**(2): p. 197-211.
19. Thomas, J.P., et al., *Protective action of phospholipid hydroperoxide glutathione peroxidase against membrane-damaging lipid peroxidation. In situ reduction of phospholipid and cholesterol hydroperoxides.* J Biol Chem, 1990. **265**(1): p. 454-61.

20. Maiorino, M., et al., *Reactivity of phospholipid hydroperoxide glutathione peroxidase with membrane and lipoprotein lipid hydroperoxides.* Free Radic Res Commun, 1991. **12-13 Pt 1**: p. 131-5.
21. Ursini, F., M. Maiorino, and C. Gregolin, *The selenoenzyme phospholipid hydroperoxide glutathione peroxidase.* Biochim Biophys Acta, 1985. **839**(1): p. 62-70.
22. Ursini, F., M. Maiorino, and A. Roveri, *Phospholipid hydroperoxide glutathione peroxidase (PHGPx): more than an antioxidant enzyme?* Biomed Environ Sci, 1997. **10**(2-3): p. 327-32.
23. Brigelius-Flohe, R., et al., *Phospholipid-hydroperoxide glutathione peroxidase. Genomic DNA, cDNA, and deduced amino acid sequence.* J Biol Chem, 1994. **269**(10): p. 7342-8.
24. Schneider, M., et al., *Embryonic expression profile of phospholipid hydroperoxide glutathione peroxidase.* Gene Expr Patterns, 2006. **6**(5): p. 489-94.
25. Pushpa-Rekha, T.R., et al., *Rat phospholipid-hydroperoxide glutathione peroxidase. cDNA cloning and identification of multiple transcription and translation start sites.* J Biol Chem, 1995. **270**(45): p. 26993-9.
26. Schneider, M., et al., *Mitochondrial glutathione peroxidase 4 disruption causes male infertility.* FASEB J, 2009. **23**(9): p. 3233-42.
27. Moreno, S.G., et al., *Testis-specific expression of the nuclear form of phospholipid hydroperoxide glutathione peroxidase (PHGPx).* Biol Chem, 2003. **384**(4): p. 635-43.
28. Pfeifer, H., et al., *Identification of a specific sperm nuclei selenoenzyme necessary for protamine thiol cross-linking during sperm maturation.* FASEB J, 2001. **15**(7): p. 1236-8.
29. Conrad, M., et al., *The nuclear form of phospholipid hydroperoxide glutathione peroxidase is a protein thiol peroxidase contributing to sperm chromatin stability.* Mol Cell Biol, 2005. **25**(17): p. 7637-44.
30. Borchert, A., N.E. Savaskan, and H. Kuhn, *Regulation of expression of the phospholipid hydroperoxide/sperm nucleus glutathione peroxidase gene. Tissue-specific expression pattern and identification of functional cis- and trans-regulatory elements.* J Biol Chem, 2003. **278**(4): p. 2571-80.
31. Ho, Y.S., et al., *Mice deficient in cellular glutathione peroxidase develop normally and show no increased sensitivity to hyperoxia.* J Biol Chem, 1997. **272**(26): p. 16644-51.
32. Ho, Y.S., et al., *Mice lacking catalase develop normally but show differential sensitivity to oxidant tissue injury.* J Biol Chem, 2004. **279**(31): p. 32804-12.
33. Sato, H., et al., *Redox imbalance in cystine/glutamate transporter-deficient mice.* J Biol Chem, 2005. **280**(45): p. 37423-9.
34. Yant, L.J., et al., *The selenoprotein GPX4 is essential for mouse development and protects from radiation and oxidative damage insults.* Free Radic Biol Med, 2003. **34**(4): p. 496-502.
35. Yoo, S.E., et al., *Gpx4 ablation in adult mice results in a lethal phenotype accompanied by neuronal loss in brain.* Free Radic Biol Med, 2012. **52**(9): p. 1820-7.
36. Weitzel, F. and A. Wendel, *Selenoenzymes regulate the activity of leukocyte 5-lipoxygenase via the peroxide tone.* J Biol Chem, 1993. **268**(9): p. 6288-92.
37. Sutherland, M., et al., *Evidence for the presence of phospholipid hydroperoxide glutathione peroxidase in human platelets: implications for its involvement in the regulatory network of the 12-lipoxygenase pathway of arachidonic acid metabolism.* Biochem J, 2001. **353**(Pt 1): p. 91-100.
38. Imai, H., et al., *Suppression of leukotriene formation in RBL-2H3 cells that overexpressed phospholipid hydroperoxide glutathione peroxidase.* J Biol Chem, 1998. **273**(4): p. 1990-7.
39. Conrad, M., et al., *12/15-lipoxygenase-derived lipid peroxides control receptor tyrosine kinase signaling through oxidation of protein tyrosine phosphatases.* Proc Natl Acad Sci U S A, 2010. **107**(36): p. 15774-9.
40. Brigelius-Flohe, R., et al., *Interleukin-1-induced nuclear factor kappa B*

activation is inhibited by overexpression of phospholipid hydroperoxide glutathione peroxidase in a human endothelial cell line. Biochem J, 1997. **328 (Pt 1)**: p. 199-203.
41. Widlansky, M.E., et al., *The clinical implications of endothelial dysfunction.* J Am Coll Cardiol, 2003. **42**(7): p. 1149-60.
42. Montezano, A.C. and R.M. Touyz, *Reactive oxygen species, vascular Noxs, and hypertension: focus on translational and clinical research.* Antioxid Redox Signal, 2014. **20**(1): p. 164-82.
43. Cai, H. and D.G. Harrison, *Endothelial dysfunction in cardiovascular diseases: the role of oxidant stress.* Circ Res, 2000. **87**(10): p. 840-4.
44. De Keulenaer, G.W., et al., *Oscillatory and steady laminar shear stress differentially affect human endothelial redox state: role of a superoxide-producing NADH oxidase.* Circ Res, 1998. **82**(10): p. 1094-101.
45. Hsieh, H.J., et al., *Shear-induced endothelial mechanotransduction: the interplay between reactive oxygen species (ROS) and nitric oxide (NO) and the pathophysiological implications.* J Biomed Sci, 2014. **21**: p. 3.
46. Sugamura, K. and J.F. Keaney, Jr., *Reactive oxygen species in cardiovascular disease.* Free Radic Biol Med, 2011. **51**(5): p. 978-92.
47. Rajagopalan, S., et al., *Angiotensin II-mediated hypertension in the rat increases vascular superoxide production via membrane NADH/NADPH oxidase activation. Contribution to alterations of vasomotor tone.* J Clin Invest, 1996. **97**(8): p. 1916-23.
48. Rueckschloss, U., N. Duerrschmidt, and H. Morawietz, *NADPH oxidase in endothelial cells: impact on atherosclerosis.* Antioxid Redox Signal, 2003. **5**(2): p. 171-80.
49. Virdis, A., et al., *Role of NAD(P)H oxidase on vascular alterations in angiotensin II-infused mice.* J Hypertens, 2004. **22**(3): p. 535-42.
50. Redon, J., et al., *Antioxidant activities and oxidative stress byproducts in human hypertension.* Hypertension, 2003. **41**(5): p. 1096-101.
51. Wingler, K. and H.H. Schmidt, *Good stress, bad stress--the delicate balance in the vasculature.* Dtsch Arztebl Int, 2009. **106**(42): p. 677-84.
52. Touyz, R.M., *Reactive oxygen species, vascular oxidative stress, and redox signaling in hypertension: what is the clinical significance?* Hypertension, 2004. **44**(3): p. 248-52.
53. Droge, W., *Free radicals in the physiological control of cell function.* Physiol Rev, 2002. **82**(1): p. 47-95.
54. Brigelius-Flohe, R., A. Banning, and K. Schnurr, *Selenium-dependent enzymes in endothelial cell function.* Antioxid Redox Signal, 2003. **5**(2): p. 205-15.
55. Gorlach, A. and T. Kietzmann, *Superoxide and derived reactive oxygen species in the regulation of hypoxia-inducible factors.* Methods Enzymol, 2007. **435**: p. 421-46.
56. Feil, R., et al., *Regulation of Cre recombinase activity by mutated estrogen receptor ligand-binding domains.* Biochem Biophys Res Commun, 1997. **237**(3): p. 752-7.
57. Kleinman, H.K. and G.R. Martin, *Matrigel: basement membrane matrix with biological activity.* Semin Cancer Biol, 2005. **15**(5): p. 378-86.
58. Sen, M., et al., *Orthotopic expression of human 15-lipoxygenase (LO)-1 in the dorsolateral prostate of normal wild-type C57BL/6 mouse causes PIN-like lesions.* Prostaglandins Other Lipid Mediat, 2006. **81**(1-2): p. 1-13.
59. Giavazzi, R., et al., *Distinct role of fibroblast growth factor-2 and vascular endothelial growth factor on tumor growth and angiogenesis.* Am J Pathol, 2003. **162**(6): p. 1913-26.
60. Giavazzi, R., et al., *Modulation of tumor angiogenesis by conditional expression of fibroblast growth factor-2 affects early but not established tumors.* Cancer Res, 2001. **61**(1): p. 309-17.
61. D'Amato, R.J., et al., *Thalidomide is an inhibitor of angiogenesis.* Proc Natl Acad Sci U S A, 1994. **91**(9): p. 4082-5.
62. Wang, Y., et al., *Ephrin-B2 controls VEGF-induced angiogenesis and lymphangiogenesis.* Nature, 2010. **465**(7297): p. 483-6.

63. Hara-Kaonga, B., et al., *Variable recombination efficiency in responder transgenes activated by Cre recombinase in the vasculature.* Transgenic Res, 2006. **15**(1): p. 101-6.
64. Schneider, M., et al., *Absence of glutathione peroxidase 4 affects tumor angiogenesis through increased 12/15-lipoxygenase activity.* Neoplasia, 2010. **12**(3): p. 254-63.
65. Gualandris, A., et al., *Basic fibroblast growth factor overexpression in endothelial cells: an autocrine mechanism for angiogenesis and angioproliferative diseases.* Cell Growth Differ, 1996. **7**(2): p. 147-60.
66. Bombeli, T., et al., *Apoptotic vascular endothelial cells become procoagulant.* Blood, 1997. **89**(7): p. 2429-42.
67. Naiche, L.A. and V.E. Papaioannou, *Cre activity causes widespread apoptosis and lethal anemia during embryonic development.* Genesis, 2007. **45**(12): p. 768-75.
68. Kamimura, W., et al., *Effect of vitamin E on alloxan-induced mouse diabetes.* Clin Biochem, 2013. **46**(9): p. 795-8.
69. Chi, C., et al., *Vitamin E-deficiency did not exacerbate partial skin reactions in mice locally irradiated with X-rays.* J Radiat Res, 2011. **52**(1): p. 32-8.
70. Cui, X., *Reactive oxygen species: the achilles' heel of cancer cells?* Antioxid Redox Signal, 2012. **16**(11): p. 1212-4.
71. Baynes, J.W., *Role of oxidative stress in development of complications in diabetes.* Diabetes, 1991. **40**(4): p. 405-12.
72. Federico, A., et al., *Mitochondria, oxidative stress and neurodegeneration.* J Neurol Sci, 2012. **322**(1-2): p. 254-62.
73. Harman, D., *Aging: a theory based on free radical and radiation chemistry.* J Gerontol, 1956. **11**(3): p. 298-300.
74. Goel, S., et al., *Normalization of the vasculature for treatment of cancer and other diseases.* Physiol Rev, 2011. **91**(3): p. 1071-121.
75. Jain, R.K., *Normalization of tumor vasculature: an emerging concept in antiangiogenic therapy.* Science, 2005. **307**(5706): p. 58-62.
76. Heirman, I., et al., *Blocking tumor cell eicosanoid synthesis by GP x 4 impedes tumor growth and malignancy.* Free Radic Biol Med, 2006. **40**(2): p. 285-94.
77. Brigelius-Flohe, R. and A. Kipp, *Glutathione peroxidases in different stages of carcinogenesis.* Biochim Biophys Acta, 2009. **1790**(11): p. 1555-68.
78. Kris-Etherton, P.M., et al., *Antioxidant vitamin supplements and cardiovascular disease.* Circulation, 2004. **110**(5): p. 637-41.
79. Glynn, R.J., et al., *Effects of random allocation to vitamin E supplementation on the occurrence of venous thromboembolism: report from the Women's Health Study.* Circulation, 2007. **116**(13): p. 1497-503.
80. Guo, X., et al., *Overexpression of peroxiredoxin 4 attenuates atherosclerosis in apolipoprotein E knockout mice.* Antioxid Redox Signal, 2012. **17**(10): p. 1362-75.
81. Khurana, R., et al., *Role of angiogenesis in cardiovascular disease: a critical appraisal.* Circulation, 2005. **112**(12): p. 1813-24.
82. Lappalainen, H., et al., *Mast cells in neovascularized human coronary plaques store and secrete basic fibroblast growth factor, a potent angiogenic mediator.* Arterioscler Thromb Vasc Biol, 2004. **24**(10): p. 1880-5.

5 Anhang

5.1 Publikationen

5.1.1 Absence of Glutathione Peroxidase 4 Affects Tumor Angiogenesis Through Increased 12/15-Lipoxygenase Activity.

Schneider M, **Wortmann M**, Mandal PK, Arpornchayanon W, Jannasch K, Alves F, Strieth S, Conrad M, Beck H.

Neoplasia. 2010 Mar;12(3):254-63.

NEOPLASIA
www.neoplasia.com

Volume 12 Number 3 March 2010 pp. 254–263 254

Absence of Glutathione Peroxidase 4 Affects Tumor Angiogenesis through Increased 12/15-Lipoxygenase Activity[1]

Manuela Schneider[*,†], Markus Wortmann[*], Pankaj Kumar Mandal[†], Warangkana Arpornchayanon[*,‡], Katharina Jannasch[§], Frauke Alves[§], Sebastian Strieth[‡], Marcus Conrad[†,2] and Heike Beck[*,2]

[*]Walter Brendel Center of Experimental Medicine, Ludwig-Maximilians-University, Munich, Germany; [†]Institute of Clinical Molecular Biology and Tumor Genetics, Helmholtz Zentrum München, German Research Center for Environmental Health, Munich, Germany; [‡]Department of Otorhinolaryngology, Ludwig-Maximilians-University, Munich, Germany; [§]Department of Hematology and Oncology, University Medicine Göttingen, Göttingen, Germany

Abstract

The selenoenzyme glutathione peroxidase 4 (GPx4) has been described to control specific cyclooxygenases (COXs) and lipoxygenases (LOXs) that exert substantiated functions in tumor growth and angiogenesis. Therefore, we hypothesized a putative regulatory role of GPx4 during tumor progression and created transformed murine embryonic fibroblasts with inducible disruption of GPx4. GPx4 inactivation caused rapid cell death *in vitro*, which could be prevented either by lipophilic antioxidants or by 12/15-LOX–specific inhibitors, but not by inhibitors targeting other LOX isoforms or COX. Surprisingly, transformed *GPx4*$^{+/-}$ cells did not die when grown in Matrigel but gave rise to tumor spheroids. Subcutaneous implantation of tumor cells into mice resulted in knockout tumors that were indistinguishable in volume and mass in comparison to wild-type tumors. However, further analysis revealed a strong vascular phenotype. We observed an increase in microvessel density as well as a reduction in the number of large diameter vessels covered by smooth muscle cells. This phenotype could be linked to increased 12/15-LOX activity that was accompanied by an up-regulation of basic fibroblast growth factor and down-regulation of vascular endothelial growth factor A protein expression. Indeed, pharmacological inhibition of 12/15-LOX successfully reversed the tumor phenotype and led to "normalized" vessel morphology. Thus, we conclude that GPx4, through controlling 12/15-LOX activity, is an important regulator of tumor angiogenesis as well as vessel maturation.

Neoplasia (2010) 12, 254–263

Abbreviations: αSMA, α-smooth muscle actin; bFGF, basic fibroblast growth factor; COX, cyclooxygenase; ECM, extracellular matrix; FITC, fluorescein isothiocyanate; fpVCT, flat-panel volume computed tomography; GPx4, glutathione peroxidase 4; HODE, hydroxy octadecadienoic acid; LOX, lipoxygenase; MEF, murine embryonic fibroblast; MTT, thiazolyl blue tetrazolium bromide; PlGF, placenta growth factor; TAM, 4-hydroxy-tamoxifen, tamoxifen; tMEF, transformed murine embryonic fibroblast; VEGF-A, vascular endothelial growth factor A

Address all correspondence to: Dr. Heike Beck, Walter Brendel Center of Experimental Medicine, Ludwig-Maximilians-University, Marchioninistr. 15, 81377 Munich, Germany. E-mail: heike.beck@med.uni-muenchen.de; or Dr. Marcus Conrad, Institute of Clinical Molecular Biology and Tumor Genetics, Helmholtz Zentrum München, German Research Center for Environmental Health, Marchioninistr. 25, 81377 Munich, Germany. E-mail: marcus.conrad@helmholtz-muenchen.de

[1]This work was supported by the DFG-Priority Programme SPP1190 to H.B., M.C., and F.A.

[2]These authors contributed equally to this work.

Received 19 October 2009; Revised 22 December 2009; Accepted 29 December 2009

DOI 10.1593/neo.91782

Introduction

The selenoenzyme glutathione peroxidase 4 (GPx4) was initially described as an important intracellular antioxidant enzyme for the protection of membranes by its unique capacity to reduce phospholipid hydroperoxides [1]. Later, GPx4 has been considered to be involved in eicosanoid synthesis by controlling cyclooxygenase (COX) and lipoxygenase (LOX) activities [2]. Because these enzymes require basal amounts of lipid hydroperoxides for their activation [3,4], the modulation of GPx4 activity should effectively influence COX and LOX activities and thus eicosanoid synthesis. Indeed, aberrant arachidonic acid metabolism has been demonstrated to play a crucial role in carcinogenesis and tumor angiogenesis [5]. Thus, pharmacological targeting of GPx4, which in turn influences arachidonic acid metabolism, can be considered as a promising strategy to interfere with the tumor-host communication. Yet, it has remained obscure if there is specificity of GPx4 toward distinct LOX and COX isoforms and if an unbalanced regulation of distinct enzymes may influence tumor development *in vivo* [6]. Our recent study using inducible inactivation of *GPx4* in cells and mice provided unequivocal evidence that GPx4 effectively prevents oxidative stress–induced cell death by specifically controlling 12/15-LOX [7,8]. The impact of 12/15-LOX (or the corresponding human ortholog 15-LOX-1) on carcinogenesis seems quite complex, and its role in cancer development and progression is controversially discussed [9]. 12/15-LOX shows increased expression in normal tissues and benign lesions, but not in carcinomas of the bladder, breast, colon, lung, or prostate [10–14]. However, other studies suggested that the 12/15-LOX product, 13-*S*-hydroxyoctadecadienoic acid (13-HODE), enhances colon carcinogenesis [15]. Moreover, 13-HODE has been shown to enhance cell proliferation and to potentiate the mitogenic response to epidermal growth factor (EGF) in different cell types such as BALB/c 3T3, Syrian hamster embryo (SHE) cells [16], as well as human pancreatic adenocarcinomas [16,17]. In addition, overexpression of the human ortholog 15-LOX-1 induces extracellular signal–related kinase 1/2 phosphorylation, decreased p21 (cip/WAF1) expression, and increased colon cancer growth [18]. Conversely, Kim et al. [19] described an antiproliferative effect of 15-LOX-1 in colorectal cancer cells associated with p53 phosphorylation. In line with these results, Shureiqi et al. reported that 13-HODE induces apoptosis and cell cycle arrest in colorectal cancer cells [20]. Studies analyzing the biological relevance of 12/15-LOX in the vascular system seem similarly inconsistent, and 12/15-LOX has been described to either promote or inhibit neovascularization. Here, we hypothesize a putative regulatory role of GPx4 during carcinogenesis. We strongly believe that our genetic model of inducible GPx4 disruption is an ideal model to study tumor progression and tumor angiogenesis in the context of modified linoleic acid metabolism because GPx4 ablation specifically leads to changes in 12/15-LOX activity.

Materials and Methods

Cell Line and Reagents

The 4-hydroxy-tamoxifen (TAM)–inducible *GPx4* knockout murine embryonic fibroblasts (MEFs) were used as described by Seiler et al. [7]. All cell culture reagents were purchased from Invitrogen (Karlsruhe, Germany). MEFs were cultured at 37°C under 5% CO_2 and 5% O_2 in Dulbecco's modified Eagle medium supplemented with 10% fetal bovine serum, 2 mM L-glutamine, 100 U/ml penicillin, and 100 μg/ml streptomycin. To maintain the viability of the cells after induction of GPx4 deletion by adding TAM, cells were always maintained in the presence of (±)-6-hydroxy-2,5,7,8-tetramethylchromane-2-carboxylic acid (Trolox; 1 μM, #56510; Sigma-Aldrich, Deisenhofen, Germany), a water-soluble analog of α-tocopherol (see MTT Assay for Cell Viability section). Tumor cells were harvested near confluence by brief trypsination in 0.25% trypsin/EDTA solution, washed several times, and placed in sterile phosphate-buffered saline (PBS) shortly before implantation. The pan-COX-inhibitor indomethacin (I7378), the pan-LOX-inhibitor NDGA (N5023), and the 12/15-LOX–specific inhibitors Baicalein (#465119) and PD146176 (P4620) as well as 4-hydroxy-tamoxifen (H7904) were purchased from Sigma-Aldrich. pBJ3Ω *c-Myc* and pUC EJ6.6 *Ha-ras*^{V12} were a kind gift from Dr. Hartmut Land. Each time before performing an *in vitro* or *in vivo* assay, GPx4-deleted cells were thoroughly washed with PBS to remove Trolox. Furthermore, an aliquot of the cells was checked for GPx4 expression by quantitative polymerase chain reaction (PCR; see below). As a second control, another aliquot was plated under normal cell culture conditions without adding Trolox, and cell death was analyzed within the next 48 to 72 hours (see below).

Transformation of Conditional GPx4-Deficient MEFs

For oncogenic transformation, *GPx4*-deficient MEFs were cotransduced with *c-Myc*– and *ha-ras*^{V12}–expressing lentiviruses. Soft agar assays were conducted to select for transformed cells. The assay was performed in 60-mm dishes (BD Falcon; Becton Dickinson, Heidelberg, Germany) containing two layers of soft agar. The top and bottom layers were 0.3% and 0.4% agarose, respectively, in Dulbecco's modified Eagle medium supplemented with 10% fetal bovine serum. A total of 2×10^4 of the *c-Myc*– and *ha-ras*–infected cells were added to the top layer before pouring. Single-cell colonies were isolated approximately 2 to 3 weeks after culturing at 37°C and 5% CO_2. Single-cell clones were individually expanded, and GPx4 deletion was tested later in each of the established cell lines by adding TAM (±Trolox) followed by analysis of GPx4 expression (see quantitative reverse transcription [RT]–PCR) and cell death, respectively (see MTT Assay for Cell Viability section).

Immunoblot Analysis

Cell lysates and tumor tissue lysates, protein concentration determination, and immunoblot analysis of GPx4 were performed as described previously [7]. *Ha-ras*^{V12} and *c-Myc* expression was confirmed using anti–*Ha-ras* (#3965; Cell Signaling Technology, New England Biolaboratories, Frankfurt am Main, Germany) and anti–*c-Myc* antibodies (sc-788; Santa Cruz Biotechnology, Heidelberg, Germany).

MTT Assay for Cell Viability

Cells were plated in 96-well plates at 1×10^4 cells per well and incubated overnight. Cells were treated either with Trolox (a water-soluble analog of α-tocopherol; #56510; Sigma-Aldrich), with the pan-COX inhibitor indomethacin, the general LOX inhibitor NDGA and the 12/15-LOX-specific inhibitors Baicalein and PD146176 for 72 hours at various concentrations. Then, 10 μl of 5 mg/ml 3-(4,5-dimethylthiazol-2-yl)-2,5-diphenyltetrazolium bromide (MTT; M2003; Sigma-Aldrich) in PBS was added to 100 μl of culture media. Plates were incubated for 4 hours, and the formazan precipitate was redissolved in 200 μl of 0.04N HCl in isopropanol. The absorbance at

540 nm was recorded using a Sunrise microplate absorbance reader (Tecan, Crailsheim, Germany).

Three-dimensional BD Matrigel Assay

Three days before starting the assay, deletion of *GPx4* was induced by adding TAM to the cell culture medium. To ensure survival of the cells, Trolox, which fully complements GPx4 deficiency *in vitro* (see MTT Assay for Cell Viability section), was given as a supplement to the medium.

Two types of frozen Matrigel (Matrigel as well as Growth Factor–reduced Matrigel; #356234 and #35623; Becton Dickinson GmbH) were thawed overnight at 4°C, and 200 μl of each undiluted Matrigel was placed on 24-well plates and incubated for 1 hour at 37°C. Thereafter, tGPx4 knockout as well as control cells were thoroughly washed with PBS to remove Trolox. Cells were counted and 5×10^4 cells each were reconstituted in 20 μl of culture medium ± TAM. Finally, cells were plated on the BD Matrigel layer, coated with 200 μl of undiluted Matrigel, and incubated for an additional hour at 37°C. Normal cell culture medium ± TAM was added on the top layer. In parallel, the same amount of wild-type and knockout cells was plated on uncoated 24-well plates ± TAM, and GPx4 deletion was verified by analyzing cell death within the next 48 to 72 hours.

The average number of spheroids per well was determined after 14 days of growth in both types of Matrigel. Pictures were taken from triplicate experiments.

RNA Isolation, Reverse Transcription, and Quantitative RT-PCR

Cells were kept 72 hours under the conditions described above adding either TAM and Trolox or Trolox alone to the cell culture medium. Total RNA was extracted with the Qiagen RNA isolation kit (RNeasy Mini Kit #74106; Qiagen, Hilden, Germany), and residual genomic DNA was removed by the RNase-Free DNase Set (#79254; Qiagen). RNA was reverse-transcribed into complementary DNA as described before [21]. Real-time PCR was performed with Lightcycler in a reaction volume of 10 μl using SYBR Green I (LC-FastStart DNA Master^{Plus}, #03 515 885 001; Roche, Mannheim, Germany) according to the manufacturer's protocol. Primers were used at a final concentration of 0.5 μM each. An initial denaturation step at 95°C for 10 minutes was followed by 40 cycles of denaturation (95°C, 1 second), annealing (65°C, 10 seconds), and extension (72°C, 20 seconds). Standard curve was prepared using four dilutions of complementary DNA obtained from mouse embryonic fibroblasts. Relative messenger RNA levels were normalized to β-actin messenger RNA levels in the same samples. Primer sequences are as follows: GPx4 A forward (5′-GCA ACC AGT TTG GGA GGC AGG AG-3′), GPx4 B reverse (5′-CCT CCA TGG GAC CAT AGC GCT TC-3′); β-actin forward (5′-CTA CGA GGG CTA TGC TCT CCC-3′) and reverse (5′-CCG GAC TCA TCG TAC TCC TGC-3′).

In Vivo *Tumor Model*

For *in vivo* implantation studies, cells were kept for at least 72 hours under TAM and Trolox, and the knockout was verified as described above. Before injecting the cells, cells were washed thoroughly with PBS to remove TAM and Trolox. After cell counting, 5×10^6 *c-Myc/Ha-ras*^{V12}–transformed *GPx4*-deficient or *GPx4*-proficient MEFs diluted in 100 μl of sterile PBS were implanted subcutaneously into the flanks of C57BL/6 or severe combined immunodeficient (SCID) mice, respectively. Tumors were collected 16 days after implantation (n = 8 mice per group). Tumor volume was calculated by caliber measurement according to the following formula: V (mm^3) = (length × width × high) × π/6. For the *in vivo* pharmacological studies, mice were treated with Baicalein (1.5 mg/kg in Tween 20) orally every second day beginning at day 3 after tumor cell implantation.

Mice were kept under standard conditions with food and water *ad libitum* (ssniff, Soest, Germany). All animal experiments were performed in compliance with the German Animal Welfare Law and have been approved by the institutional committee on animal experimentation and the government of Upper Bavaria.

Hematoxylin-Eosin Histology

Five-micrometer sections of 4% (wt./vol. in PBS) paraformaldehyde-fixed and paraffin-embedded tumor material were stained as described [22].

Immunohistochemistry and Image Analysis

Tumor tissue samples were snap frozen in liquid nitrogen and stored at −80°C. Ten-micrometer frozen sections were prepared using a cryotome (HM 560; Microm, Walldorf, Germany) and mounted on poly-L-lysine–coated glass slides (Menzel, Braunschweig, Germany). Immunostaining was performed using a phospho–histone H3 antibody (1:200; # 9701; Cell Signaling Technology, New England Biolaboratories) for proliferating cells, a CD31 antibody (1:800; BM 4086B; Acris Antibodies, Hiddenhausen, Germany) for endothelial cells, an α-smooth muscle cell antibody (1:200, A2547; Sigma-Aldrich) to mark endothelial coverage by vascular smooth muscle cells/pericytes and the ApopTag Peroxidase *In Situ* Apoptosis Detection Kit (S7100; Serologicals Corporation, Millipore, Schwalbach, Germany) for the detection of apoptotic nuclei according to the manufacturers' recommendations. Immunoperoxidase staining was performed using the Vector ABC Kit and Vector DAB Kit (Vector Laboratories, Linaris, Wertheim-Bettingen, Germany).

Quantification of Proliferation and Apoptosis

The number of proliferating or apoptotic cells, respectively, was determined in a genotype-blinded fashion in 10 random microscopic visual fields at 200-fold magnification and quantified using pixel-based thresholds in a computer-assisted image analysis software (KS400 Imaging System; Carl Zeiss Vision, Hallbergmoos, Germany) defined as positively stained area per total area.

Quantification of Blood Vessel Density

The number of total blood vessels was determined in a genotype-blinded fashion by counting the number of blood vessels in 10 random microscopic visual fields at 200-fold magnification. Blood vessel density, defined as percentage of CD31-positive staining per unit area, was quantified using pixel-based thresholds in a computer-assisted image analysis software (KS400 Imaging System; Carl Zeiss Vision).

Quantification of Pericyte-Covered Tumor Vessels

Tumor sections were double-stained with anti-CD31 antibody for endothelial cells, and anti–α-smooth muscle actin (αSMA) antibodies for smooth muscle cells/pericytes. The number of α-smooth muscle cell–covered vessels was determined in a genotype-blinded fashion in 10 random microscopic visual fields at 200-fold magnification.

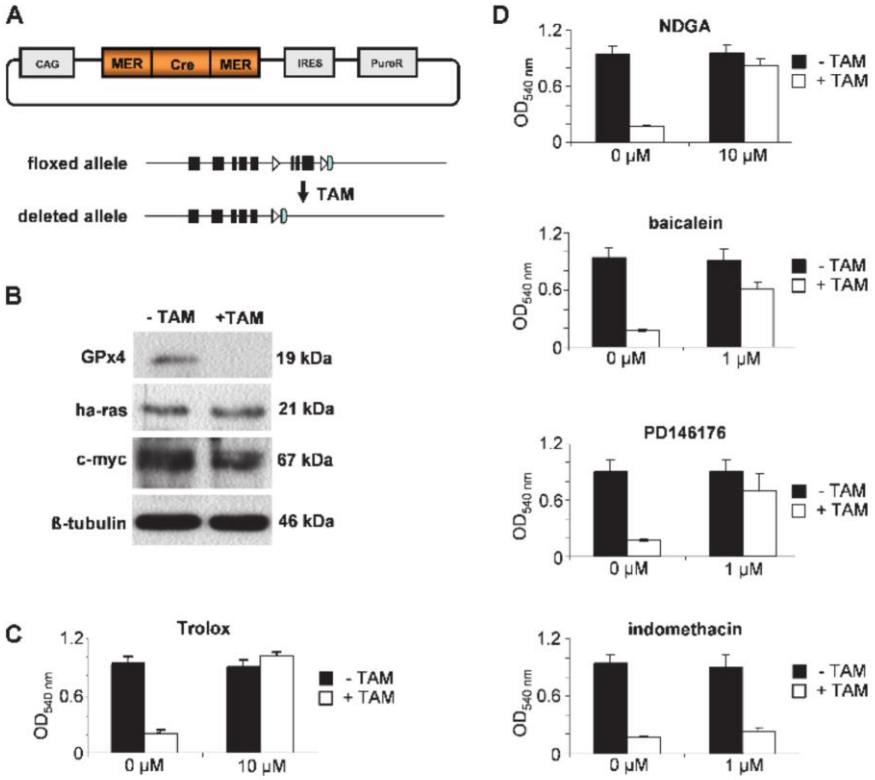

Figure 1. Inducible deletion of GPx4 in transformed cells leads to rapid cell death, which can be prevented by Trolox or 12/15-LOX inhibitors. (A) MEFs isolated from conditional *GPx4* knockout mice were transfected with a TAM-inducible GPx4 knockout system [7]. MERCreMER (*MER* = mutated estrogen receptor) is retained in the cytosol. On addition of TAM, MERCreMER translocates to the nucleus where Cre-mediated deletion of the floxed *GPx4* alleles occurs. (B) Immunoblot analysis with a monoclonal antibody directed against murine GPx4 peptide shows strongly reduced GPx4 protein levels after TAM administration (upper panel). TAM-inducible GPx4 MEFs were transformed with the oncogenes *c-Myc* and *Ha-ras*^{V12} using lentivirus-mediated gene transfer. The expression of both oncogenes was confirmed by immunoblot analysis (lower panel). (C) TAM-induced cell death of *GPx4* knockout MEFs can be prevented by Trolox or (D) by the general LOX inhibitor NDGA and the 12/15-LOX specific inhibitors Baicalein and PD146176 but not by the general COX inhibitor indomethacin. Cell viability was determined 72 hours after TAM treatment by MTT assay. Trolox, NDGA, Baicalein, or PD146176 treatment caused a statistically significant increase in cell viability compared with cell viability in nontreated GPx4-deleted cells.

In Vivo Fluorescence Microscopy

Experiments were performed in male C57BL/6 mice (8-10 weeks old, 25-35 g, $n = 4$ mice per group). A dorsal skinfold chamber was implanted under anesthesia (subcutaneous injection of 75 mg of ketamine hydrochloride/25 mg xylazine per kilogram body weight) as described [23]. Animals were allowed to recover from the chamber implantation surgery for 2 to 3 days before tumor cells were inoculated into the skinfold chamber preparation.

Before measurement of vessel diameter and vessel density at days 7, 10, and 14 after tumor cell implantation, animals were placed in a polycarbonate tube and were injected intravenously with 0.1 ml of a fluorescein isothiocyanate (FITC)–labeled dextran solution (5% in 0.9% NaCl, M_W = 200,000, FD20; Sigma-Aldrich).

The chamber preparation was mounted on an individually designed microscope stage (Axioplan; Zeiss, Jena, Germany), and tumor vascularization was observed by using a 20× objective (LD acroplan; Zeiss). Epi-illumination was achieved with a 100-W mercury lamp with a fluorescence filter for FITC (excitation, 450-490 nm; emission, 515-525 nm). Images of microvessels in five areas of the tumor were acquired by using a CCD camera (AVC D7; Sony, Tokyo, Japan), displayed on a video monitor and recorded on digital tapes by using a video recorder (SVO-9500MD; Sony) for offline analysis.

Flat-Panel Volume Computed Tomography Imaging

Mice were imaged with flat-panel volume computed tomography (fpVCT), a nonclinical volume computed tomography prototype (GE Global Research, Niskayuna, NY) as described [24,25]. In brief, mice were anesthetized with vaporized isoflurane at 0.8% to 1% concentration, centered on the fpVCT gantry axis of rotation, and placed perpendicularly to the *z*-axis of the system. At distinct time points, iodine-containing contrast agent, 150 µl of Isovist 300 (Bayer-Schering, Berlin, Germany) per mouse, was applied intravenously approximately 30 seconds before scan, and for better demonstration of small blood vessels, the blood pool agent eXia 160 (Binito Biomedical Inc, Ottawa, Canada) was administered intravenously 90 seconds before each scan as described by Jannasch et al. [25]. All data sets were acquired with the same protocol: 500 views per rotation, 4 seconds rotation time, 360 used detector rows, tube voltage of 80 kilovolt (peak), and a current of 100 mA. A modified Feldkamp algorithm was used for image reconstruction resulting in

isotropic high-resolution volume data sets (512 × 512 matrix, with an isotropic voxel size of approximately 100 μm). For tumor segmentation and volume estimation, data sets were analyzed with voxtools 3.0.64 Advantage Workstation 4.2 (GE Healthcare, UK).

Enzyme-Linked Immunosorbent Assay for Vascular Endothelial Growth Factor A, Placenta Growth Factor, and Basic Fibroblast Growth Factor

Lysates from GPx4 knockout and control tumors as well as cell culture supernatants from both types of cells were prepared, and enzyme-linked immunosorbent assays (ELISAs) for vascular endothelial growth factor (VEGF; MMV00), placenta growth factor (PlGF; MP200), and basic fibroblast growth factor (bFGF, DFB50; all purchased from R&D Systems GmbH, Wiesbaden-Nordenstadt, Germany) were performed as described in the accompanying Quantikine ELISA protocols. All ELISA results were read on a Sunrise microplate absorbance reader (Tecan) at an absorbance of 450 nm, with wavelength correction at 550 nm, and calculated according to the manufacturers' recommendations. Total protein concentrations of tumor homogenates and supernatants were measured with the BCA Protein Assay Kit (#23227; Pierce, Fisher Scientific GmbH, Schwerte, Germany).

Statistical Analysis

Statistical analysis was performed using SigmaStat software. The statistical significance of the results was tested by Student's t test. $P < .05$ was considered statistically significant. Results were expressed as mean ± SD.

Results

Transformation of Inducible GPx4 Knockout MEFs with the Oncogenes c-Myc and Ha-ras^{V12}

To investigate the impact of GPx4 depletion on tumorigenesis, we took advantage of our recently established TAM-inducible *GPx4* knockout fibroblasts (Figure 1*A*) [7]. These cells were cotransduced with *c-Myc*– or *Ha-ras^{V12}*–expressing lentiviruses. To establish stably transformed cell lines, colony formation assays were performed, which allowed to isolate single-cell colonies after 2 to 3 weeks of growth in soft agar. Single-cell clones were individually expanded, and the expression of both oncogenes *c-Myc* and *Ha-ras^{V12}* was confirmed by immunoblot analysis (Figure 1*B*). All the following experiments were performed using the *c-Myc*– or *Ha-ras^{V12}*–transformed TAM-inducible *GPx4* knockout fibroblasts (tGPx4).

As shown previously, inducible depletion of GPx4 in nontransformed MEFs caused rapid cell death within 48 hours after knockout induction, which could be prevented either by α-tocopherol or by 12/15-LOX–specific inhibitors. Water-soluble antioxidants and 5-LOX– and COX-specific inhibitors were shown to be ineffective in preventing cell death [7]. To address whether transformed *GPx4* knockout cells behave differently with respect to cell proliferation and cell survival, the knockout was induced by TAM in the presence and absence of Trolox, an α-tocopherol analog, and various LOX and COX inhibitors. Cell viability was determined by MTT assay 72 hours after TAM treatment. As illustrated in Figure 1, *C* and *D*, cell death of transformed *GPx4* knockout cells could be prevented by Trolox, NDGA, Baicalein, and the 12/15-LOX–specific inhibitor PD146176, but not by the COX inhibitor indomethacin. Hence, in terms of cell viability *in vitro*, transformed *GPx4*-null cells do not substantially deviate from the nontransformed parental cell lines.

tGPx4-Deficient MEFs Form Tumor Spheroids in Three-dimensional Extracellular Matrix

One characteristic of tumor cells is their ability to form three-dimensional structures in reconstituted extracellular matrix (ECM) such as BD Matrigel, a solubilized basement membrane preparation extracted from the Engelbreth-Holm-Swarm mouse sarcoma [26]. Interaction of tumor cells with the ECM is thought to be a critical event in controlling angiogenesis and tumor growth. To compare the (tumor cell) behavior of *GPx4*-deficient and -proficient transformed MEFs, cells were plated in between two layers of BD Matrigel to obtain a three-dimensional culture assay.

Unexpectedly, *tGPx4*-null cells embedded in three-dimensional BD Matrigel survived and indeed formed tumor cell colonies (Figure 2*B*). Such colonies were similar in appearance and number (17.53 ± 6.51; Figure 2, *B* and *E*) compared with the colonies formed by control cells (17.60 ± 2.67; Figure 2, *A* and *E*). To test whether survival of *GPx4*-deficient MEFs was dependent on the growth factor content of BD

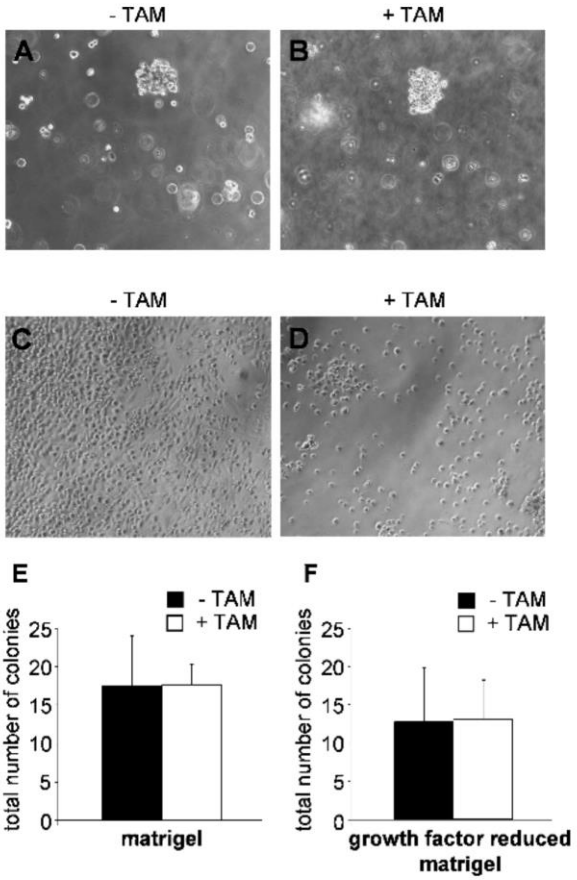

Figure 2. *GPx4* knockout MEFs survive in BD Matrigel. TAM-induced *GPx4* knockout MEFs and uninduced control cells were either embedded in BD Matrigel (A and B) or plated on normal culture dishes (C and D). After 14 days in BD Matrigel, *GPx4* knockout cells formed tumor spheroids (B and E) that were comparable in appearance and number to tumor spheroids formed by control cells (A and E). Similar results were obtained when tumor cells were embedded in Growth Factor–reduced Matrigel (F). In contrast, *GPx4* knockout cells plated on normal dishes died within 48 hours (D).

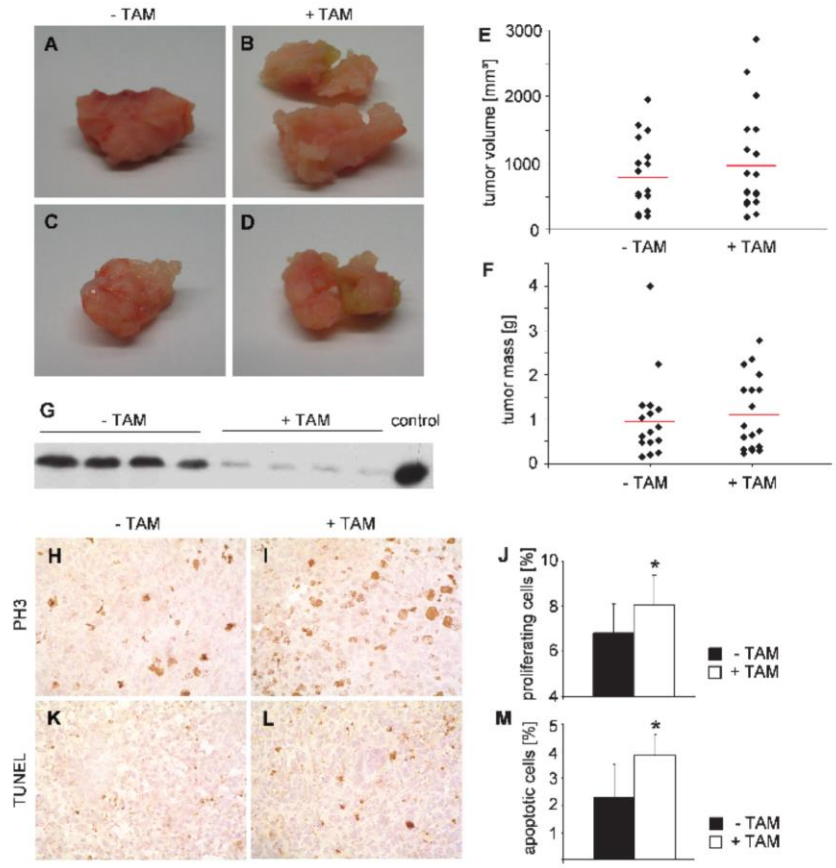

Figure 3. GPx4-deficient transformed MEFs are capable to form tumors *in vivo* (A–D) and display elevated tumor proliferation and apoptosis (H–M). (A–F) *c-Myc*/*Ha-ras*^{V12}–transformed GPx4-deficient MEFs were implanted subcutaneously into C57BL/6 mice. Tumors were collected 16 days after implantation. Control and GPx4 knockout tumors did not show a significant difference in the macroscopic appearance (A–D), tumor volume (E), and tumor mass (F). (G) Deletion of GPx4 in the tumors was confirmed by immunoblot analysis. (H–J) Immunohistologic analysis revealed a higher proliferation rate in *GPx4* knockout tumors (I) compared with control tumors (H) using PH3 antibody as marker for proliferation. (K–M) TUNEL staining demonstrated more apoptotic cells in tumors derived from GPx4-deficient tumor cells (L) compared with control tumors (M).

Matrigel, cell survival and colony formation were tested in parallel in BD Growth Factor–reduced Matrigel. No significant difference in the number of colonies could be found between the two types cells, although the overall number of colonies was reduced under the conditions of limited growth factor availability (12.77 ± 7.07 control colonies *vs* 13 ± 5.24 knockout colonies; Figure 2*F*). In contrast, a strong reduction in cell number of *tGPx4*-null cells seeded on uncoated plates was observed after 48 hours (Figure 2*D*), whereas wild-type cells survived (Figure 2*C*).

Transformed GPx4-Deficient MEFs Form Tumors with Higher Mitotic Activity but Also an Increased Number of Apoptotic Cells

Because transformed *GPx4*-deficient cells died under normal cell culture conditions, but survived and formed colonies when plated in ECM-like BD Matrigel, we asked whether *tGPx4*-deficient cells generate tumors *in vivo*. To this end, *tGPx4*-deficient MEFs and the corresponding noninduced control cells were subcutaneously injected into the flanks of C57BL/6 mice. Tumor growth was monitored every second day, and tumors were harvested and analyzed at day 16 after tumor cell injection. Surprisingly, *GPx4*-deficient and GPx4 control tumors revealed no significant difference with regard to morphologic appearance (Figure 3, *A* and *D*), tumor volume (1399.49 ± 767.21 *vs* 1427.86 ± 1088.49 mm^3; Figure 3*E*) and tumor mass (1.77 ± 0.72 *vs* 1.62 ± 1.58 g; Figure 3*F*). To exclude the possibility that tumors arose from noninduced wild-type cells in the TAM-treated group, GPx4 expression in tumor tissue was analyzed by immunoblot analysis with a GPx4-specific antibody. As illustrated in Figure 3*G*, tumor lysates showed strongly reduced GPx4 expression, indicating that tumors were indeed derived from *tGPx4*-null cells.

Interestingly, immunohistochemical staining using the proliferation marker phospho–histone H3 revealed an increase in the proliferation rate of *GPx4*-deficient tumors (8.08 ± 2.07%) compared with control tumors (6.82 ± 2.08%; Figure 3, *H–J*). Whereas tumors from both groups displayed regions of necrosis, the portion of apoptotic cells was higher in *GPx4*-deficient tumors (3.85 ± 0.78%) than in control tumors (2.30 ± 1.22%) as detected by TUNEL staining (Figure 3, *K–M*).

To quantitate the precise tumor growth and progression over time in a noninvasive fashion, we applied the high-resolution imaging technique, fpVCT. By virtual isolation of the tumor from the acquired isotropic high-resolution fpVCT data sets, tumor volumes were calculated automatically by considering all three dimensions, allowing the generation of precise growth kinetics for each tumor over time. Single fpVCT scans of the entire mice after application of an iodine-containing contrast agent were performed three times per week beginning at day 3 after tumor cell inoculation. In addition, at day 7 and day 14 after tumor cell implantation, we applied the blood pool contrast agent eXia 160 to illustrate the intratumoral vascular network as well as the vessel recruitment from the host in response to the developing tumor. Evaluation of *GPx4*-deficient tumors and control tumors over time by fpVCT imaging yielded no differences in tumor size and progression. Furthermore, contrast medium–containing blood vessels with sizes greater than 150 μm in diameter around and within the tumors were determined. The observed recruitment of host vessels by the tumors as well as the characteristics of large diameter tumor vessels was comparable within the two groups (Figure 4, *A–D*).

Increased Number of Microvessels in GPx4-Deficient Tumors

GPx4-deficient tumors displayed a higher rate of apoptotic cells, nevertheless an increase in tumor cell proliferation. Therefore, no significant alterations about tumor size, tumor weight, or growth rate could be determined between GPx4-deficient tumors and control tumors. In the next step, we performed CD31 immunostaining to evaluate tumor vascularization. Analysis of serial sections for the CD31-positive area demonstrated a markedly increased number of small microvessels in *GPx4*-deficient tumors (total vessel number, 364 ± 119.21), whereas control tumors displayed decreased total vessel numbers (279.73 ± 83.79; Figure 5, *A–D*). However, it is noteworthy that, in control tumors, the mean vessel area was clearly augmented compared with GPx4 knockout tumors (mean ±SEM: 100.26 ± 10.35 *vs* 83.94 ± 12.69 μm^2).

To analyze the density of effectively perfused tumor vessels *in vivo*, *tGPx4*-deficient MEFs and control cells were implanted into the dorsal skinfold chamber. Tumor cells were implanted 3 days after chamber preparation, and *in vivo* fluorescence microscopy was performed at days 7, 10, and 14 after intravenous administration of FITC-dextran, respectively. At days 7 and 10, no differences were observed in vessel diameter and vessel density between *GPx4*-deficient and control tumors. However, at day 14, *GPx4*-null tumors showed a significantly higher functional microcapillary density (262.96 ± 13.72) than control tumors (202.26 ± 13.97; Figure 5, *E–G*), whereas control tumors had a significantly increased tumor vessel diameter and caliber size (15.93 ± 0.60 *vs* 9.95 ± 0.47; Figure 5, *E*, *F*, and *H*).

Decreased Number of αSMA-Covered Vessels

Tumor vessels were also characterized with respect to smooth muscle cell/pericyte coverage by staining tumor sections with anti-CD31 and anti-αSMA antibodies; smooth muscle cell–positive vessels were defined as CD31-positive structures associated with αSMA-positive cells. Analysis of double-stained sections revealed a statistically significant reduction in αSMA-positive vessels in GPx4 knockout tumors when compared with control tumors (7.21 ± 1.81 *vs* 12.25 ± 0.76; Figure 6, *A–C*).

VEGF-A, PlGF, and bFGF Levels of Tumors Derived from tGPx4 Deficient Cells Were Similar to Control Tumors

Because GPx4 knockout tumors displayed a higher microvessel density that was associated with poor mural cell coverage, we wondered if this might be due to an increased endothelial growth factor production by GPx4 knockout tumors. Therefore, we quantified the amount of VEGF-A, PlGF, and bFGF in tumor tissue lysates. Surprisingly, all endothelial growth factor levels obtained from control tumors (VEGF-A, 479.61 ± 220.55 pg/ml; PlGF, 221.41 ± 151.27 ng/μg; bFGF, 272.63 ± 125.33 pg/μg) did not differ from the values obtained from GPx4 knockout tumors (VEGF-A, 555.63 ± 432.29 pg/μg; PlGF, 257.04 ±

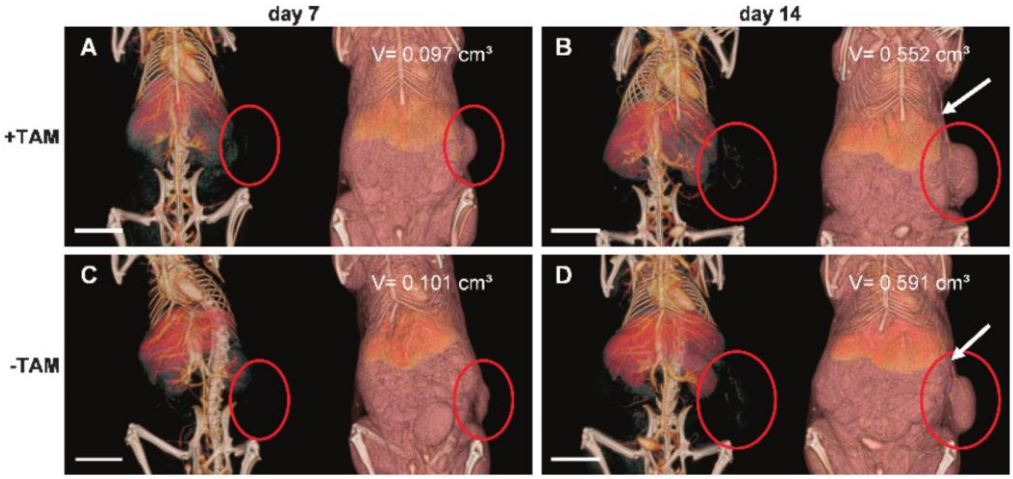

Figure 4. *In vivo* imaging by fpVCT showed no significant alterations for *GPx4*-null tumors. SCID mice with tumors derived from either GPx4-knockout cells or control cells were scanned over time using fpVCT in combination with the blood pool agent eXia 160. Representative pictures from fpVCT data sets show that 7 days after implantation of tumor cells, tumors with comparable volumes formed in both groups (A and C), whereas vessels could not be detected (B and D); red circles indicate tumor localization. Likewise, at the end of the experiment, 14 days after tumor cell implantation, there were no differences in tumor volume and tumor vascularization between the two groups. Note that the tumors of both groups showed similar vessel recruitment (arrows). Scale bars, 10 mm.

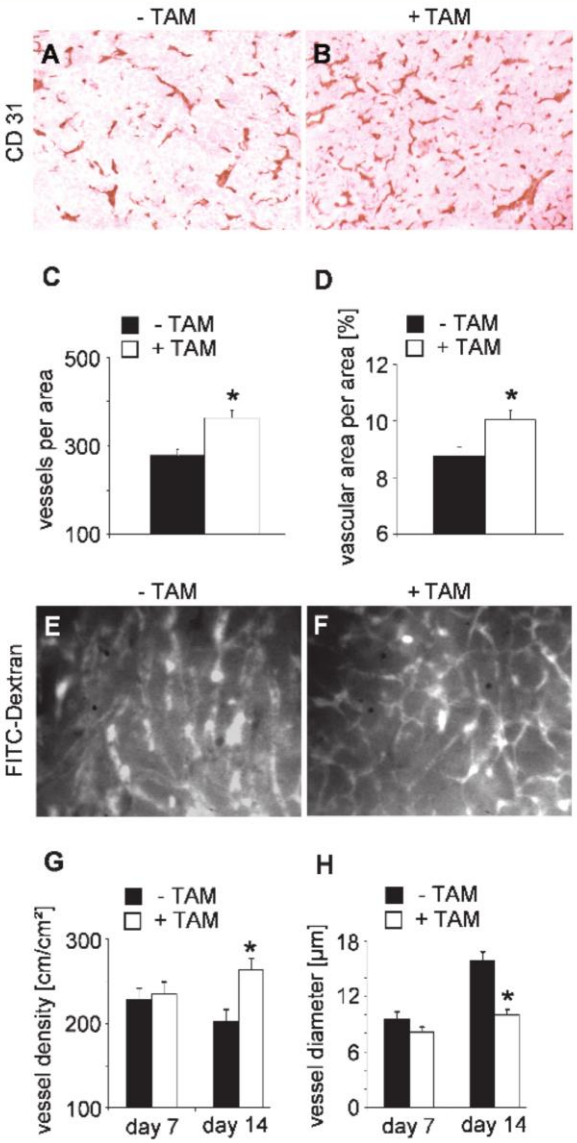

Figure 5. Altered tumor vascularization in *GPx4*-null tumors compared with control tumors. (A–D) Immunohistologic evaluation of CD31-stained tumor sections revealed higher vessel density, in particular more microvessels in *GPx4* knockout tumors. (E–H) For analysis of functional vascular density and vessel diameter, *GPx4*-deficient cells were implanted into the dorsal skinfold chamber preparations in mice. The microvessel density in knockout tumors is significantly increased (E–G). However, newly formed vessels had thinner diameter and markedly reduced vessel lumina in contrast to control tumors (E, F, and H).

83.82 ng/µg; bFGF, 233.03 ± 67.26 pg/µg). Because the SD in tumor tissue samples was high, we also analyzed cell culture supernatants after induction of GPx4 deletion (see below).

Increased bFGF and Decreased VEGF-A Levels in Supernatants of GPx4-Deleted tMEFs

Quantification of VEGF-A, PlGF, and bFGF levels in supernatants of GPx4-deleted tMEFs and control cells revealed a decrease in VEGF-A protein expression levels (729.4 ± 29.38 pg/µg in control supernatants *vs* 204.8 ± 6.13 pg/µg in GPx4 knockout supernatants), no change in the levels of PlGF (2.49 ± 1.29 ng/µg in control *vs* 2.13 ± 0.76 ng/µg in GPx4 knockout supernatants), as well as a strong increase in bFGF expression levels (14.6 ± 6.37 pg/µg in control *vs* 38.4 ± 8.66 pg/µg in GPx4 knockout supernatants). The increase of bFGF is in accordance with data from the literature describing that the 12/15-LOX product 13-HODE is an inducer of bFGF [27].

Baicalein Treatment of Tumor-Bearing Mice Reverses the Vascular Alterations in GPx4-Deficient Tumors

Baicalein, a specific LOX inhibitor, was originally described as an inhibitor of platelet-type 12-LOX, but later also reported to inhibit human 15-LOX [28]. Moreover, Baicalein has already been successfully used for treating neurological disorders in mice [29,30]. Because cell death of *tGPx4* knockout cells could be prevented by Baicalein *in vitro*, we sought to address whether the effects of GPx4 disruption and perturbed 12/15-LOX activity might be reverted by Baicalein administration *in vivo*. For this reason, *GPx4* knockout and GPx4 control tumor-bearing mice were treated daily by intraperitoneal injections of Baicalein. Immunohistologic analyses of Baicalein-treated tumor tissue revealed a clear reduction in microvessel density (untreated GPx4 knockout tumors 8.40 ± 0.45% *vs* treated knockout tumors 6.54 ± 0.85%; Figure 7, *A–C*), which was accompanied by an increase in tumor vessel diameters and mural cell coverage evaluated by αSMA-positive vessels (untreated GPx4 knockout tumors 7.21 ± 1.81 *vs* treated knockout tumors 9.22 ± 2.55; Figure 7*D*). Tumor vessel density and smooth muscle cell/pericyte coverage in Baicalein-treated control tumors revealed no difference compared with the untreated control group (tumor vessel

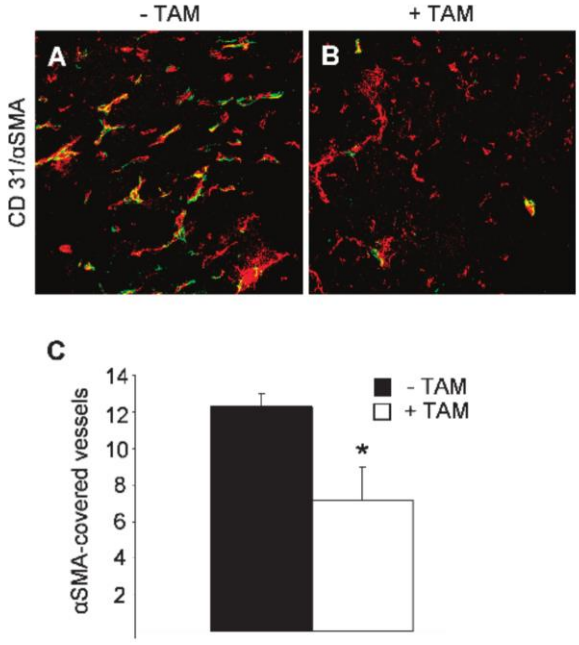

Figure 6. Vessels of *GPx4*-null tumors show diminished pericyte coverage. To further analyze vessel morphology, double staining for CD31 and αSMA was performed on tumor sections (A and B). We observed a reduced number of pericyte covered vessels in GPx4 knockout tumors when compared with control tumors (C).

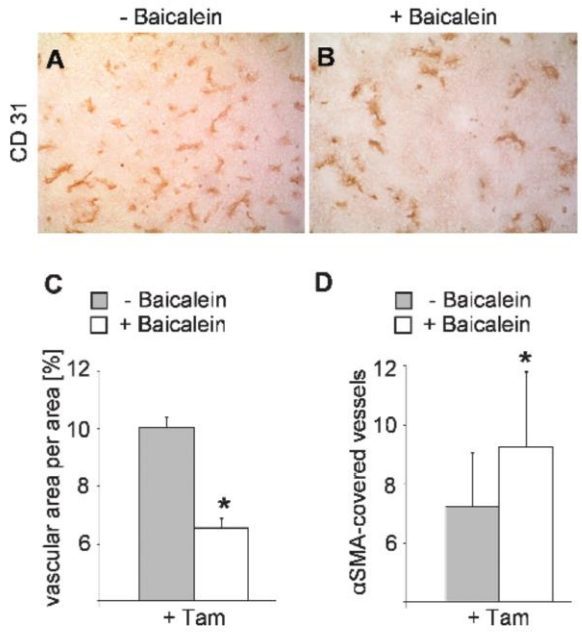

Figure 7. Baicalein treatment reversed the vascular alterations in *GPx4* knockout tumors. The increased microvessel density (A–C) as well as the reduced number of vessels covered by smooth muscle cells in *GPx4* knockout tumors (D) could be reverted by Baicalein administration *in vivo*. Vascular alterations were evaluated by CD31 immunohistochemistry as well as by CD31/αSMA double staining. Note the strong reduction of the overall vascular area (C) as well as the increase of the number of smooth muscle cell covered vessels (D) after Baicalein treatment.

density 8.79 ± 0.29% in untreated control tumors *vs* tumor vessel density 8.40 ± 0.42% in Baicalein-treated control tumors).

Discussion

Numerous studies focusing on the relationship between polyunsaturated fatty acid metabolism and carcinogenesis have identified novel promising compounds targeting COX and LOX activities for anticancer therapies [5,31]. Our recent findings, which identified GPx4 as an important regulator of LOX-catalyzed arachidonic and linoleic acid metabolism by specifically keeping 12/15-LOX activity on a low level [7], prompted us to investigate the function of GPx4 in tumorigenesis and tumor angiogenesis. Therefore, we transformed TAM-inducible *GPx4* knockout MEFs with the oncogenes *c-Myc* and *Ha-ras*^{V12}. Like in the nontransformed parental cell line, inducible GPx4 disruption caused massive cell death *in vitro*, which could be prevented by lipophilic antioxidants such as Trolox as well as by broad-range LOX inhibitors or 12/15-LOX–specific inhibitors.

Contrary to our expectations *tGPx4*-deficient cells survived when embedded into BD Matrigel as well as into Growth Factor–reduced Matrigel and formed three-dimensional "tumor spheroids," which were comparable to spheroids formed by tGPx4 wild-type cells. When implanted subcutaneously into mice, *tGPx4*-deficient cells formed tumors that were indistinguishable from wild-type tumors regarding tumor mass or volume. However, further analysis revealed a strong vascular phenotype.

Tumors derived from tGPx4-deficient cells displayed more microvessels. This phenotype was combined with a reduced number of large diameter vessels as well as a reduction of endothelial tubes covered by smooth muscle cells. Because overexpression of 15-LOX-1 in human prostate cancer cell line PC-3 led to high levels of VEGF-A secretion and therefore enhanced tumor angiogenesis [32], we were interested to analyze whether GPx4-deficient tumors also produce higher levels of VEGF-A. Interestingly, elevated 12/15-LOX activity in tGPx4 cells did not result in increased VEGF-A protein levels in tumor tissues. In addition, neither PlGF nor bFGF protein expression levels were increased *in vivo*. However, analysis of cell supernatants derived from GPx4-deficient and -proficient tMEFs revealed even a decrease of VEGF-A protein expression levels and, at the same time, an increase in bFGF expression levels. The increase of bFGF protein expression levels is in accordance with previous data, showing that the 12/15-LOX product 13-HODE can induce this proangiogenic growth factor. Altogether, results from various studies investigating the biological relevance of 12/15-LOX in the vascular system seem rather inconsistent. 12/15-LOX expression and function have been extensively studied in endothelial cells, smooth muscle cells, and atherosclerotic animal models, where it was shown to play a role in vascular remodeling as well as in the progression of atherosclerotic lesions [33,34]. Conversely, tumor studies demonstrated that the enzyme and its metabolites can either promote or inhibit neovascularization. For example, tumor formation and angiogenesis were inhibited in transgenic mice overexpressing 15-LOX-1 in endothelial cells [35]. In line with these data, Viita et al. [36] showed antiangiogenic action of 15-LOX-1 in a model of hindlimb ischemia. Here, 15-LOX-1 significantly decreased all angiogenic effects induced by VEGF-A and PlGF, including capillary perfusion, vascular permeability, vasodilatation, and increase in capillary number.

One explanation for such inconsistent observations is that 12/15-LOX overexpression might not necessarily result in an increased activity of the enzyme. However, our genetic model of GPx4 ablation leads to increased 12/15-LOX activity, and application of specific 12/15-LOX inhibitors specifically prevents cell death *in vitro*. Interestingly, no up-regulation of 12/15-LOX RNA or protein can be observed after GPx4 deletion. A second explanation might be that various tumor cell types might behave in a different way when exposed to altered 12/15-LOX activity.

By treating our GPx4-deprived tumor-bearing mice with the broad-range LOX inhibitor Baicalein, we could successfully reverse the vascular alterations. Thus, we conclude that GPx4 through controlling 12/15-LOX activity is an important regulator of tumor angiogenesis as well as vessel maturation. Second, modulating 12/15-LOX activity through GPx4 might be an interesting way to reshape tumor vessels.

Acknowledgments

The authors thank Hartmut Land for providing the pBJΩ *c-Myc* and pUC EJ6.6 *Ha-ras*^{V12} plasmids. The authors also thank Wolfgang Schmahl for fruitful discussions, Heidi Förster and Matthias Semisch for excellent technical assistance, and Sarah Greco and Christian Dullin for excellent support running the fpVCT.

References

[1] Ursini F, Maiorino M, Valente M, Ferri L, and Gregolin C (1982). Purification from pig liver of a protein which protects liposomes and biomembranes from peroxidative degradation and exhibits glutathione peroxidase activity on phosphatidylcholine hydroperoxides. *Biochim Biophys Acta* **710**, 197–211.

[2] Imai H, Narashima K, Arai M, Sakamoto H, Chiba N, and Nakagawa Y (1998). Suppression of leukotriene formation in RBL-2H3 cells that overexpressed phospholipid hydroperoxide glutathione peroxidase. *J Biol Chem* **273**, 1990–1997.

[3] Hemler ME, Crawford CG, and Lands WE (1978). Lipoxygenation activity of purified prostaglandin-forming cyclooxygenase. *Biochemistry* **17**, 1772–1779.

[4] Lands WE (1985). Interactions of lipid hydroperoxides with eicosanoid biosynthesis. *J Free Radic Biol Med* **1**, 97–101.

[5] Fürstenberger G, Krieg P, Müller-Decker K, and Habenicht AJR (2006). What are cyclooxygenases and lipoxygenases doing in the driver's seat of carcinogenesis? *Int J Cancer* **119**, 2247–2254.

[6] Conrad M, Schneider M, Seiler A, and Bornkamm GW (2007). Physiological role of phospholipid hydroperoxide glutathione peroxidase in mammals. *Biol Chem* **388**, 1019–1025.

[7] Seiler A, Schneider M, Förster H, Roth S, Wirth EK, Culmsee C, Plesnila N, Kremmer E, Rådmark O, Wurst W, et al. (2008). Glutathione peroxidase 4 senses and translates oxidative stress into 12/15-lipoxygenase dependent– and AIF-mediated cell death. *Cell Metab* **8**, 237–248.

[8] Loscalzo J (2008). Membrane redox state and apoptosis: death by peroxide. *Cell Metab* **8**, 182–183.

[9] Shureiqi I and Lippman SM (2001). Lipoxygenase modulation to reverse carcinogenesis. *Cancer Res* **61**, 6307–6312.

[10] Shureiqi I, Wojno KJ, Poore JA, Reddy RG, Moussalli MJ, Spindler SA, Greenson JK, Normolle D, Hasan AA, Lawrence TS, et al. (1999). Decreased 13-*S*-hydroxyoctadecadienoic acid levels and 15-lipoxygenase-1 expression in human colon cancers. *Carcinogenesis* **20**, 1985–1995.

[11] Shappell SB, Olson SJ, Hannah SE, Manning S, Roberts RL, Masumori N, Jisaka M, Boeglin WE, Vader V, Dave DS, et al. (2003). Elevated expression of 12/15-lipoxygenase and cyclooxygenase-2 in a transgenic mouse model of prostate carcinoma. *Cancer Res* **63**, 2256–2267.

[12] Gonzalez AL, Roberts RL, Massion PP, Olson SJ, Shyr Y, and Shappell SB (2004). 15-Lipoxygenase-2 expression in benign and neoplastic lung: an immunohistochemical study and correlation with tumor grade and proliferation. *Hum Pathol* **35**, 840–849.

[13] Subbarayan V, Xu X, Kim J, Yang P, Hoque A, Sabichi AL, Llansa N, Mendoza G, Logothetis CJ, Newman RA, et al. (2005). Inverse relationship between 15-lipoxygenase-2 and PPAR-gamma gene expression in normal epithelia compared with tumor epithelia. *Neoplasia* **7**, 280–293.

[14] Tang DG, Bhatia B, Tang S, and Schneider-Broussard R (2007). 15-Lipoxygenase 2 (15-LOX2) is a functional tumor suppressor that regulates human prostate epithelial cell differentiation, senescence, and growth (size). *Prostaglandins Other Lipid Mediat* **82**, 135–146.

[15] Hsi LC, Wilson L, Nixon J, and Eling TE (2001). 15-Lipoxygenase-1 metabolites down-regulate peroxisome proliferator–activated receptor gamma via the MAPK signaling pathway. *J Biol Chem* **276**, 34545–34552.

[16] Eling TE and Glasgow WC (1994). Cellular proliferation and lipid metabolism: importance of lipoxygenases in modulating epidermal growth factor–dependent mitogenesis. *Cancer Metastasis Rev* **13**, 397–410.

[17] Yip-Schneider MT, Barnard DS, Billings SD, Cheng L, Heilman DK, Lin A, Marshall SJ, Crowell PL, Marshall MS, and Sweeney CJ (2000). Cyclooxygenase-2 expression in human pancreatic adenocarcinomas. *Carcinogenesis* **21**, 139–146.

[18] Yoshinaga M, Buchanan FG, and DuBois RN (2004). 15-LOX-1 inhibits p21 (Cip/WAF 1) expression by enhancing MEK-ERK 1/2 signaling in colon carcinoma cells. *Prostaglandins Other Lipid Mediat* **73**, 111–122.

[19] Kim J, Baek SJ, Bottone FG, Sali T, and Eling TE (2005). Overexpression of 15-lipoxygenase-1 induces growth arrest through phosphorylation of p53 in human colorectal cancer cells. *Mol Cancer Res* **3**, 511–517.

[20] Shureiqi I, Chen D, Lee JJ, Yang P, Newman RA, Brenner DE, Lotan R, Fischer SM, and Lippman SM (2000). 15-LOX-1: a novel molecular target of nonsteroidal anti-inflammatory drug-induced apoptosis in colorectal cancer cells. *J Natl Cancer Inst* **92**, 1136–1142.

[21] Beck H, Semisch M, Culmsee C, Plesnila N, and Hatzopoulos AK (2008). Egr-1 regulates expression of the glial scar component phosphacan in astrocytes after experimental stroke. *Am J Pathol* **173**, 77–92.

[22] Conrad M, Jakupoglu C, Moreno SG, Lippl S, Banjac A, Schneider M, Beck H, Hatzopoulos AK, Just U, Sinowatz F, et al. (2004). Essential role for mitochondrial thioredoxin reductase in hematopoiesis, heart development, and heart function. *Mol Cell Biol* **24**, 9414–9423.

[23] Yuan F, Salehi HA, Boucher Y, Vasthare US, Tuma RF, and Jain RK (1994). Vascular permeability and microcirculation of gliomas and mammary carcinomas transplanted in rat and mouse cranial windows. *Cancer Res* **54**, 4564–4568.

[24] Missbach-Guentner J, Dullin C, Kimmina S, Zientkowska M, Domeyer-Missbach M, Malz C, Grabbe E, Stühmer W, and Alves F (2008). Morphologic changes of mammary carcinomas in mice over time as monitored by flat-panel detector volume computed tomography. *Neoplasia* **10**, 663–673.

[25] Jannasch K, Dullin C, Heinlein C, Krepulat F, Wegwitz F, Deppert W, and Alves F (2009). Detection of different tumor growth kinetics in single transgenic mice with oncogene-induced mammary carcinomas by flat-panel volume computed tomography. *Int J Cancer* **125**, 62–70.

[26] Kleinman HK and Martin GR (2005). Matrigel: basement membrane matrix with biological activity. *Semin Cancer Biol* **15**, 378–386.

[27] Sen M, McHugh K, Hutzley J, Philips BJ, Dhir R, Parwani AV, and Kelavkar UP (2006). Orthotopic expression of human 15-lipoxygenase (LO)-1 in the dorsolateral prostate of normal wild-type C57BL/6 mouse causes PIN-like lesions. *Prostaglandins Other Lipid Mediat* **81**, 1–13.

[28] Deschamps JD, Kenyon VA, and Holman TR (2006). Baicalein is a potent *in vitro* inhibitor against both reticulocyte 15-human and platelet 12-human lipoxygenases. *Bioorg Med Chem* **14**, 4295–4301.

[29] van Leyen K, Kim HY, Lee S, Jin G, Arai K, and Lo EH (2006). Baicalein and 12/15-lipoxygenase in the ischemic brain. *Stroke* **37**, 3014–3018.

[30] Lapchak PA, Maher P, Schubert D, and Zivin JA (2007). Baicalein, an antioxidant 12/15-lipoxygenase inhibitor improves clinical rating scores following multiple infarct embolic strokes. *Neuroscience* **150**, 585–591.

[31] Pidgeon GP, Lysaght J, Krishnamoorthy S, Reynolds JV, O'Byrne K, Nie D, and Honn KV (2007). Lipoxygenase metabolism: roles in tumor progression and survival. *Cancer Metastasis Rev* **26**, 503–524.

[32] Kelavkar UP, Nixon JB, Cohen C, Dillehay D, Eling TE, and Badr KF (2001). Overexpression of 15-lipoxygenase-1 in PC-3 human prostate cancer cells increases tumorigenesis. *Carcinogenesis* **22**, 1765–1773.

[33] Cyrus T, Witztum JL, Rader DJ, Tangirala R, Fazio S, Linton MF, and Funk CD (1999). Disruption of the 12/15-lipoxygenase gene diminishes atherosclerosis in apo E-deficient mice. *J Clin Invest* **103**, 1597–1604.

[34] Shen J, Herderick E, Cornhill JF, Zsigmond E, Kim HS, Kühn H, Guevara NV, and Chan L (1996). Macrophage-mediated 15-lipoxygenase expression protects against atherosclerosis development. *J Clin Invest* **98**, 2201–2208.

[35] Harats D, Ben-Shushan D, Cohen H, Gonen A, Barshack I, Goldberg I, Greenberger S, Hodish I, Harari A, Varda-Bloom N, et al. (2005). Inhibition of carcinogenesis in transgenic mouse models over-expressing 15-lipoxygenase in the vascular wall under the control of murine preproendothelin-1 promoter. *Cancer Lett* **229**, 127–134.

[36] Viita H, Markkanen J, Eriksson E, Nurminen M, Kinnunen K, Babu M, Heikura T, Turpeinen S, Laidinen S, Takalo T, et al. (2008). 15-Lipoxygenase-1 prevents vascular endothelial growth factor A– and placental growth factor–induced angiogenic effects in rabbit skeletal muscles via reduction in growth factor mRNA levels, NO bioactivity, and down-regulation of VEGF receptor 2 expression. *Circ Res* **102**, 177–184.

5.1.2 Combined Deficiency in Glutathione Peroxidase 4 (Gpx4) and Vitamin E Causes Multi-Organ Thrombus Formation and Early Death in Mice.

Wortmann M*, Schneider M*, Pircher J, Hellfritsch J, Aichler M, Vegi N, Koelle P, Kuhlencordt P, Walch A, Pohl U, Bornkamm GW, Conrad M, Beck H.

Circ Res. 2013 Aug 2;113(4):408-17. Epub 2013 Jun 14. (* equal contribution)

Circulation Research
JOURNAL OF THE AMERICAN HEART ASSOCIATION

American Heart Association®

Combined Deficiency in Glutathione Peroxidase 4 (Gpx4) and Vitamin E Causes Multi-Organ Thrombus Formation and Early Death in Mice

Markus Wortmann, Manuela Schneider, Joachim Pircher, Juliane Hellfritsch, Michaela Aichler, Naidu Vegi, Pirkko Koelle, Peter Kuhlencordt, Axel Walch, Ulrich Pohl, Georg W. Bornkamm, Marcus Conrad and Heike Beck

Circ Res. published online June 14, 2013;
Circulation Research is published by the American Heart Association, 7272 Greenville Avenue, Dallas, TX 75231

Print ISSN: 0009-7330. Online ISSN: 1524-4571

Integrative Physiology

Combined Deficiency in Glutathione Peroxidase 4 and Vitamin E Causes Multiorgan Thrombus Formation and Early Death in Mice

Markus Wortmann,* Manuela Schneider,* Joachim Pircher, Juliane Hellfritsch, Michaela Aichler, Naidu Vegi, Pirkko Kölle, Peter Kuhlencordt, Axel Walch, Ulrich Pohl, Georg W. Bornkamm, Marcus Conrad, Heike Beck

Rationale: **Growing evidence indicates that oxidative stress contributes markedly to endothelial dysfunction. The selenoenzyme glutathione peroxidase 4 (Gpx4) is an intracellular antioxidant enzyme important for the protection of membranes by its unique activity to reduce complex hydroperoxides in membrane bilayers and lipoprotein particles. Yet a role of Gpx4 in endothelial cell function has remained enigmatic.**

Objective: **To investigate the role of Gpx4 ablation and subsequent lipid peroxidation in the vascular compartment in vivo.**

Methods and Results: **Endothelium-specific deletion of Gpx4 had no obvious impact on normal vascular homeostasis, nor did it impair tumor-derived angiogenesis in mice maintained on a normal diet. In stark contrast, aortic explants from endothelium-specific Gpx4 knockout mice showed a markedly reduced number of endothelial branches in sprouting assays. To shed light onto this apparent discrepancy between the in vivo and ex vivo results, we depleted mice of a second antioxidant, vitamin E, which is normally absent under ex vivo conditions. Therefore, mice were fed a vitamin E–depleted diet for 6 weeks before endothelial deletion of Gpx4 was induced by 4-hydroxytamoxifen. Surprisingly, ≈80% of the knockout mice died. Histopathological analysis revealed detachment of endothelial cells from the basement membrane and endothelial cell death in multiple organs, which triggered thrombus formation. Thromboembolic events were the likely cause of various clinical pathologies, including heart failure, renal and splenic microinfarctions, and paraplegia.**

Conclusions: **Here, we show for the first time that in the absence of Gpx4, sufficient vitamin E supplementation is crucial for endothelial viability. (*Circ Res*. 2013;113:408-417.)**

Key Words: α-tocopherol ■ endothelium, vascular ■ oxidant stress ■ thrombosis ■ vascular endothelial function

Peroxidation of lipids and the formation of bioactive lipid peroxidation products have been implicated in a number of pathophysiological processes, including inflammation and atherogenesis.[1,2] The selenoenzyme glutathione peroxidase 4 (Gpx4), 1 of 8 glutathione peroxidases in mammals, is an intracellular antioxidant enzyme unique for its activity to reduce phospholipid hydroperoxides in membrane bilayers.[3,4] In addition, Gpx4 can react with hydrogen peroxide and a wide range of lipid hydroperoxides, including those derived from lipoprotein particles and from cholesterol and cholesteryl esters.[4–6] Disruption of Gpx4 in the mouse leads to early embryonic lethality at embryonic day 7.5.[7,8] Inducible mouse embryonic fibroblasts (MEFs) isolated from conditional Gpx4 knockout mice die shortly after knockout induction.[9] Cell death progression downstream of Gpx4 inactivation was linked to increased 12/15 lipoxygenase-derived lipid peroxidation rather than accumulation of water-soluble oxygen radicals. Increased lipid peroxidation causes cell death in a caspase-independent, apoptosis-inducing factor–mediated manner.[9] Remarkably, cell death of inducible Gpx4 knockout

Original received September 4, 2012; revision received June 13, 2013; accepted June 14, 2013. In May 2013, the average time from submission to first decision for all original research papers submitted to *Circulation Research* was 15 days.

From the Walter Brendel Centre of Experimental Medicine, Munich Heart Alliance, Munich Cluster for Systems Neurology (SyNergy), Ludwig-Maximilians-University, Munich, Germany (M.W., M.S., J.P., J.H., U.P., H.B.); Institute for Stroke and Dementia Research, University of Munich Medical Center, Munich, Germany (M.S.); Research Unit Analytical Pathology, Institute of Pathology (M.A., A.W.), and Institute for Developmental Genetics (M.C.), German Research Center for Environmental Health, Helmholtz Zentrum München, Neuherberg, Germany; Institute of Experimental Cancer Research, Comprehensive Cancer Center and University Hospital Ulm, Ulm, Germany (N.V.); Department of Vascular Medicine, Medizinische Klinik und Poliklinik IV, Klinikum der Ludwig-Maximilians-Universität München, München, Germany (P. Kölle, P. Kuhlencordt); and Institute of Clinical Molecular Biology and Tumor Genetics, German Research Center for Environmental Health, Helmholtz Zentrum München, Munich, Germany (G.W.B.).

*These authors contributed equally.

The online-only Data Supplement is available with this article at http://circres.ahajournals.org/lookup/suppl/doi:10.1161/CIRCRESAHA.113.279984/-/DC1.

Correspondence to Heike Beck, Walter Brendel Centre of Experimental Medicine, Ludwig-Maximilians-University, Marchioninistrasse 15, 81377 Munich, Germany (e-mail Heike.Beck@med.uni-muenchen.de); or Marcus Conrad, Helmholtz Zentrum München, Institute for Developmental Genetics, Ingolstädter Landstraße 1, 85764 Neuherberg, Germany (e-mail marcus.conrad@helmholtz-muenchen.de).

Nonstandard Abbreviations and Acronyms

EC	endothelial cell
eEPC	embryonic endothelial progenitor cell
Gpx4	glutathione peroxidase 4
Gpx4^{iECKO}	tamoxifen-inducible endothelial-specific Gpx4 knockout mice
Gpx4^{control}	control littermates to Gpx4^{iECKO} mice
MDA	malondialdehyde
MEF	mouse embryonic fibroblasts
TUNEL	terminal deoxynucleotidyl transferase dUTP nick-end labeling

MEFs and primary neurons could be prevented by supplementation of the lipophilic antioxidant vitamin E (α-tocopherol). In contrast, water-soluble antioxidants proved to be largely ineffective, indicating that Gpx4 acts mainly at the membranous compartment. In accordance, transformed Gpx4-deleted MEFs died in vitro after knockout induction.[10] However, when implanted subcutaneously into wild-type mice, these cells survived and formed tumors. This suggests that a less toxic, more protective environment is present in vivo to which higher levels of lipophilic antioxidants in serum may contribute.[10]

Because the ability of cells to upregulate intrinsic antioxidant enzymes is fundamentally important in protecting cells from enhanced oxidative stress,[11–13] several studies addressed whether overexpression of Gpx4 might also increase the resistance of the cell against high levels of lipid hydroperoxides. Indeed, Gpx4 overexpression in smooth muscle cells lowered oxidized low-density lipoprotein–induced proliferation compared with untransfected smooth muscle cells.[14] In accordance, overexpression of Gpx4 in apolipoprotein E–deficient mice (*ApoE*$^{-/-}$) inhibited the development of atherosclerosis by decreasing lipid peroxidation.[15] Remarkably, such mice displayed a diminished number of dying endothelial cells (ECs). Furthermore, high amounts of Gpx4 markedly decreased the sensitivity against hydrogen peroxide–induced cytotoxicity in ECs in vitro.[16] These results indicate the importance of Gpx4 in maintaining EC function and vascular wall integrity and prompted us to study the as-yet unexplored role of this redox enzyme in resting and proliferating ECs in vivo.

In view of the fact that oxidative stress and augmented lipid peroxidation have been identified as important detrimental determinants in cardiovascular diseases, we were surprised that endothelial loss of Gpx4 produced no obvious phenotype under baseline conditions or under forced angiogenesis after tumor cell implantation. However, the combined loss of endothelial Gpx4 expression plus dietary depletion of the lipophilic antioxidant vitamin E dramatically impaired vascular homeostasis and resulted in multifocal thrombus formation. Our study reveals that in the absence of Gpx4, vitamin E is essentially required for the homeostasis of blood vessels in the adult mouse.

Methods

Mice

To analyze the biological significance of Gpx4 expression in vascular ECs in vivo, we interbred *Gpx4$^{lox/lox}$* mice[9] with transgenic mice expressing the tamoxifen-inducible recombinase CreERT2 under control of the endothelial Cdh5 promoter (a kind gift from Dr Ralf Adams, MPI Münster).[17] These mice were further crossed with *Gpx4$^{lox/lox}$*, *Gpx4$^{lox/wt}$*, and *Gpx4$^{wt/wt}$* mice to generate litters containing *Gpx4$^{lox/lox}$Cdh5(PAC)-CreERT2* (referred to as *Gpx4^{iECKO}*) and control littermates (referred to as *Gpx4^{control}*; Figure 1A). Control littermates

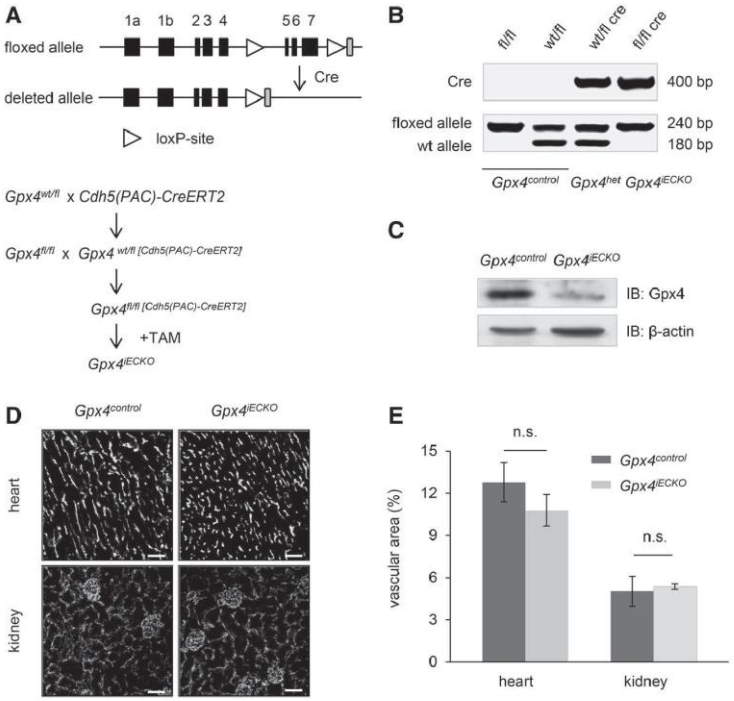

Figure 1. Generation and characterization of *Gpx4^{iECKO}* mice. **A**, Endothelium-specific *Gpx4* knockout strategy. Outline of the generation of the conditional *Gpx4* knockout allele (**top**) and breeding scheme used to generate tamoxifen (TAM)-inducible endothelium-specific *Gpx4* knockout mice (*Gpx4^{iECKO}*). **B**, Genotyping of tail DNA biopsies. A band of 400 bp indicates the presence of the Cre transgene. A 180-bp band indicates the wild-type (wt) allele, and the 240-bp band corresponds to the floxed *Gpx4* allele. **C**, Mouse lung endothelial cells were isolated from tamoxifen-treated *Gpx4^{iECKO}* mice and control littermates (*Gpx4^{control}*). Successful deletion of Gpx4 was verified by immunoblotting. **D** and **E**, No difference in vascular density in heart and kidney tissue was observed between *Gpx4^{iECKO}* and *Gpx4^{control}* mice (n=5). Analysis was performed by immunofluorescence staining with the endothelial cell marker CD31 (**D**) and by quantification of the CD31-positive area (**E**). Data are represented as mean±SEM. ns Indicates not significant. Scale bars=50 μm.

include mice of the following genotypes: *Gpx4*$^{lox/lox}$, *Gpx4*$^{lox/wt}$, and *Gpx4*$^{lox/wt}$ *Cdh5(PAC)-CreERT2*. To activate Cre recombinase in mice carrying the Cdh5(PAC)-CreERT2 transgene, 4-hydroxytamoxifen (T5648, Sigma-Aldrich, Deisenhofen, Germany) was administered by oral gavage on 5 consecutive days followed by a final sixth oral application 1 week thereafter (30 µg tamoxifen per gram body weight per day, diluted in corn oil; C8267, Sigma-Aldrich). The same tamoxifen treatment protocol was applied to control mice.

All mice were kept under standard conditions with food (ssniff, Soest, Germany) and water ad libitum. Mice with dietary depletion of vitamin E received a special diet (No. 15791-147 vitamin E–depleted diet [ssniff] containing 7 mg/kg vitamin E as compared with 55 mg/kg in normal chow) for ≥6 weeks before knockout induction. In a second set of experiments, the order of the events was inverted: First, endothelium-specific *Gpx4* deletion was induced. The dietary depletion of vitamin E was initiated 6 weeks later. In both settings, the vitamin E–depleted diet was applied to knockout and control mice. Animal experiments were performed in compliance with the German Animal Welfare Law and had been approved by the Institutional Committee on Animal Experimentation and the Government of Upper Bavaria.

Isolation of ECs From Heart and Lung Tissue

Two weeks after the last tamoxifen application, ECs isolated from heart and lung tissue were analyzed by Western blotting to confirm the loss of endothelial Gpx4 expression.

Isolation of ECs was performed using a rat antimouse CD31 antibody (1:50; BM 4086, Acris Antibodies GmbH, Herford, Germany), goat antirat IgG Micro Beads (20 µL per 10^7 cell; No.130-048-501, Miltenyi Biotec, Bergisch Gladbach, Germany), and MACS MS Columns (No. 130-042-201, Miltenyi Biotec) according to the manufacturer manual.

Depletion of ECs From Brain Tissue

One hemisphere of the brain (3 *Gpx4*^{iECKO} and 3 *Gpx4*^{control} mice) was cut into pieces of ≈1 mm^3 and homogenized using the Neural Tissue Dissociation Kit (130-092-628, Miltenyi Biotec). The single-cell solution was filtered through a 70-µm cell strainer, rinsed 3 times, and centrifuged at 400*g* for 10 minutes at 4°C. Depletion of the ECs was accomplished using a rat antimouse CD31 antibody (1:50; BM4086, Acris Antibodies), goat antirat IgG Micro Beads (20 µL per 10^7 cells; Miltenyi Biotec), and MACS LD columns (No. 130042901, Miltenyi Biotec) according to the manufacturer's recommendations.

Immunoblotting

Detection of Gpx4 in isolated ECs was achieved with a monoclonal peptide antibody specific for Gpx4. The monoclonal rat C-terminal antibody 1B4 was produced as described previously.[9] Each blot was reprobed for actin (1:1000; A2066, Sigma-Aldrich). Semiquantitative analysis was performed using the Wasabi imaging software (Hamamatsu Photonics Deutschland, Herrsching, Germany).

Cell Lines and Reagents

Lewis Lung Carcinoma cells were cultured at 37°C under 5% CO_2 and 5% O_2 in Dulbecco modified Eagle medium (No. 41965-039, Invitrogen, Karlsruhe, Germany), supplemented with 10% fetal bovine serum (S 0115 Biochrom, Berlin, Germany), 2 mmol/L L-glutamine (No.25030032, Invitrogen), and 100 U/mL penicillin/streptomycin (No. 15140-122, Invitrogen).

Histology

Five-micrometer sections of 4% (wt/vol, in PBS) paraformaldehyde-fixed and paraffin-embedded material were stained with hematoxylin-eosin as described[18] or with the Masson-Goldner staining kit (No. 100485, Merck Millipore, Billerica, MA) according to the manufacturer's instructions.

Immunohistochemistry and Image Analysis

Organ samples and tumor tissue samples were snap-frozen in liquid nitrogen and stored at −80°C. Immunohistochemistry and immunofluorescence were performed as described previously.[19] Immunostaining was analyzed using the Olympus BX41 microscope in combination with the CAMEDIA C-5050 digital camera and Olympus DP-Soft software version 3.2 (Olympus, Tokyo, Japan).

Ex Vivo Mouse Aortic Ring Angiogenesis Assay

Ex vivo angiogenesis was studied by culturing mouse aortic rings in a 3-dimensional Matrigel matrix. Aortic rings of *Gpx4*^{iECKO} mice and control littermates were cultured in the presence or absence of (±)-6-hydroxy-2,5,7,8-tetramethylchromane-2-carboxylic acid (Trolox; 1 µmol/L; No. 56510; Sigma-Aldrich), a water-soluble analog of vitamin E.[10,20]

Embryonic Endothelial Progenitor Cells

To gain further insight into the role of Gpx4 in the endothelial compartment, we used embryonic endothelial progenitor cells (eEPCs), which were isolated from *Gpx4*$^{lox/lox}$ and *Gpx4*$^{wt/lox}$ mouse embryos at embryonic day 7.5.[21] These cells were stably transfected with tamoxifen-inducible MERCreMER (MER indicates mutated estrogen receptor) as described.[9]

To maintain the viability of cells after inducing the deletion of Gpx4 by tamoxifen treatment, cells were cultured in the presence of 1 µmol/L Trolox (Sigma-Aldrich).

Quantification of Blood Vessel Density

Blood vessel density, defined as percentage of CD31-positive staining per area, was quantified using pixel-based thresholds in a computer-assisted image analysis software (KS400 Image System, Carl Zeiss Vision, Jena, Germany).

Quantification of Ex Vivo Angiogenesis

Microvessel outgrowth was studied with an Olympus microscope at appropriate magnification using phase-contrast microscopy. Image analysis was performed with the Aqual software as described before.[22] After generation of a binary image, the following semiautomatic measurements were performed: the number of microvessels, the maximal microvessel length, and the total number of branches.

Hemodynamic Parameters and Endothelial Function In Vivo

Arteriolar resting tone and endothelial function were investigated in arterioles of the cremaster muscle and calculated as described previously.[23]

Determination of Serum Malondialdehyde Levels by High-Performance Liquid Chromatography

Blood samples were obtained from the facial vein 10 days after the final tamoxifen application. Whole-blood samples were kept at room temperature for 20 minutes followed by centrifugation at 3000*g* for 10 minutes at 4°C. The serum was collected, and high-performance liquid chromatography analysis was performed as described previously.[24,25]

Statistical Analysis

Statistical analysis was performed using SigmaStat 2.0 software (Jandel GmbH, Erkrath, Germany). Experimental values are expressed as mean±SEM unless otherwise stated. Statistically significant differences between groups were calculated by the Student *t* test or ANOVA followed by Bonferroni correction. Nongaussian-distributed data were analyzed by the nonparametric Kruskal-Wallis test for nonpaired data. Values of $P<0.05$ were considered significant.

Results

Generation and Histopathological Analysis of *Gpx4*^{iECKO} Mice

The breeding strategy for the generation and genotyping of *Gpx4*^{iECKO} mice is depicted in Figure 1A and 1B. Two weeks after the last tamoxifen application, endothelial loss of Gpx4

expression was verified in ECs isolated from either heart or lung tissue by Western blotting (Figure 1C). Semiquantitative analysis of endothelial Gpx4 expression revealed a 75% reduction in *Gpx4*^{iECKO} (100% in control mice versus 24.8±4.0% in Gpx4^{iECKO} mice; endothelial Gpx4 expression of control mice was arbitrarily set to 100%). In contrast, after the depletion of ECs from brain tissue, no difference in Gpx4 expression was detectable between *Gpx4*^{iECKO} and control mice by Western blot analysis, indicating that nonendothelial tissue is not affected by the endothelium-specific deletion of Gpx4 (100% in *Gpx4*^{control} and 108±15% in *Gpx4*^{iECKO} mice, Gpx4 expression of control mice was arbitrarily set to 100%). *Gpx4*^{iECKO} mice developed no obvious phenotype within 6 months (the maximum observation period) after knockout induction. Survival rate was analyzed for 15 *Gpx4*^{iECKO} mice and 21 control mice. The control group involved the following genotypes: *Gpx4*$^{lox/lox}$ (10 animals), *Gpx4*$^{lox/wt}$ (2 animals), and *Gpx4*$^{lox/wt}$ *Cdh5(PAC)-CreERT2* (9 animals). Immunohistological analysis of the vasculature of various organs (eg, heart, liver, lung, spleen, brain, and kidney) did not reveal any morphological abnormalities in response to endothelial Gpx4 deletion such as vessel density and vessel integrity (exemplarily shown for heart and renal tissue in Figure 1D and 1E).

Tumor Growth and Angiogenesis Are Not Hindered in *Gpx4*^{iECKO} Mice

Because endothelial deletion of Gpx4 did not result in any obvious impairment of vascular homeostasis, we addressed whether it might affect the growth of new blood vessels using a tumor model to study tumor-derived angiogenesis. Subcutaneous implantation of Lewis Lung Carcinoma cells tumor cells into *Gpx4*^{iECKO} and control littermates, resulted in tumors of similar volume and mass (Figure 2A). Quantification of vascularization by CD31 immunohistochemistry revealed no differences between the experimental groups in either vascular density (Figure 2B) or the number of vascular structures (data not shown).

Aortic Explants Derived From *Gpx4*^{iECKO} Mice Show Significantly Impaired Branching

Although the adult vasculature in induced *Gpx4*^{iECKO} mice revealed no abnormal morphology, we asked whether a difference might be unmasked ex vivo. Therefore, aortic explants from *Gpx4*^{iECKO} (n=5) and control littermates (n=5) were cultured for a period of 10 days (Figure 3A). Although the decrease in the number of sprouts from aortic explants of *Gpx4*^{iECKO} mice as compared with controls was not statistically significant (Figure 3B), a significant reduction in both the number of branches (Figure 3C) and sprout length was detectable in the knockout explants (Figure 3D).

In a second set of experiments, we tested whether the addition of Trolox, a water-soluble analog of the lipophilic antioxidant vitamin E, to the cell culture medium was able to restore a normal branching pattern in aortic rings derived from *Gpx4*^{iECKO} mice (Online Figure I). Trolox supplementation rescued the number of branches in knockout explants compared with nontreated explants to a significant extent (Online Figure IA and IB). The increase in the overall sprout length observed on Trolox treatment did, however, not reach statistical significance (Online Figure ID).

Inducible Depletion of *Gpx4* in Mouse eEPCs Leads to Massive Cell Death

We have shown previously that disruption of the Gpx4 gene in MEFs and in c-myc/ha-ras–transformed MEFs caused rapid cell death.[9,10] As a more relevant cellular model for ECs, we generated a tamoxifen-inducible knockout cell system using eEPCs harboring 1 or 2 loxP-flanked *Gpx4* alleles (Online Figure IIA and IIB). These cells were subsequently transfected with MerCreMer, allowing the tamoxifen-dependent inducible depletion of Gpx4. Tamoxifen treatment induced cell death in *Gpx4*$^{lox/lox}$ but not in *Gpx4*$^{wt/lox}$ eEPCs within 72 hours (Online Figure IIC), which could be fully compensated by Trolox, ruling out deleterious side effects of tamoxifen (Online Figure IID).

Vitamin E Deprivation In Vivo Causes Sudden Death or Paralysis in a Fraction of *Gpx4*^{iECKO} Mice

Considering that Gpx4-mediated cell death in eEPCs could be prevented by vitamin E and that ex vivo cultured ECs from *Gpx4*^{iECKO} mice revealed marked defects in vascular branching, whereas endothelium-specific Gpx4 knockout mice show no obvious vascular defects, we asked whether the vitamin E content in the chow may compensate for endothelial Gpx4 deletion. To address this, we replaced the normal mouse diet, which is generally enriched in vitamin E (55 mg/kg vitamin E), by a vitamin E–deprived diet (7 mg/kg vitamin E) for ≥6 weeks before deletion of endothelial Gpx4. Strikingly, 80% of the *Gpx4*^{iECKO} mice maintained on this vitamin E–deprived diet died within 3 weeks or suffered from severe paralysis (3 of 18) after the final tamoxifen application (Figure 4) and had to be euthanized.

In the protocol used above, deletion of Gpx4 is induced by tamoxifen-induced activation of Cre recombinase under conditions of dietary vitamin E deprivation. Ubiquitous transient Cre activation has been shown to induce double-strand breaks and

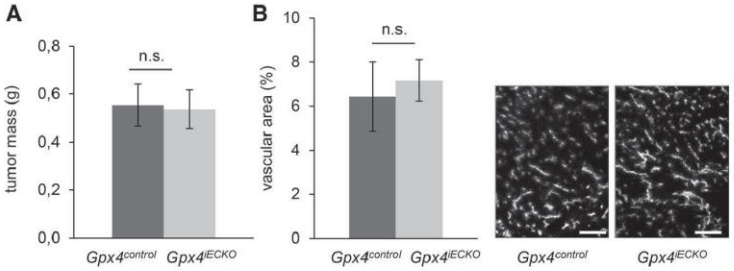

Figure 2. Endothelial loss of Gpx4 does not affect tumor growth or tumor-derived angiogenesis. A and **B**, Subcutaneous tumor cell implantation in *Gpx4*^{iECKO} (n=10) or *Gpx4*^{control} mice (n=10) results in tumors of similar mass (**A**) and vascularization (**B**). Data are represented as mean±SEM. ns Indicates not significant. Scale bars=50 μm.

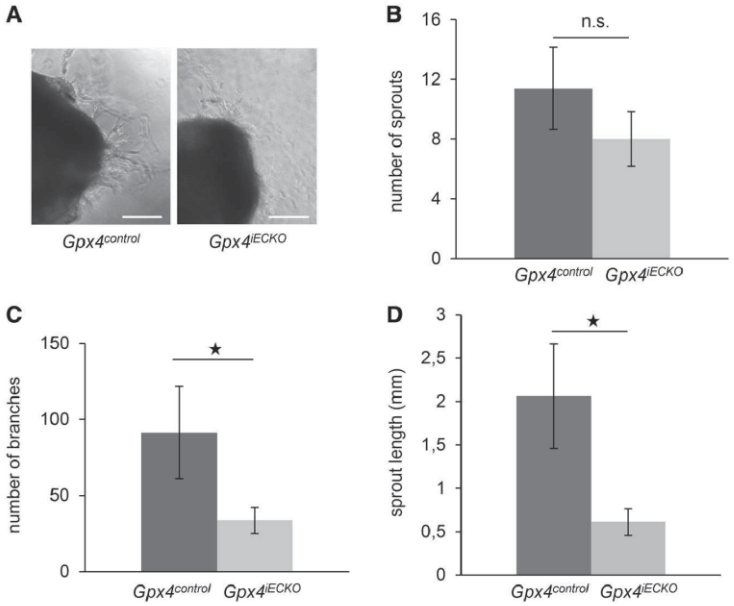

Figure 3. Aortic explants derived from *Gpx4*^{iECKO} mice show impaired branching. **A** through **D**, Aortic ring explants from *Gpx4*^{iECKO} mice (n=5) have similar numbers of sprouts compared with *Gpx4*^{control} mice (n=5; **A** and **B**). However, the number of branches (**C**) and the overall length of sprouts are significantly decreased (**D**). Data are represented as mean±SEM. ns indicates not significant. Scale bars=200 μm. **P*<0.05.

growth inhibition in mammalian cells in vitro[26] and severe toxicity in mice in vivo,[27] which may dramatically aggravate the phenotype when the gene of interest is deleted. To rule out the possibility that Cre toxicity may be responsible for the phenotype or may severely contribute to a composite phenotype in combination with Gpx4 loss and vitamin E deprivation, we inverted the order of events. After endothelium-specific deletion of *Gpx4,* mice were allowed to recover from Cre toxicity and to adapt to the deletion of Gpx4 for 6 weeks before vitamin E was restricted. The inverted protocol resulted in a slightly alleviated phenotype. Only 1 sudden death was observed in the group of *Gpx4*^{iECKO} mice (10 animals). Five other mice had to be euthanized because their general condition was poor. One of these mice suffered from myocardial infarction; 1 mouse suffered from hemiparesis; and another showed forelimb paralysis. The 2 remaining mice demonstrated multiple microthrombotic events in the kidneys. In the control group, 1 animal (*Gpx4*$^{lox/lox}$) suffered from bite injury and had to be euthanized; all other mice survived without developing any symptoms (observation period, 6 months). The control group was composed of the following animals: *Gpx4*$^{lox/lox}$ (10 animals), *Gpx4*$^{lox/wt}$ (1 animal), and *Gpx4*$^{lox/wt}$ *Cdh5(PAC)-CreERT2* (5 animals; Online Figure III).

Although we cannot formally discriminate between an adaptive response (activation of other enzymatic antioxidant systems other than Gpx4 after genetic ablation of Gpx4 or aggravation of the phenotype by the combined toxic action of Cre recombinase activity in concert with Gpx4 deletion and vitamin E depletion), this experiment allowed to make 2 crucially important points: First, there is no other antioxidant system than vitamin E that might take over the function of Gpx4 after adaptation to Gpx4 deletion, and second, Cre toxicity could be definitively ruled out as critical culprit of the phenotype.

Vitamin E–Depleted Diet Increases the Risk of Thrombosis in *Gpx4*^{iECKO} Mice

Because of paraplegia of some mice (2 of 18 mice suffered from hindlimb paralysis, 1 of 18 from forelimb paralysis), we

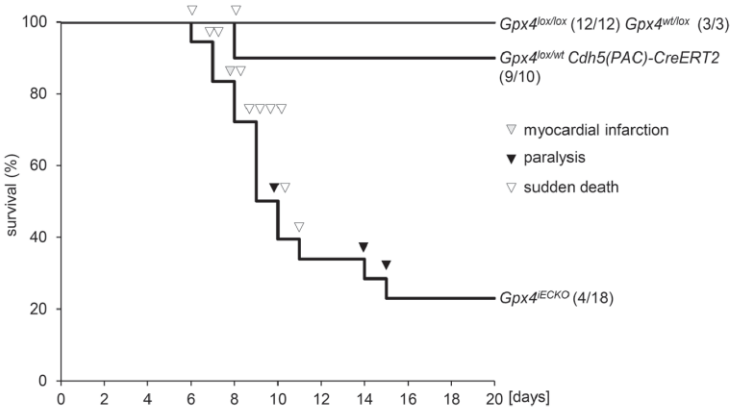

Figure 4. Vitamin E–depleted diet results in sudden death of *Gpx4*^{iECKO} mice. Approximately 80% of *Gpx4*^{iECKO} mice either die or suffer from paralysis when maintained on a vitamin E–depleted diet.

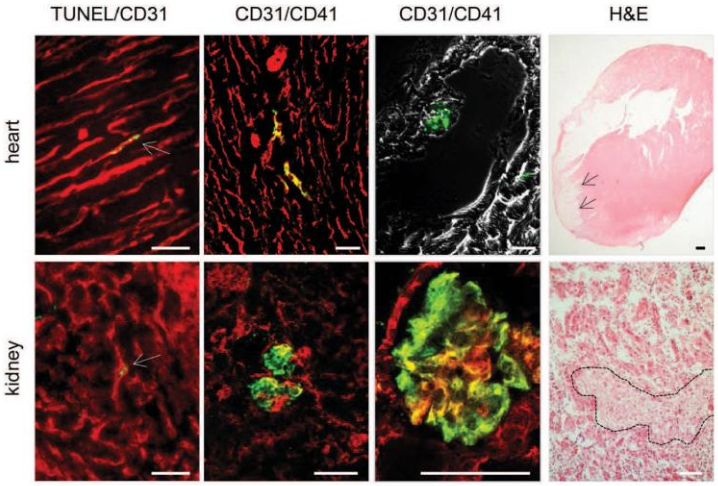

Figure 5. Thrombus formation in *Gpx4*^{iECKO} mice receiving a vitamin E–deprived diet. Endothelial cell death (**left**; endothelial cells are detected by CD31 immunofluorescence [red], terminal deoxynucleotidyl transferase dUTP nick-end labeling (TUNEL)-positive cells are marked in green) in heart (**top**) and renal (**bottom**) tissue results in thrombus formation (**middle**). CD41 immunofluorescence (green) stains aggregated platelets within different vascular beds (as marked by CD31 immunofluorescence staining in red). Thrombus formation results in multiple pathological conditions such as myocardial infarction (**top** and **right**, indicated by **arrows**) or renal infarction (**bottom** and **right**, outlined). Scale bars=50 μm. H&E indicates hematoxylin and eosin.

hypothesized that thrombus formation might be one of the underlying reasons for paraplegia and sudden death in *Gpx4*^{iECKO} mice. Indeed, a systemic histological analysis of different organs confirmed our assumption (Figure 5). One possible reason for the thromboembolic events in *Gpx4*^{iECKO} mice might be EC death because dying ECs are known to be procoagulant.[28] Therefore, we analyzed sections from multiple organs by combined CD31/terminal deoxynucleotidyl transferase dUTP nick-end labeling (TUNEL) staining. In fact, single TUNEL-positive ECs were detectable in lung, kidney, liver, and heart tissue of *Gpx4*^{iECKO} mice (exemplarily shown for heart and renal tissue in Figure 5; left column, top and bottom), which was in sharp contrast to control littermates in which no TUNEL-positive ECs could be detected.

Immunofluorescence staining with an antibody against CD41 further verified platelet aggregation and thrombus formation in various organs (exemplarily shown for heart and renal tissue in Figure 5; middle columns, top and bottom). Such thrombus formation resulted in multiple pathologies like myocardial infarction (Figure 5, right column, top) or microinfarctions in the kidney (Figure 5, right column, bottom). Microinfarctions and microbleedings could also be detected in various organs and tissues such as spleen, liver, and others (not shown). Intriguingly, paralyzed mice had microbleedings within the spinal cord (Figure 6A). Further analysis of the spinal cord and spinal nerves revealed multiple intravascular thrombi (inset in Figure 6B). Such thrombus formation might be responsible for the observed spinal nerve degeneration (Figure 6B), which was not detectable in *Gpx4*^{control} mice (Figure 6C).

Mean Arterial Blood Pressure and Heart Rate

To address whether the endothelium-specific disruption of Gpx4 in combination with vitamin E depletion has any functional consequences on the vascular tone, mean arterial blood pressure and heart rates were determined. Mean arterial blood pressure was significantly elevated in *Gpx4*^{iECKO} mice compared with control mice (79±2 versus 69±3 mm Hg, respectively; n=6 each; $P<0.05$). In contrast, heart rate was not different between *Gpx4*^{iECKO} mice and control mice (226±13 versus 218±35 bpm, respectively; Table).

Resting Arteriolar Tone and Acetylcholine-Induced Dilation

A total of 76 arterioles from 7 control mice and 79 arterioles from 6 *Gpx4*^{iECKO} mice were investigated. Maximal diameters of the arterioles were not significantly different between control littermates (38 μm; range, 18–69 μm) and *Gpx4*^{iECKO} mice (35 μm; range, 16–70 μm). The arterioles in untreated preparations showed varying normalized diameters (from 0.25–1.00); however, normalized diameter was lower in *Gpx4*^{iECKO} mice compared with control littermates (0.78±0.02 versus 0.89±0.02; $P<0.05$), corresponding to an increased arteriolar resting tone. In contrast, acetylcholine-dependent vasodilation (expressed as percent of maximal vessel dilation) as an indicator of endothelial function was not significantly different in *Gpx4*^{iECKO} mice compared with control mice either in response to low acetylcholine (1 μmol/L; 24±5% versus 17±4% in control mice) or in response to high acetylcholine concentrations (10 μmol/L; 83±3% versus 75±3% in control mice). Correspondingly, the response to 1 μmol/L norepinephrine (which was used to normalize the vessel tone for the investigation of acetylcholine-induced vasodilation) was similar in *Gpx4*^{iECKO} and control littermates (normalized vessel diameter after norepinephrine, 0.48±0.02 in *Gpx4*^{iECKO} mice versus 0.47±0.02 in controls). Results are shown in the Table.

Increased Lipid Peroxidation in Vitamin E–Depleted Gpx4^{iECKO} Mice

Malondialdehyde (MDA) is one of the most established indicators of lipid peroxidation.[29] MDA determinations by high-performance liquid chromatography of freshly collected blood samples from mice kept on a standard diet revealed no difference in the MDA levels between control mice (n=6) and *Gpx4*^{iECKO} littermates (n=6; 13.06±2.25 versus 11.71±2.14 μmol/L). However, when mice received a vitamin E–depleted diet, significantly higher MDA plasma levels were observed in *Gpx4*^{iECKO} mice (14.7±3.07 in control mice versus 20.04±2.87 μmol/L in *Gpx4*^{iECKO} mice; Figure 6D).

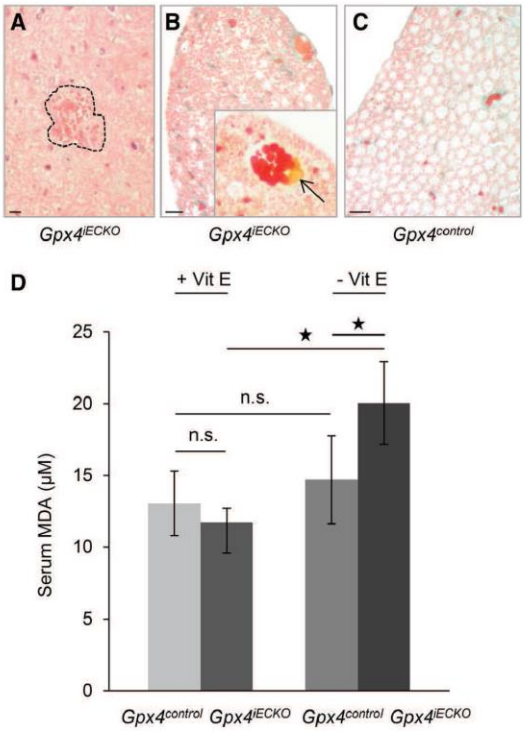

Figure 6. Spinal nerve degeneration in *Gpx4*^{iECKO} mice maintained on a vitamin E–deprived diet. A through **C**, Histological analysis of the spinal cord and the spinal nerves of paralyzed *Gpx4*^{iECKO} mice revealed microbleedings (marked by a dotted line) within the spinal cord (**A**) and spinal nerve degeneration (**B**). Intravascular thrombus formation (**inset** in **B**, marked by an **arrow**) was observed only in *Gpx4*^{iECKO} and not in *Gpx4*^{control} mice (**C**). **D**, Serum levels of malondialdehyde (MDA) were not elevated in *Gpx4*^{iECKO} mice (n=6) compared with wild-type littermates (n=6) on standard diet. However, when mice received a vitamin E–deprived diet, MDA serum levels of *Gpx4*^{iECKO} mice (n=6) were significantly higher than those of *Gpx4*^{control} mice (n=7). ns indicates not significant. Scale bars=20 µm. *P<0.05.

Vitamin E Depletion Leads to EC Ablation in *Gpx4*^{iECKO} Mice

Analysis of the aorta and renal glomeruli by transmission electron microscopy revealed partial ablation of ECs from the basement membrane in *Gpx4*^{iECKO} mice kept on a vitamin E–depleted diet (Figure 7, right column). Control littermates that were also kept on a vitamin E–depleted diet revealed no obvious phenotype (Figure 7, left column) except that single mitochondria in renal ECs seemed swollen.

Discussion

The endothelium maintains vascular homeostasis through multiple complex interactions with cells in the vessel wall and vessel lumen.[30] Considerable evidence suggests that oxidative stress is an important contributing factor in endothelial dysfunction.[31] The functional role of endothelium-expressed Gpx4 in the maintenance of vascular homeostasis in vivo has not been explored to date.

Table. Hemodynamic Parameters and Microvascular Function

	Gpx4^{control}	*Gpx4*^{iECKO}
Hemodynamic parameters		
Animals, n	6	6
Mean arterial blood pressure, mm Hg	69±3	79±2*
Heart rate, bpm	218±35	226±13
Microvascular parameters		
Animals, n	7	6
Vessels, n	76	79
Maximal vessel diameter, µm	38±11	35±11
Normalized resting diameter (resting diameter/maximal diameter)	0.89±0.02	0.78±0.21*
Normalized diameter after norepinephrine (1 µmol/L; diameter after norepinephrine/maximal diameter)	0.47±0.02	0.48±0.02
Acetylcholine (1 µmol/L)–induced vasodilation, % of maximal dilation	17±4	24±5
Acetylcholine (10 µmol/L) induced vasodilation, % of maximal dilation	75±3	83±3

*P<0.05.

Hence, we strived to uncover the biological significance of Gpx4 and its interplay with vitamin E in resting and proliferating ECs in vivo. Interestingly, vascular integrity was not affected when Gpx4 alone was deleted in the endothelium. Similarly, tumor-induced angiogenesis in *Gpx4*^{iECKO} mice was comparable to that in wild-type littermates, indicating an efficient backup system under in vivo conditions. Two observations led us to the assumption that the backup system might be available only in vivo, not in ex vivo, cell systems: First, *Gpx4*^{iECKO} mice display significantly impaired angiogenesis in an ex vivo aortic ring angiogenesis assay; second, Gpx4 knockout eEPCs rapidly die when explanted in culture. Indeed, although vitamin E is not a component of the EC growth medium, the applied mouse diet is highly supplemented with vitamin E. To substantiate our hypothesis that vitamin E in the diet is masking the genetic loss of Gpx4 in vascular ECs in vivo, mice were fed a vitamin E–depleted diet for ≥6 weeks before the deletion of Gpx4. Strikingly, the combined reduction of vitamin E and loss of endothelial Gpx4 expression resulted in fatal outcome in the majority of mice; ≈80% of the Gpx4^{iECKO} mice either suffered from paralysis (3 of 18) or suddenly died within 3 weeks after the final tamoxifen application (14 of 18). To allow adaptation of the mice to Gpx4 deletion in the endothelial system and to exclude toxic side effects of induced Cre recombinase activity, the order of events was inverted. After deletion of Gpx4 by tamoxifen administration, mice were allowed to adapt and to recover from Cre toxicity for 6 weeks before the vitamin E–depleted diet was initiated. With this reverse protocol, a mitigated phenotype was observed (delayed onset and fewer affected animals). Nonetheless, the same pathological findings could be demonstrated in more than half of the animals (6 of 10). The confirmation of the phenotype in the reciprocal protocol provided definitive proof for the backup function of vitamin E for Gpx4 deficiency in ECs in vivo and excluded Cre toxicity as a putative culprit in provoking the observed phenotype.

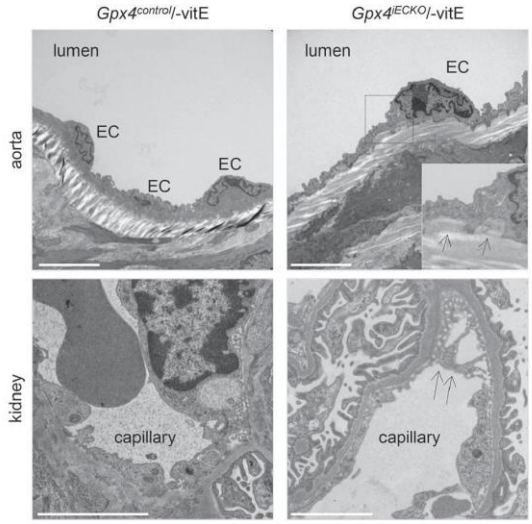

Figure 7. Detachment of endothelial cells (ECs) in *Gpx4*^{iECKO} mice maintained on a vitamin E–depleted diet. Analysis of the aorta (**top**) and of renal glomeruli (**bottom**) by transmission electron microscopy revealed a partial detachment of endothelial cells from the basement membrane (indicated by **arrows**, **right**) in *Gpx4*^{iECKO} mice maintained on a vitamin E–depleted diet (n=3), but not in control littermates (n=4). Scale bars=3 µm.

Nevertheless, because there was a severity difference between the 2 groups, we cannot absolutely exclude that Cre activation exacerbated the phenotype. Because the induced deletion of Gpx4 results in lipid peroxidation–induced cell death in different kinds of cultured cells,[9,10,32] we hypothesized that *Gpx4*^{iECKO} mice may also suffer from increased lipid peroxidation. As expected, serum levels of MDA, the most frequently used biomarker for enhanced lipid peroxidation,[29] were elevated in the serum of vitamin E–depleted *Gpx4*^{iECKO} mice, but not in serum of control littermates or of *Gpx4*^{iECKO} mice kept on a standard diet. Because several lipid peroxidation derivatives are known to induce EC apoptosis,[33,34] we analyzed whether we could detect dying ECs. Indeed, TUNEL-positive ECs were observed in different organs of vitamin E–depleted *Gpx4*^{iECKO} mice but not in organs of control mice or of mice on a standard diet. Detailed analysis of EC morphology by transmission electron microscopy supported this observation. Vitamin E–depleted *Gpx4*^{iECKO} mice revealed a partial detachment of ECs from the basal membrane in the aorta and renal glomeruli. In control littermates, which also received vitamin E–depleted diet, only a single swollen mitochondria (heterozygous and wild-type mice) and a few myelinosomes within ECs (heterozygous animals) were detected. Because proper endothelial function is crucial for the maintenance of vascular homeostasis, we further analyzed animals receiving the vitamin E–depleted diet for hemodynamic parameters and microvascular function. Indeed, *Gpx4*^{iECKO} mice displayed an elevated resting arteriolar vessel tone, which was associated with a significantly higher mean arterial blood pressure. These observations suggest that the combined deficiency of Gpx4 and vitamin E in ECs may decrease endothelial vasodilators and limit endothelial function, which in turn could contribute to the thromboembolic events. In contrast, rats deprived of dietary vitamin E have been shown to exhibit a decrease in the relaxation response to acetylcholine and elevated MDA serum levels.[35] However, species-specific differences and differences in the composition and duration of the diet (35 instead of 6 weeks) might account for these variations.

In view of the fact that dying ECs are well known to contribute to a prothrombotic state,[28] we paid special attention to signs of thrombotic events. The first indication for thrombus formation came from mice suffering either from hindlimb or forelimb paralysis, which was substantiated by autopsy analyses. Two mice revealed macroscopically visible infarct areas either in liver or in myocardium. A detailed analysis of different tissues and organs unveiled platelet aggregation and thus thrombus formation in renal, spleen and liver tissue, myocardium, and spinal cord. Macroinfarctions and microinfarctions and microbleedings were also evident in these organs.

Conclusively, endothelial deletion of Gpx4 and dietary vitamin E depletion highly increase the risk of life-threatening thrombus formation in mice. Interestingly, although oxidative stress is a central cause of endothelial dysfunction, data from vitamin E supplementation studies in patients do not reveal a uniform picture. A number of large-scale randomized trials have been disappointing concerning the prevention of cancer or of major cardiovascular events by vitamin E supplementation.[36–39] However, the Women's Health Study addressed whether vitamin E supplementation for 10 years may decrease the risk of cardiovascular disease. It is noteworthy that vitamin E supplementation reduced the risk of venous thromboembolism, especially for women with a previous history of venous thromboembolism or genetic predisposition.[40] Our data provide conclusive evidence that vitamin E acts as a highly efficient backup system in the prevention of lipid peroxidation processes when other systems are impaired.

Acknowledgments

We thank Heidi Förster, Uta Mamrak, Dorothee Gössel, and Matthias Semisch for excellent technical assistance. We thank Julian Kirsch for his careful reading of the article and his detailed comments and suggestions for further improvement.

Sources of Funding

This work was supported by the Deutsche Forschungsgemeinschaft (DFG) priority Program SPP 1190 to H. Beck and M. Conrad, the Friedrich-Baur Stiftung to H. Beck, the FöFoLe program of the Ludwig-Maximilians University Munich to H. Beck, and a DFG grant (CO 291/2–3) to M. Conrad.

Disclosures

None.

References

1. Esterbauer H, Wäg G, Puhl H. Lipid peroxidation and its role in atherosclerosis. *Br Med Bull*. 1993;49:566–576.
2. Ylä-Herttuala S. Oxidized LDL and atherogenesis. *Ann N Y Acad Sci*. 1999;874:134–137.
3. Imai H, Nakagawa Y. Biological significance of phospholipid hydroperoxide glutathione peroxidase (PHGPx, GPx4) in mammalian cells. *Free Radic Biol Med*. 2003;34:145–169.
4. Maiorino M, Thomas JP, Girotti AW, Ursini F. Reactivity of phospholipid hydroperoxide glutathione peroxidase with membrane and lipoprotein lipid hydroperoxides. *Free Radic Res Commun*. 1991;12-13(pt 1):131–135.

5. Thomas JP, Maiorino M, Ursini F, Girotti AW. Protective action of phospholipid hydroperoxide glutathione peroxidase against membrane-damaging lipid peroxidation: in situ reduction of phospholipid and cholesterol hydroperoxides. *J Biol Chem*. 1990;265:454–461.
6. Sattler W, Maiorino M, Stocker R. Reduction of HDL- and LDL-associated cholesterylester and phospholipid hydroperoxides by phospholipid hydroperoxide glutathione peroxidase and Ebselen (PZ 51). *Arch Biochem Biophys*. 1994;309:214–221.
7. Yant LJ, Ran Q, Rao L, Van Remmen H, Shibatani T, Belter JG, Motta L, Richardson A, Prolla TA. The selenoprotein GPX4 is essential for mouse development and protects from radiation and oxidative damage insults. *Free Radic Biol Med*. 2003;34:496–502.
8. Imai H, Hirao F, Sakamoto T, Sekine K, Mizukura Y, Saito M, Kitamoto T, Hayasaka M, Hanaoka K, Nakagawa Y. Early embryonic lethality caused by targeted disruption of the mouse PHGPx gene. *Biochem Biophys Res Commun*. 2003;305:278–286.
9. Seiler A, Schneider M, Förster H, Roth S, Wirth EK, Culmsee C, Plesnila N, Kremmer E, Rådmark O, Wurst W, Bornkamm GW, Schweizer U, Conrad M. Glutathione peroxidase 4 senses and translates oxidative stress into 12/15-lipoxygenase dependent- and AIF-mediated cell death. *Cell Metab*. 2008;8:237–248.
10. Schneider M, Wortmann M, Mandal PK, Arpornchayanon W, Jannasch K, Alves F, Strieth S, Conrad M, Beck H. Absence of glutathione peroxidase 4 affects tumor angiogenesis through increased 12/15-lipoxygenase activity. *Neoplasia*. 2010;12:254–263.
11. Sneddon AA, Wu HC, Farquharson A, Grant I, Arthur JR, Rotondo D, Choe SN, Wahle KW. Regulation of selenoprotein GPx4 expression and activity in human endothelial cells by fatty acids, cytokines and antioxidants. *Atherosclerosis*. 2003;171:57–65.
12. Thomas JP, Geiger PG, Girotti AW. Lethal damage to endothelial cells by oxidized low density lipoprotein: role of selenoperoxidases in cytoprotection against lipid hydroperoxide- and iron-mediated reactions. *J Lipid Res*. 1993;34:479–490.
13. Lu D, Maulik N, Moraru II, Kreutzer DL, Das DK. Molecular adaptation of vascular endothelial cells to oxidative stress. *Am J Physiol*. 1993;264:C715–C722.
14. Brigelius-Flohé R, Maurer S, Lötzer K, Böl G, Kallionpää H, Lehtolainen P, Viita H, Ylä-Herttuala S. Overexpression of PHGPx inhibits hydroperoxide-induced oxidation, NFkappaB activation and apoptosis and affects oxLDL-mediated proliferation of rabbit aortic smooth muscle cells. *Atherosclerosis*. 2000;152:307–316.
15. Guo Z, Ran Q, Roberts LJ II, Zhou L, Richardson A, Sharan C, Wu D, Yang H. Suppression of atherogenesis by overexpression of glutathione peroxidase-4 in apolipoprotein E-deficient mice. *Free Radic Biol Med*. 2008;44:343–352.
16. Brigelius-Flohé R, Friedrichs B, Maurer S, Streicher R. Determinants of PHGPx expression in a cultured endothelial cell line. *Biomed Environ Sci*. 1997;10:163–176.
17. Wang Y, Nakayama M, Pitulescu ME, Schmidt TS, Bochenek ML, Sakakibara A, Adams S, Davy A, Deutsch U, Lüthi U, Barberis A, Benjamin LE, Mäkinen T, Nobes CD, Adams RH. Ephrin-B2 controls VEGF-induced angiogenesis and lymphangiogenesis. *Nature*. 2010;465:483–486.
18. Conrad M, Jakupoglu C, Moreno SG, Lippl S, Banjac A, Schneider M, Beck H, Hatzopoulos AK, Just U, Sinowatz F, Schmahl W, Chien KR, Wurst W, Bornkamm GW, Brielmeier M. Essential role for mitochondrial thioredoxin reductase in hematopoiesis, heart development, and heart function. *Mol Cell Biol*. 2004;24:9414–9423.
19. Beck H, Acker T, Wiessner C, Allegrini PR, Plate KH. Expression of angiopoietin-1, angiopoietin-2, and tie receptors after middle cerebral artery occlusion in the rat. *Am J Pathol*. 2000;157:1473–1483.
20. Conrad M, Sandin A, Förster H, Seiler A, Frijhoff J, Dagnell M, Bornkamm GW, Rådmark O, Hooft van Huijsduijnen R, Aspenström P, Böhmer F, Ostman A. 12/15-lipoxygenase-derived lipid peroxides control receptor tyrosine kinase signaling through oxidation of protein tyrosine phosphatases. *Proc Natl Acad Sci U S A*. 2010;107:15774–15779.
21. Hatzopoulos AK, Folkman J, Vasile E, Eiselen GK, Rosenberg RD. Isolation and characterization of endothelial progenitor cells from mouse embryos. *Development*. 1998;125:1457–1468.
22. Boettcher M, Gloe T, de Wit C. Semiautomatic quantification of angiogenesis. *J Surg Res*. 2010;162:132–139.
23. Wölfle SE, Schmidt VJ, Hoyer J, Köhler R, de Wit C. Prominent role of KCa3.1 in endothelium-derived hyperpolarizing factor-type dilations and conducted responses in the microcirculation in vivo. *Cardiovasc Res*. 2009;82:476–483.
24. Grotto D, Santa Maria LD, Boeira S, Valentini J, Charão MF, Moro AM, Nascimento PC, Pomblum VJ, Garcia SC. Rapid quantification of malondialdehyde in plasma by high performance liquid chromatography-visible detection. *J Pharm Biomed Anal*. 2007;43:619–624.
25. Moselhy HF, Reid RG, Yousef S, Boyle SP. A specific, accurate, and sensitive measure of total plasma malondialdehyde by HPLC. *J Lipid Res*. 2013;54:852–858.
26. Loonstra A, Vooijs M, Beverloo HB, Allak BA, van Drunen E, Kanaar R, Berns A, Jonkers J. Growth inhibition and DNA damage induced by Cre recombinase in mammalian cells. *Proc Natl Acad Sci U S A*. 2001;98:9209–9214.
27. Higashi AY, Ikawa T, Muramatsu M, Economides AN, Niwa A, Okuda T, Murphy AJ, Rojas J, Heike T, Nakahata T, Kawamoto H, Kita T, Yanagita M. Direct hematological toxicity and illegitimate chromosomal recombination caused by the systemic activation of CreERT2. *J Immunol*. 2009;182:5633–5640.
28. Bombeli T, Karsan A, Tait JF, Harlan JM. Apoptotic vascular endothelial cells become procoagulant. *Blood*. 1997;89:2429–2442.
29. Nielsen F, Mikkelsen BB, Nielsen JB, Andersen HR, Grandjean P. Plasma malondialdehyde as biomarker for oxidative stress: reference interval and effects of life-style factors. *Clin Chem*. 1997;43:1209–1214.
30. Widlansky ME, Gokce N, Keaney JF Jr, Vita JA. The clinical implications of endothelial dysfunction. *J Am Coll Cardiol*. 2003;42:1149–1160.
31. Davignon J, Ganz P. Role of endothelial dysfunction in atherosclerosis. *Circulation*. 2004;109:III27–III32.
32. Yoo MH, Gu X, Xu XM, Kim JY, Carlson BA, Patterson AD, Cai H, Gladyshev VN, Hatfield DL. Delineating the role of glutathione peroxidase 4 in protecting cells against lipid hydroperoxide damage and in Alzheimer's disease. *Antioxid Redox Signal*. 2010;12:819–827.
33. Jian W, Arora JS, Oe T, Shuvaev VV, Blair IA. Induction of endothelial cell apoptosis by lipid hydroperoxide-derived bifunctional electrophiles. *Free Radic Biol Med*. 2005;39:1162–1176.
34. Herbst U, Toborek M, Kaiser S, Mattson MP, Hennig B. 4-Hydroxynonenal induces dysfunction and apoptosis of cultured endothelial cells. *J Cell Physiol*. 1999;181:295–303.
35. Hubel CA, Griggs KC, McLaughlin MK. Lipid peroxidation and altered vascular function in vitamin E-deficient rats. *Am J Physiol*. 1989;256:H1539–H1545.
36. The effect of vitamin E and beta carotene on the incidence of lung cancer and other cancers in male smokers: the Alpha-Tocopherol, Beta Carotene Cancer Prevention Study Group. *N Engl J Med*. 1994;330:1029–1035.
37. Lonn E, Bosch J, Yusuf S, Sheridan P, Pogue J, Arnold JM, Ross C, Arnold A, Sleight P, Probstfield J, Dagenais GR; HOPE and HOPE-TOO Trial Investigators. Effects of long-term vitamin E supplementation on cardiovascular events and cancer: a randomized controlled trial. *JAMA*. 2005;293:1338–1347.
38. Lee IM, Cook NR, Gaziano JM, Gordon D, Ridker PM, Manson JE, Hennekens CH, Buring JE. Vitamin E in the primary prevention of

cardiovascular disease and cancer: the Women's Health Study: a randomized controlled trial. *JAMA*. 2005;294:56–65.
39. Violi F, Cangemi R, Sabatino G, Pignatelli P. Vitamin E for the treatment of cardiovascular disease: is there a future? *Ann N Y Acad Sci*. 2004;1031:292–304.
40. Glynn RJ, Ridker PM, Goldhaber SZ, Zee RY, Buring JE. Effects of random allocation to vitamin E supplementation on the occurrence of venous thromboembolism: report from the Women's Health Study. *Circulation*. 2007;116:1497–1503.

Novelty and Significance

What Is Known?

- It is currently believed that lipid peroxidation contributes to the pathogenesis of cardiovascular diseases.
- Glutathione peroxidase 4 (Gpx4) protects cells from detrimental effects of lipid peroxidation and tissue degeneration.
- Gpx4 controls lipid peroxidation and caspase-independent cell death, both of which can be prevented by vitamin E supplementation in vitro.

What New Information Does This Article Contribute?

- Inducible knockout of Gpx4 in the endothelium does not cause endothelial dysfunction.
- Lowering vitamin E in mouse diet induces lipid peroxidation in endothelial cells, leading to detachment of the basement membrane and endothelial cell death in Gpx4 knockout mice.
- Endothelial cell death secondary to Gpx4 loss and vitamin E deprivation cause thromboembolic events, multiple microinfarctions, and early death of Gpx4 knockout mice, establishing a close link between vitamin E and proper Gpx4 function in vivo.

Uncontrolled oxidative degradation of lipids and lipid peroxidation could lead to tissue injury and cell death. The selenoenzyme Gpx4 reduces lipid hydroperoxides, thus preventing lipid peroxidation. Previous knockout studies in mice have corroborated the importance of Gpx4 in embryogenesis, neuroprotection, retina protection, hair follicle morphogenesis, and male fertility. Moreover, the inducible knockout of Gpx4 in fibroblasts induces massive lipid peroxidation and caspase-independent cell death, which can be rescued by the lipophilic antioxidant vitamin E. Nevertheless, a synergistic effect of vitamin E and Gpx4 has not been rigorously addressed in vivo. Here, we show that the inducible loss of Gpx4 in the endothelium does not cause overt endothelial dysfunction. However, when dietary intake of vitamin E was lowered, the endothelium-specific Gpx4 knockout mice developed progressive endothelial dysfunction and endothelial cell death, which in turn caused thromboembolic events, microinfarctions, and death. These studies establish synergistic actions of vitamin E and selenium-dependent Gpx4 and imply that proper Gpx4 expression and function, along with adequate vitamin E availability, are essential for proper endothelial physiology.

SUPPLEMENTAL MATERIAL

Methods

Genotyping

Tail probes were lysed in 250 µl of DirectPCR Tail reagent (#31-101-T, PEQLAB, Erlangen, Germany) supplemented with 0.3 mg/ml Proteinase K (#03115836001, Roche Applied Sciences, Mannheim, Germany) at 55°C under continuous agitation for 12 hours. Subsequently, Proteinase K was inactivated by incubating at 85°C for 45 min after which probes were stored at 4°C before genotyping. The following primers were used: PFforw1 (5'-ACT CCC CGT GGA ACT GTG AGC TTT GTGC-3'), PFrev1 (5'-GTG TAC CAC GTA GGT A CAGTGTCTGC-3'), CreD (5'-CAC GAC CAA GTG ACA GCA ATG CTG-3') and CreE (5'-CA G GTA GTT ATT CGG ATC ATC AGC-3').

Isolation of endothelial cells from heart and lung tissue

Two weeks following the last tamoxifen application, ECs isolated from heart and lung tissue were analyzed by western blotting to confirm the loss of endothelial Gpx4 expression. Mice were sacrificed and heart and lungs were immediately explanted. After rinsing in PBS, these organs were cut into pieces of approximately 1 mm^3. A single cell suspension was established by incubating these pieces in Collagenase A (0.2 mg/ml in PBS, #10103586001, Roche Diagnostics, Mannheim, Germany) for one hour under continuous agitation. Subsequently, the suspension was centrifuged at 400g for 10 min at 4°C. The pellet was diluted in ice cold Endothelial Cell Growth Medium MV 2 (C-22221, PromoCell, Heidelberg, Germany) and filtered through a 70µm cell strainer. Isolation of ECs was performed using a rat anti-mouse CD31 antibody (1:50, BM 4086, Acris Antibodies GmbH, Herford, Germany), goat anti-rat IgG Micro Beads (20 µl per 10^7 cell, #130-048-501, Miltenyi Biotec, Bergisch Gladbach, Germany) and MACS MS Columns (#130-042-201, Miltenyi Biotec) according to the manufacturer's manual.

Immunoblotting

Isolated ECs were lysed in protein lysis buffer (20 mM Tris, 137 mM NaCl, 2 mM EDTA, 10% Glycerol, 0.1% Sodium deoxycholate, pH 7.4) supplemented with a protease inhibitor cocktail (Roche, Mannheim, Germany). Protein quantification was performed using the BCA™ Protein Assay (Perbio, Fisher-Scientific, Schwerte, Germany). Detection of Gpx4 was achieved with a monoclonal peptide antibody specific for Gpx4. The monoclonal rat C-terminal antibody 1B4 was produced as described previously.[9] Each blot was reprobed for actin (1:1000, A2066, Sigma-Aldrich). The appropriate HRP-conjugated secondary antibodies were purchased from Dianova (1:5000, Dianova GmbH, Hamburg, Germany). Visualization was achieved by use of the ECL™ detection reagent (GE Healthcare Europe GmbH, Freiburg, Germany). Semiquantitative analysis was performed using the Wasabi imaging software (Hamamatsu Photonics Deutschland, Herrsching, Germany).

Immunohistochemistry and image analysis

Sections were stained with the following antibodies: CD31 antibody (1:200, BM4086, Acris Antibodies) to label ECs and CD41 (1:200, GTX76007, Acris Antibodies) to detect platelet aggregation. Omission of the primary antibody served as negative control. The following secondary antibodies were used: goat anti-rat Alexa 488-conjugated IgG as well as goat anti-rat Alexa 568-conjugated IgG (1:200, all antibodies were purchased from Molecular Probes, Invitrogen) and biotinylated goat anti-rat IgG (1:200, Dianova, Hamburg, Germany). Slides for peroxidase staining were incubated with Peroxidase-conjugated streptavidin (Vectastain

KIT ABC, Vector Laboratories, Linaris, Wertheim-Bettingen, Germany). Thereafter, slides were incubated with Vector® DAB kit or AEC kit (Vector Laboratories,).
Dying cells were stained using the ApopTag Fluorescein In Situ Apoptosis Detection Kit (S 7110, Serologicals Corporation, Millipore GmbH, Schwalbach, Germany) according to the manufacturer´s recommendations.
Sections were counterstained with hematoxylin, and mounted with elvanol. Sections for immunofluorescence were counterstained with DAPI (4,6-diamidino-2-phenylindole). Immunostaining was analyzed using the Olympus BX41 microscope in combination with the digital camera CAMEDIA C-5050 and the software Olympus DP-Soft v3.2 (Olympus, Tokio, Japan).

Ex Vivo Mouse Aortic Ring Angiogenesis Assay
Ex vivo angiogenesis was studied by culturing mouse aortic rings in a three-dimensional Matrigel matrix. Thoracic aortas were removed from mice sacrificed by cervical dislocation and immediately transferred into ice-cold PBS. The peri-aortic fibroadipose tissue was carefully removed with microdissecting forceps and iridectomy scissors, paying special attention not to damage the aortic wall. One millimeter long aortic rings were sectioned and extensively rinsed in PBS. These ring-shaped explants were embedded into a 48-well plate pre-coated with 40 µl of a 1:1 mixture of Matrigel (#354234, BD Biosciences, Heidelberg, Germany) and Endothelial Cell Growth Medium MV 2 (C-22022, PromoCell). The aortic rings were covered with 40 µl of the same mixture and incubated at 37°C, 5% O2 and 5% CO2 in Endothelial Cell Growth Medium MV 2 for 14 days. Medium was changed every third day. In a second set of experiments aortic rings of $Gpx4^{iECKO}$ mice (n=5) as well as control littermates (n=6) were cultured in the presence or absence of (±)-6-hydroxy-2,5,7,8-tetramethylchromane-2-carboxylic acid (Trolox; 1 µM, #56510; Sigma-Aldrich), a water-soluble analog of vitamin E.

Hemodynamic parameters and endothelial function *in vivo*
Two weeks following the last tamoxifen application (and 8 weeks after the vitamin E depleted diet was started), but prior to the development of clinical manifestations mice were anesthetized by intraperitoneal application of fentanyl (0.04 mg/kg; CuraMED Pharma GmbH, Karlsruhe, Germany), medetomidine (0.4 mg/kg; Pfizer GmbH, Berlin, Germany), and midazolam (4 mg/kg; Ratiopharm GmbH, Ulm, Germany). A catheter was placed into the left femoral artery, and mean arterial blood pressure (MAP) and heart rate were measured using the PowerLab *16/35* data acquisition system (ADInstruments Germany, Spechbach, Germany). Arteriolar resting tone and endothelial function were investigated in arterioles of the cremaster muscle and calculated as described previously.[23] Due to a relatively large normalized resting diameter in both groups, which was probably due to the anesthesia, norepinephrine (1 µmol/L; Sanofi Aventis Germany, Frankfurt, Germany) was added to the superfusion buffer to normalize vessel tone for the subsequent investigation of acetylcholine-dependent changes in vessel diameter. At the end of each experiment, the maximal vasodilatory capacity of each vessel was determined by combined superfusion with acetylcholine (30 µmol/L), adenosine (30 µmol/L) and A769662 (100 µmol/L), an activator of AMP-activated protein kinase. Measurements of the inner diameter of the vessels were normalized to the maximal possible dilation and expressed as percent of maximal dilation using the formula: $(D_{after\ treatment} - D_{before\ treatment})/(D_{Max} - D_{before\ treatment}) \times 100$.

Transmission Electron Microscopy (TEM)
Tissue was fixed with 2.5% glutaraldehyde in 0.1 M sodium cacodylate buffer pH 7.4 (Science Services, Munich, Germany), postfixed with 2% osmium tetraoxide, dehydrated in gradual ethanol (30-100%) and propylene oxide and embedded in Epon (Merck, Darmstadt,

Germany). Semithin sections were stained with toluidine blue. Ultrathin sections of 50 nm were collected on 200 mesh copper grids, stained with uranyl acetate and lead citrate before examination with a Zeiss Libra 120 Plus transmission electron microscope (Carl Zeiss NTS GmbH ,Oberkochen, Germany). Pictures were acquired using a Slow Scan CCD-camera and iTEM software (Olympus Soft Imaging Solutions, Münster, Germany).

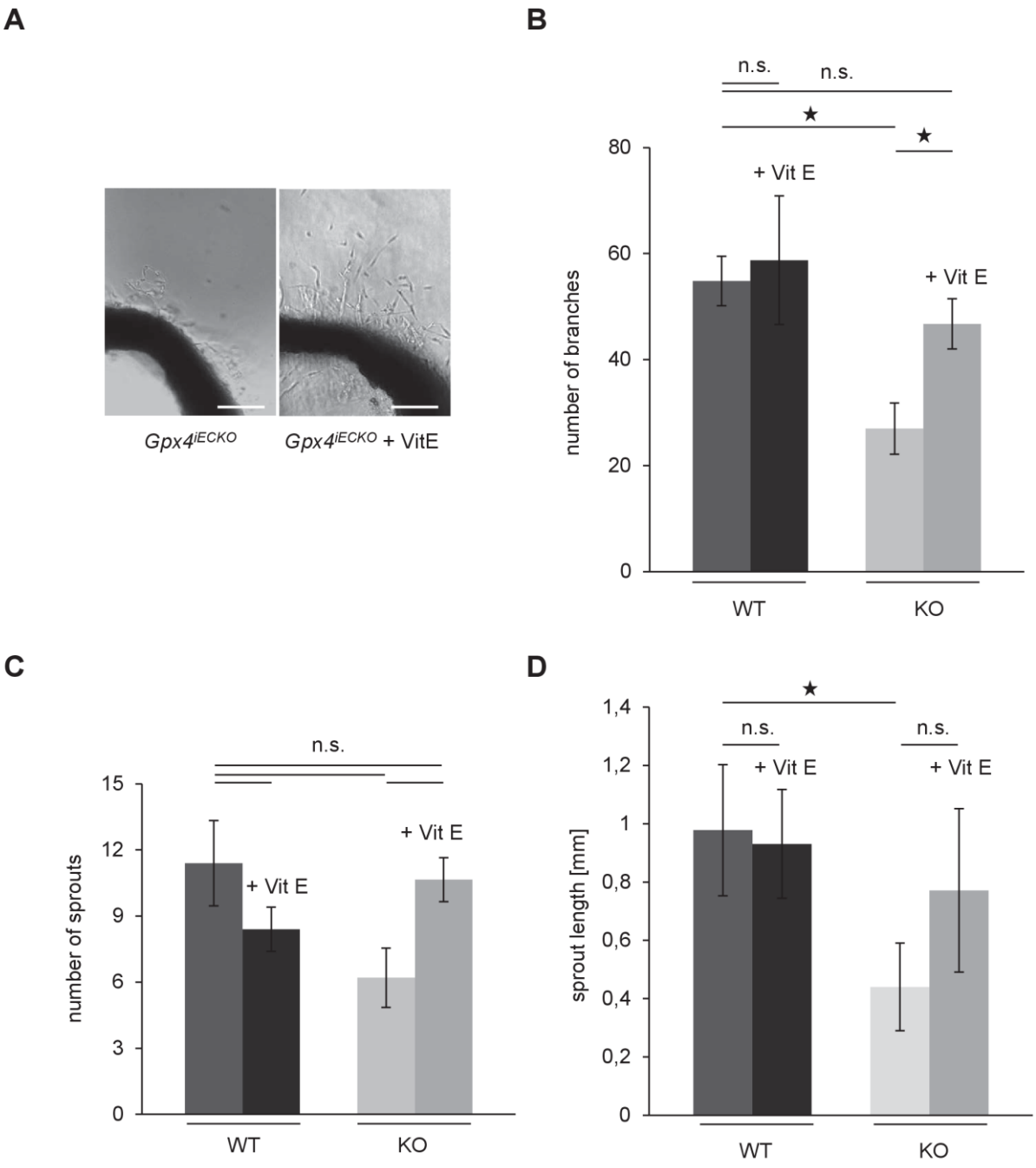

Online Figure I. Recovery of branching of aortic explants derived from *Gpx4*^{iECKO} mice by addition of Vitamin E

A-D Addition of Vitamin E is able to reestablish the decreased branching of aortic explants derived from *Gpx4*^{iECKO} mice (**A,B**). Vitamin E does not significantly influence the number of sprouts derived from aortic ring explants from WT (n=6) or KO mice (n=5) (**C**). The significantly reduced overall sprout length of explants from KO mice does not fully recover when Vitamin E is added to the cell culture medium (**D**). Data are represented as mean ± SEM (A,B) or as mean ± SD (C). n.s. not significant, * $p < 0.05$. Scale bars 200µm.

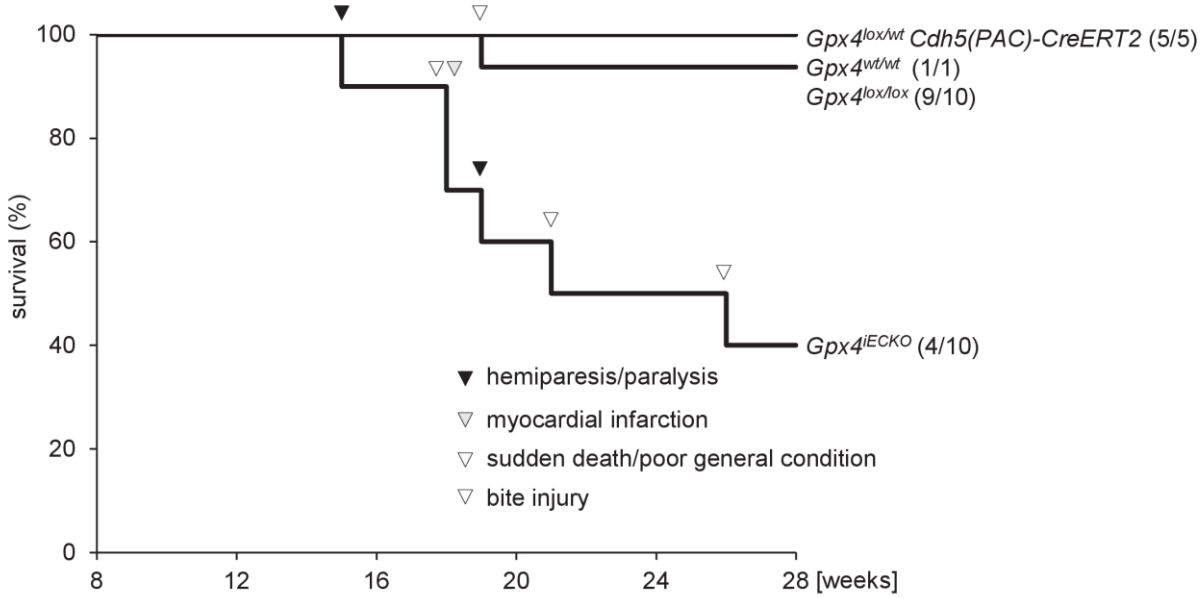

Online Figure III. Adaptation to endothelial deletion of *Gpx4* resulted in a slightly alleviated phenotype when mice were fed a vitamin E-depleted diet
On a standard diet, endothelial depletion of *Gpx4* did not result in any obvious phenotype within the first 6 weeks following knockout induction. Subsequent administration of a vitamin E-depleted diet, however, caused the onset of thrombus-induced pathological conditions in more than half of the $Gpx4^{iECKO}$ mice.

5.2 Danksagung

Die Promotion stellt *per definitionem* den Nachweis dar, dass man eigenständig wissenschaftliche Fragestellungen bearbeiten kann. Insofern gilt mein Dank allen, die mich auf dem Weg zur Fertigstellung dieser Arbeit begleitet und geprägt haben. An erster Stelle sind hier Herr Prof. Dr. Ulrich Pohl und Frau PD Dr. Heike Beck genannt, die mir die Promotion am Walter Brendel Zentrum für experimentelle Medizin in München ermöglicht und mich während der Jahre am Institut auf meinem nicht immer einfachen Weg zur Dissertation unterstützt haben.

Mein tiefster Dank gilt Dr. Marcus Conrad, der mich durch seine grenzenlose Motivation und Faszination für das Projekt immer wieder begeistert hat, mir jederzeit mit Rat und Tat zur Seite gestanden hat und der über die Jahre in München nicht nur zu einem Mentor, sondern auch zu einem guten Freund geworden ist.

Danke an die Doktorandinnen und Doktoranden, die die Zeit am Walter Brendel Zentrum zu einem unvergesslichen Lebensabschnitt gemacht haben, sei es beim Feiern von Erfolgen oder beim Verarbeiten von Niederlagen. Mein besonderer Dank gilt hierbei Juliane Hellfritsch, Julian Kirsch, Judith Pagel, Joachim Pircher, Tamara Perisic und Katja Stangl.

Obwohl sie in der Autorenliste der meisten Publikationen nie auftauchen, tragen die technischen Assistentinnen und Assistenten durch ihr Wissen, Engagement und Ihre Hilfe fundamental zu den meisten wissenschaftlichen Arbeiten bei. Insofern Danke an Heidi Förster, Matthias Semisch und Dorothea Gössel.

Ein jahrelanges wissenschaftliches Engagement parallel zum Studium, besonders in den Prüfungs- und Examensphasen ist nur möglich, wenn man durch seine Familie, Freunde und Bekannte den notwendigen Rückhalt und Ausgleich hat.

Zuerst sind hier mein Vater und meine Großeltern genannt, denen ich diese Arbeit ganz besonders widme. Mein tiefster Dank gilt aber auch meiner Mutter Renate und meiner Schwester Susanne.

Ein besonderer Dank für Ihre unendliche Geduld und Ihre Hilfe bei der Fertigstellung dieser Arbeit geht an meine Freundin Daniela.

Obwohl oder gerade weil ich viel Zeit im Labor und am Schreibtisch verbracht habe, hat die Zeit mit meinen Freunden eine ganz besondere Bedeutung für mich, auch wenn sie oft viel zu kurz kommt. Einen besonderen Dank an Alex, Lisa, Florian, Anna Franziska, Franziska, Kerstin, Christian und Christian, Felix, Katja, Sonja, Franziska, Christoph und alle anderen, die mich auf diesem Weg begleitet haben und sicherlich noch viele Jahre begleiten werden.